TESIS – TL142501

Preparasi dan karakterisasi glassy Ce^{3+} dan Mn^{2+}- doped $CaAl_2O_4$ powder dengan metode spray pyrolysis

A MARSHA ALVIANI

NRP. 02511650010008

DOSEN PEMBIMBING

Dr. Widyastuti., S.Si., M.Si.

Dr.Eng. Hosta Ardyananta., ST., M. Sc.

Prof. Shao-Ju Shih

PROGRAM MAGISTER

BIDANG KEAHLIAN MATERIAL INOVATIF

DEPARTEMEN TEKNIK MATERIAL

FAKULTAS TEKNOLOGI INDUSTRI

INSTITUT TEKNOLOGI SEPULUH NOPEMBER SURABAYA

2018

(*This page intentionally left blank*)

THESIS – TL142501

Preparation and characterization of glassy Ce^{3+} and Mn^{2+} -doped $CaAl_2O_4$ powder using spray pyrolysis

A MARSHA ALVIANI

NRP. 02511650010008

ADVISOR

Dr. Widyastuti., S.Si., M.Si.

Dr.Eng. Hosta Ardyananta., ST., M. Sc.

Prof. Shao-Ju Shih

MASTER DEGREE PROGRAM

MATERIAL INOVATIVE

DEPARTEMENT OF MATERIAL ENGINEERING

FACULTY OF INDUSTRIAL TECHNOLOGY

INSTITUT TEKNOLOGI SEPULUH NOPEMBER

SURABAYA

2018

(*This page intentionally left blank*)

LEMBAR PENGESAHAN

TESIS

Tesis disusun untuk memenuhi salah satu syarat memperoleh gelar
Magister Teknik
di
Institut Teknologi Sepuluh Nopember
Oleh:

A Marsha Alviani
NRP: 02511650010008
Tanggal Ujian: 25 Juli 2018
Periode Wisuda: September 2018
Disetujui Oleh:

1. **Dr. Widyastuti, S.Si., M.Si.**
   NIP. 197906202006042001 **(Pembimbing I)**
2. **Dr.Eng. Hosta Ardyananta., ST., M. Sc.**
   NIP. 198012072005011004 **(Pembimbing II)**
3. **Lukman Noerochim, S.T., M.Sc.Eng., Ph.D.**
   NIP. 197703132003121001 **(Penguji)**
4. **Sigit Tri Wicaksono, S.Si., M.Si., Ph.D.**
   NIP. 197801132002121003 **(Penguji)**
5. **Dr. Agung Imaduddin, M.Eng.**
   NIP. 197109291989121001 **(Penguji)**

Dekan Fakultas Teknologi Industri-ITS

KEMENTERIAN RISET, TEKNOLOGI, DAN PENDIDIKAN TINGGI
INSTITUT TEKNOLOGI SEPULUH NOPEMBER
FAKULTAS TEKNOLOGI INDUSTRI

Dr. Bambang Lelono Widjiantoro., S.T., M.T.
NIP 196905071995121001

M10604819
Thesis Advisor:Shao-Ju Shih

碩士學位考試委員會審定書

Qualification Form by Master's Degree Examination Committee

Department:Department of Materials Science and Engineering

Student's Name:Ayu Marsha Alviani

Thesis Title:

Preparation and characterization of glassy Ce3+ and Mn2+ -doped CaAl2O4 powder using spray pyrolysis

This is to certify that the dissertation submitted by the student named above, is qualified and approved by the Examination Committee.

Degree Examination Committee

Members' Signatures: _____

Advisor: _____

Program Director's Signature: _____

Department/Institute Chairman's Signature: _____

Date: 2018 / 06 / 28 (yyyy/mm/dd)

ABSTRAK

Inorganic luminescence material atau biasa disebut dengan phosphor telah diaplikasikan secara luas seperti security label, emergency signalling, solid state, dan laser light-emitting diodes (LEDs). Saat ini, phosphor sebagai security label dapat ditemukan di uang, paspor, dan beberapa kertas penting. Sebagai tambahan, Shih et al, menerangkan terkait amorfus gehlenite sebagai material phosphor yang memiliki distribusi partikel yang baik. Selain itu untuk membandingkan aplikasi dengan fasa amorfus, glassy phosphor akan diteliti lebih lanjut dalam riset ini. Dalam penelitian ini, calcium aluminate ($CaAl_2O_4$) digunakan karena memiliki beberapa karakteristik seperti long after glow time, stabilitas kimia yang baik, tidak beracun, harga murah, dan efisiensi kuantum yang tinggi pada visible region. Dalam penelitian ini Ce^{3+}, Mn^{2+} doped with $CaAl_2O_4$ dibuat menjadi fasa amorfus. Annealing temperature pada 800^oC pada 95%N_2/ 5%H_2 digunakan untuk mereduksi Ce^{4+} menjadi Ce^{3+} dan Mn^{4+} menjadi Mn^{2+}. Untuk mendapatkan fasa $CaAl_2O_4$:Ce^{3+}, Mn^{2+} , terdapat beberapa karakterisasi yang dilakukan. Seperti, X-ray diffraction (XRD). Untuk mengetahui morfologi permukaan digunakan scanning electron microscopy (SEM). Selain itu untuk mengetahui sifat photoluminescecne menggunakan alat photoluminescence spectra (PL), karakterisasi panjang gelombang yang digunakan pada 273 nm. Maksimum komposisi untuk meningkatkan intensitas dari sinar biru-hijau adalah 0.5%Ce^{3+} and 1%Mn^{2+} in $CaAl_2O_4$.

Kata kunci : Calcium aluminate, Ce/Mn, luminescence, amorphous

(*This page intentionally left blank*)

ABSTRACT

Inorganic luminescent materials (also known as phosphors), have been extensively studied in numerous application such as security label, emergency signalling, solid state, and laser light-emitting diodes (LEDs). Nowadays, phosphor for security labels can be found in money, passport, and other important paper. In addition, Shih et al determined that amorphous gehlenite phosphor material have a good activator particle distribution. Therefore, as compared to the application and amorphous phase superiority, glassy phosphor will be further investigated in this study. In this research calcium aluminate ($CaAl_2O_4$) is used because it has special characteristics such as long after glow time, good chemical stability, low toxicity, low cost, and high quantum efficiency in the visible region. In this study, Ce^{3+}, Mn^{2+} doped with $CaAl_2O_4$ were synthesized with amorphous phase. Annealing temperature at 800^{o}C in 95%N_2/ 5%H_2 condition was used to reduce Ce^{4+} to Ce^{3+} and Mn^{4+} to Mn^{2+}. The obtained phosphor $CaAl_2O_4$:Ce^{3+}, Mn^{2+} phase was characterized by X-ray diffraction technique (XRD). The surface morphology was determined by scanning electron microscopy (SEM). Also photoluminescence spectra (PL), characterization were done with excitation at 273 nm. The maximum composition to increase the intensity of the blue-green light is 0.5%Ce^{3+} and 1%Mn^{2+} in $CaAl_2O_4$.

Keywords: Calcium aluminate, Ce/Mn, luminescence, amorphous

(*This page intentionally left blank*)

ACKNOWLEDGEMENTS

There are many people I would like to thank for being part at this work. First of all, I would like to thank to Allah SWT, the greatest God in this world that gives me a lot of favours. Then I would like to thank to my advisor, Prof. Shao-Ju Shih for the opportunity to do a research under his supervision and always supporting me to finish this thesis on time. I would like to say many thanks to my advisor in Indonesia Dr. Widyastuti who supported me to continue for Master Degree and finished this thesis. I would like to thank to NGB lab family, Fetene, Abadi, Bo Jiang, Tim Lin, Fred, Janet, Tim Sun, Henni, Kevin, Stacey, Peggy, Chen Yan, Guang Ge, Peter, Hana, Emma, Candy, and Shun, who always helped and supported me to conduct this thesis. I would like to say thank to NGB lab alumni, Andy, Cho Wei, Dimas, and Parindra, who helped me to solve a lot of problem. I would like to thank to all of my family in Indonesia especially my mom, my father, my brother, my grandmother, my aunt, and my uncle who have encouraged me every time to finish my study. I would like to say my gratitude to my all of my friends especially my roommates, Frizka, Isabel, Yimen, Sirima Keang, and Ery. I would like to say my gratitude to Indonesian student in Material Science and Engineering Department, who always helped me, especially Bang Noto. I would like to say my gratitude to UNIMIG Taiwan, Salimah family, and all Indonesian organization in Taiwan who always supported and gave me their love. I would like to say my gratitude to ITS Career Centre team, the best partner, who always supported me. I would like to say my gratitude to Al Khansa family. I would like to say so many thanks to post crossing member, who gave me a lot of suggestion by their postcard, it made me cheerful again when I got the postcard. I also would like to say thank you for all my friends that I could not mention.

(*This page intentionally left blank*)

CONTENT

(*This page intentionally left blank*)

LIST OF TABLES

(*This page intentionally left blank*)

LIST OF FIGURES

CHAPTER 1
INTRODUCTION

1.1 Background

Inorganic luminescent materials (also known as phosphors), have been extensively studied in numerous application such as security label, emergency signalling, solid state laser, and light-emitting diodes (LEDs) (Yen, Shionoya et al. 2007, Kubrin 2014, Shih, Lin et al. 2016, Shashikala, Premkumar et al. 2017, Venkatachalaiah, Nagabhushana et al. 2017). Luminescence is the phenomena which involve absorption of energy and subsequent emission of light. Phosphors are luminescent materials that emit light when excited by radiation and these are usually microcrystalline powders or thin-films designed to provide visible colour emission. Phosphors are also used as luminescent pigments and can be used in many transparent or translucent media, such as plastic, paint, glaze, ink, rubbers, glasses and printing slurry, to produce luminous products (Mercury, De Aza et al. 2005, Darshan, Premkumar et al. 2016). Nowadays, phosphor for security labels can be found in money, passport, and other important paper. In several countries such as US, Great Britain, Germany and Japan, phosphorescent ink have been used in printing of all kind of postage stamps (Yen, Shionoya et al. 2007). In addition, Shih determined that amorphous gehlenite phosphor material have a good activator particle distribution (Shih, Lin et al. 2016). Therefore, as compared to the application and amorphous phase superiority, glassy phosphor will be further investigated in this study.

In this research calcium aluminate ($CaAl_2O_4$) is used because it has special characteristics such as long after glow time, good chemical stability, low toxicity, low cost, and high quantum efficiency in the visible region (Massiot, Trumeau et al. 1995, Shiri, Abbasi et al. 2014, Revupriya, P S Anjana et al. 2017). Rare earths (REs) are widely used as luminescence activators in photonic, opto-electronic materials and are very much useful in the technological fields such as solid state lighting and optical communications because their electronic transitions can generate intense emissions of light. The factors that motivated the researchers on RE^{3+} doped materials are their successful application as optical fibre amplifiers

(EDFAs, TDFAs,YDFAs) used as boosters, repeaters, lasers, light sources and preamplifiers in the optical networks. In the previous research, there are several activators that are doped with $CaAl_2O_4$. The activators are Dy^{3+}, Tb^{3+}, Eu^{2+}, Mn^{2+}, Mn^{3+}, Ce^{3+} etc (Katsumata, Nabae et al. 1998, Sathaporn and Niyomwas 2011, Wako 2011, Cao, Zhang et al. 2014, Wei, Wu et al. 2015, Brito 2016, Freeda and Subash 2017, Mishra, Satapathy et al. 2017, Xu, Wang et al. 2018). In some research, the activators are mixed to enhance the photoluminescence properties. For example, Wang successfully synthesized $CaAl_2O_4$ doped Ce^{3+}, Mn^{2+} to produce long lasting phosphorescence (Wang, Jia et al. 2003). Ce^{3+}, Mn^{2+} -doped $Ca_2Al_2SiO_7$ were done to emit two colors, which are green and blue, using two different methodologies by Teixera (Teixeira, Montes et al. 2014). The other case, $BaAl_2O_4$ was successfully synthesized using two activators, Ce^{3+} and Mn^{2+} (Suriyamurthy and Panigrahi 2007). Cerium have large energy gap from the 5d1 states to the nearest level ($_2F^{7/2}$) below that the 5d level serves as an efficient light emitting state. However, it has low energy to transfer electron from 4f to 5d. Furthermore, manganese have advantage to help some activators to transfer the energy of electron through the host or via such ions as Sb^{3+}, Pb^{2+}, Sn^{2+}, Ce^{3+}, and Eu^{2+}, which absorb the UV efficiently through allowed transition (Yen, Shionoya et al. 2007).

1.2 Objective

In this thesis, Ce^{3+}, Mn^{2+} doped with $CaAl_2O_4$ were synthesized with amorphous phase. The purpose of this study are :

1. To analyse the effect of annealing temperature influence photoluminescence Ce^{3+}, Mn^{2+} doped- $CaAl_2O_4$ with spray pyrolysis method.
2. To analyse the effect of reducing atmosphere influence on photoluminescence of Ce^{3+}, Mn^{2+} doped- $CaAl_2O_4$ using spray pyrolysis method.
3. To analyse the effect of Ce and Mn composition influence on photoluminescence of Ce^{3+}, Mn^{2+} doped- $CaAl_2O_4$ using spray pyrolysis method.

CHAPTER 2
LITERATURE REVIEW

2.1. Luminescence material

Luminescence is the phenomena which involve absorption of energy and subsequent emission that generate light in various wavelengths (Wako 2011, Shinde, Dhoble et al. 2012, Teixeira, Montes et al. 2014). Phosphors are material that exhibits the phenomenon of luminescence that emits light when excited by radiation to provide visible colour emission. After decades, phosphors have been prepared and some of them are widely used in many areas, such as fluorescent lamp, cathode ray tubes, security label, solid state laser, radiation delivery vehicles for cancer treatment, etc (Wako 2011, Shih, Lin et al. 2016, Mishra, Satapathy et al. 2017, Xu, Wang et al. 2018). In general, luminescence can be classified into two categories; there are afterglow duration and light source mechanism.

2.1.1 Afterglow duration

Phosphor materials have a dissimilar duration time to glow. This phenomenon is depended on the hosting material and type of the activator. There is two types of the phosphor material based on the afterglow duration. There are fluorescence and phosphorescence.

2.1.1.1 Fluorescence

Fluorescence is the emission of light with a characteristic time of less than 10^{-8} seconds (Wako 2011). Fluorescence occurs when a molecule absorbs photons from the UV-visible light spectrum (200-900 nm), causing transition to a high-energy electronic state and then emits photons as it returns to its initial state. Fluorescent stop emitting light very soon (in about 10 ns) after the exciting energy is cut off. Because reemission occurs so quickly, the fluorescence ceases as soon as the exciting source is removed, unlike phosphorescence, which persists as an afterglow. In generally, fluorescence is not affected by temperature (Ronda).

2.1.1.2 Phosphorescence

The difference between phosphorescence and fluorescence is the emission time. Phosphorescence continues for a longer time than fluorescence. Phosphorescence will happen when the recombination of the photo-generated electrons and holes is significantly delayed in a luminescent material. A less obvious but more exact definition of the difference is that the amount of time phosphorescence continues after the material has been excited may change with temperature, but in fluorescence, this decay time does not change. In phosphorescence, the gap between the ground level and the excited level is a level of intermediate energy, called a metastable level, or electron trap. It is caused by a transition between the metastable level and other levels, which is forbidden (highly improbable). Once an electron has fallen from the excited level to the metastable level (by radiation or by energy transfer to the system), it remains there until it makes a forbidden transition or until it is further excited back to the transition level. The excitation may come from thermal agitation of the neighbouring atoms or molecules (called thermoluminescence) or through optical (e.g., infrared) stimulation. The time that is needed in the metastable level, or electron trap, determines the length of time phosphorescence persists (Ronda , Yen, Shionoya et al. 2007, Wako 2011, Shinde, Dhoble et al. 2012).

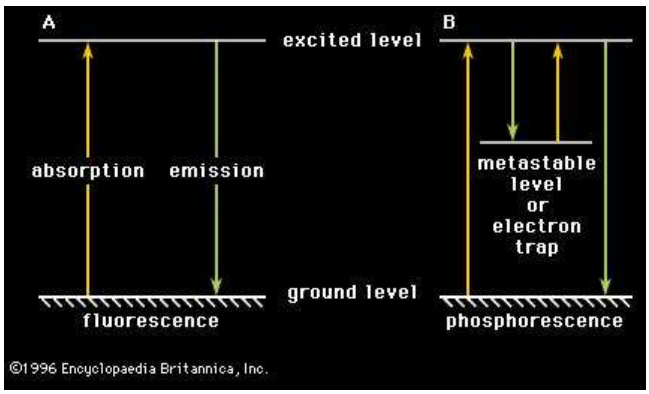

Figure 2.1. Mechanism of electron transfer in fluorescence and phosphorescence

2.1.2 Light source mechanism

There is seven types for the light source mechanism in the luminescence. There are electroluminescence, cathodoluminescence, thermoluminescence, chemiluminescence, bioluminescence, electro-chemiluminescence, and photoluminescence (PL).

2.1.2.1 Electroluminescence

Electroluminescence is the electrical phenomenon that can produce light by flow of electrons, as within certain crystals. The most common electroluminescent device is made for organic thin film (Tang, VanSlyke et al. 1989, Bharathan and Yang 1998). There are two distinct mechanisms that can produce electroluminescence in crystals pure or intrinsic and charge injection. The principal differences between the two mechanisms are that in the first, no net current passes through the phosphor (electroluminescent material) and in the second, luminescence prevails during the passage of an electric current (Shinde, Dhoble et al. 2012).

According to the process by which light is generated from a solid semiconducting material or a gas due to the application of the electric field in the form of high electric voltage (AC-Voltage). Some crystalline substances also exhibit electroluminescence (EL). When an electric current is passed through them, the electrons in the material are accelerated which in turn excite the activator ions that occupy energy levels in the chemical bond of the crystal structure by impact excitation. Electron-hole pairs get excited due to the applied field and as they recombine, they emit photons (Yen, Shionoya et al. 2007). These excited electrons emit visible light as they decay back to the ground state (Wako 2011).

2.1.2.2 Cathodoluminescence

Cathodoluminescence is the emission of light by invisible energetic electrons (cathode rays) produced by electrical discharges in vacuum tubes when they strike the glass walls of the tubes (Yen, Shionoya et al. 2007). The other name of cathode rays is electrons. Cathodoluminescence is widely applied, for

instance the electron microscope uses beams of electrons to produce high resolution images of small images (Wako 2011). For example, in 2003, Sony announced an advanced phosphor screen process using new exposure and color filter technology (Igarashi, Ihara et al. 2000), it applied thermal transfer film technology for coating phosphors, instead of the conventional slurry-spinning method that has been used worldwide since the early stage of CRT development.

2.1.2.3 Thermoluminescence

Thermoluminescence, or also known as Thermally Stimulated Luminescence (TSL), it is a phenomenon in which light is emitted by a crystalline materials which has been exposed to some radiation while being subjected to increasing heat. The heating substance at temperatures of about 450° C (842° F) and higher enables the trapped electrons to return to their normal positions, resulting in the release of energy. All phosphorescent materials have a minimum temperature; but many have a minimum triggering temperature below normal temperatures and are not normally thought of as thermoluminescent materials (Wako 2011).

Figure 2.2. Thermoluminescence of fluorite (chlorophane) (Britannica 2015)

2.1.2.4 Chemiluminescence

Occurs as a result of the energy of a chemical reaction i.e. reduction-oxidation (Redox) reaction whereby the chemical energy formed by the exothermic reaction is transformed into visible light. Sometimes the energy is directly transferred to the electrons in the chemical bonds raising them to the excited states. The electrons then emit light as they decay back to lower or ground states. Because of the slow chemical reactions light can be emitted for a longer time. Chemiluminescence is used, for instance, in the detection and concentration measurements of some atmosphere contaminants, such as NO_2 and NO. A light stick emits a form of light by chemiluminescence (Wako 2011). The widespread luminescence of such living organisms as fireflies and bacteria is based on the oxidation of luciferin in the presence of an enzyme, luciferase. Chemiluminescence that occurs in living organisms is called bioluminescence (q.v.).

2.1.2.5 Bioluminescence

As a particular class of chemiluminescence, bioluminescence is defined as the emission of light by a living organism due to some form of chemical reactions within their bodies in which chemical energy is transformed into light energy. These reactions which mostly involve the substance adenosine triphosphate (ATP) occur either inside or outside the cell. Bioluminescence is the predominant source of light in the deep ocean. Bacteria, jellies, algae, and other organisms, such as fish and squids, are able to produce light by chemicals that they have stored in their bodies. Fireflies, glow worms, some insects, insect larvae, annelids, arachnids and even species of fungi belong to forms of land bioluminescence (Wako 2011).

2.1.2.6 Electrochemiluminescence

ECL or (EL) is the phenomenon in which electrical energy is converted to luminous energy by an electrochemical reaction without thermal energy generation. It involves the production of reactive intermediates from stable precursors at the surface of an electrode. These intermediates then react under a

variety of conditions to form excited states that emit light. It is important to distinguish ECL from chemiluminescence (CL). Both ECL and CL involve the production of light by species that can undergo highly energetic electron-transfer reactions. However, luminescence in CL is initiated by the mixing of reagents and controlled by careful manipulation of fluid flows. In ECL, luminescence is initiated and controlled by switching an electrode voltage. EL finds wide application in the so-called high field electroluminescent thin film materials. These materials are different in principle from standard light emitting diode (LED) and diode lasers where electrons and holes recombine to create light. In these high field EL materials, typically rare earth and transition metal ions are doped in wide band gap materials. This phosphor layer is sandwiched between two insulators to limit the current and driven with an alternating current at high fields (Ligler and Taitt 2011, Wako 2011).

2.1.2.7 Photoluminescence (PL)

It is excitation caused by electromagnetic radiations. In solids, PL takes place when the electronic states are excited by a photon and the excitation energy is absorbed and emitted in the form of light (Kubrin 2014, Xu, Wang et al. 2018). PL consists in the radiation emitted by a crystalline or amorphous solid or by a nanostructure as a consequence of optical excitation; in particular, it derives from the radiative recombination processes of photoexcited electron–hole pairs (e–h pairs). The wide diffusion of this technique in the field of semiconductor nanostructures is motivated by the fact that it allows obtaining general information on the electronic properties and, which is of particular interest, on the quality of the nanostructures. The study of the PL spectra dependence on external parameters, such as sample temperature, energy and intensity of the exciting radiation, and applied fields (electric field, magnetic field, pressure), helps obtaining these information (Sanguinetti, Guzzi et al. 2008).

2.2 Luminescence mechanism

Luminescent materials or phosphors, which are solid inorganic materials consisting of host lattice, usually doped with impurities. The composition of impurities usually is low to enhance the efficiency of the luminescence process. If the composition is too high, the concentration quenching phenomenon will occur and it will decrease the luminescence intensity (Penghui, Xue et al. 2012). Furthermore, most of the phosphor have a white body color. Especially for fluorescent lamps, this condition is used to prevent absorption of visible light by the phosphors used. The absorption of energy, which is used to excite the luminescence, takes place by either the host lattice or by intentionally doped impurities. In most cases, the emission takes place on the impurity ions, which, when they also generate the desired emission, are called activator ions. When the activator ions show too weak an absorption, a second kind of impurities can be added (sensitizers), which absorb the energy and subsequently transfer the energy to the activators. This process involves transport of energy through the luminescent materials. Then, the emission color can be adjusted by choosing the proper impurity ion, without changing the host lattice in which the impurity ions are incorporated (Ronda). This impurities can be classified into several types, such as ns^2 -type ions, transition, metal ions, and rare earth ions (Yen, Shionoya et al. 2007). Table 2.1 shows the ions classification.

Table 2.1 Types of the activators (Yen, Shionoya et al. 2007)

Type	Atomic No	Element	Ion species
ns^2	29	Cu	Cu^-
	30	Zn	Zn^0
	31	Ga	Ga^+
	32	Ge	Ge^{2+}
	33	As	A^{s+}
	47	Ag	Ag^-
	48	Cd	Cd^0
	49	In	In^+

Type	Atomic No	Element	Ion species
ns^2	50	Sn	Sn^{2+}
	51	Sb	Sb^{3+}
	79	Au	Au^{-}
	80	Hg	Hg^{0}
	81	Tl	Tl^{+}
	82	Pb	Pb^{2+}
	83	Bi	Bi^{3+}
Transition metal ions	24	Cr	Cr^{3+}
	25	Mn	Mn^{4+}. Mn^{2+}
	26	Fe	Fe^{3+}
Rare earth ions	21	Sc	Sc^{3+}
	39	Y	Y^{3+}
	57	La	La^{3+}
	58	Ce	Ce^{3+}
	59	Pr	Pr^{3+}
	60	Nd	Nd^{3+}, Nd^{4+}
	61	Pm	Pm^{3+}
	62	Sm	Sm^{2+}, Sm^{3+}
	63	Eu	Eu^{2+}, Eu^{3+}
	64	Gd	Gd^{3+}
	65	Tb	Tb^{3+}
	66	Dy	Dy^{4+}, Dy^{3+}, Dy^{2+}
	67	Ho	Ho^{2+}, Ho^{3+}
	68	Er	Er^{3+}
	68	Tm	Tm^{3+}
	70	Yb	Yb^{2+}, Yb^{3+}
	71	Lu	Lu^{3+}

In the phosphor material, when absorption of UV or even visible light leads to emission, one speaks of optical excitation of luminescence. This process takes place in, e.g., fluorescent lamps and phosphor-converted LEDs, in which phosphors are used to at least partly change the wavelength of the radiation emitted by the LED. Optical absorption can take place on the already discussed impurities (optical centers), being either the activator ions or the sensitizer ions. Sensitizer ions are used when the optical absorption of the activator ions is too weak (e.g., because the optical transition is forbidden) to be useful in practical devices. In such a case, energy transfer from the sensitizer ions to the activator ions has to take place. The optical absorption leading to emission can also take place by the host lattice itself (band absorption). In this case one speaks of host lattice sensitization. Energy transfer from host lattice states to the activator ions (in some cases also involving sensitizers) has to take place. Figure 2.3 shows the mechanism of luminescence.

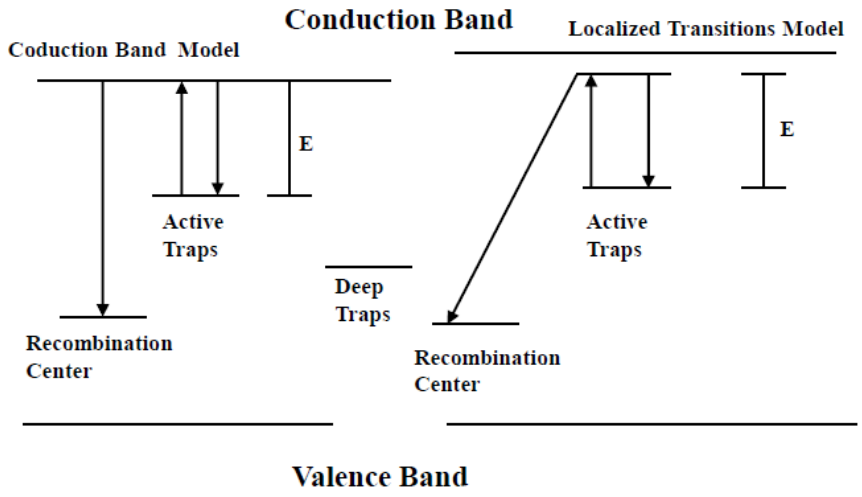

Figure 2.3. Persistent luminescence mechanism (Wako 2011)

These color spectra are described quantitatively by wavelength of light. The most common wavelength unit for describing fluorescence spectra is the nanometer (nm). The colors of the visible spectrum can be broken up into the approximate wavelength values (Guilbault 1967):

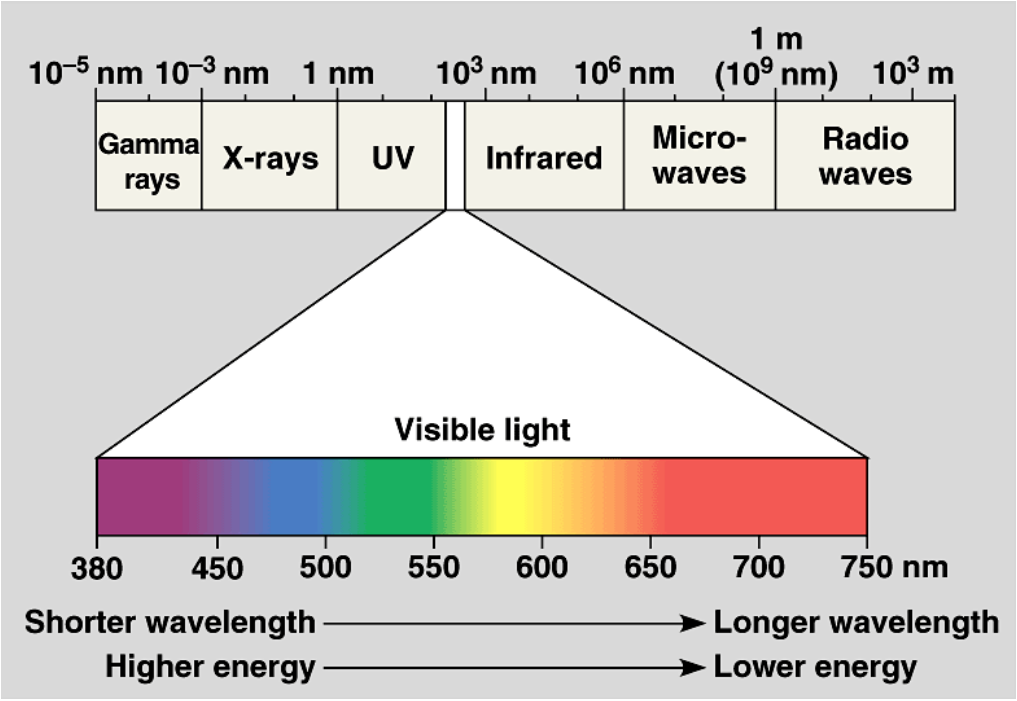

Figure 2.4 Color wavelenght

On the short-wavelength end of the visible spectrum is the near-ultraviolet (near-UV) band from 320 to 400 nm, and on the long-wavelength end is the near-

infrared (near-IR) band from 750 to approximately 2,500 nm. The broad band of light from 320 to 2,500 nm marks the limits of transparency of crown glass and window glass, and this is the band most often used in fluorescence microscopy. Some applications, especially in organic chemistry, utilize excitation light in the mid-ultraviolet band (190–320 nm), but special UV-transparent illumination optics must be used. There are several general characteristics of fluorescence spectra that pertain to fluorescence microscopy and filter design. First, although some substances have very broad spectra of excitation and emission, most fluorochromes have well-defined bands of excitation and emission.

In the luminescence process, there are several factor that affect the absorption and emission light, such as types of the activator, activator composition, annealing temperature, crystal size, specific surface area, particle morphology, atmosphere, and holding time (Sohn, Cho et al. 2000, Peng and Hong 2007, Jin, Yuanyuan et al. 2017, Park, Kim et al. 2017, Zhang, Li et al. 2017, Shih, Chou et al. 2018). Eu^{3+} doped amorphous $Ca_2Al_2SiO_7$ were done to control the particle morphology using the distinct pore agent by Shih(Shih, Chou et al. 2018). Shih defined that morphology can affect the emission intensity. $(Ca,Sr)_2Al_2SiO_7:Eu^{3+}$ were synthesized by Park (Park, Kim et al. 2017). The maximum composition for Eu^{3+} composition for $Ca_2Al_2SiO_7$ and $Sr_2Al_2SiO_7$ are 0.18 and 0.12, respectively. Park defined that increasing the composition can decrease the emission intensity, because it referred to as concentration quenching.

2.3 Luminescent security label application

Counterfeiting is a global problem, especially for companies, governments and customers. Anti-counterfeiting technology is needed to make the genuine item harder to copy and easier to authenticate are therefore important for the protection of brands and valuable documents (Andres, Hersch et al. 2014, Kumar, Singh et al. 2016). Luminescence tags or labels are appreciated security elements for protecting authenticable articles. One way to incorporate luminescent materials as luminescent security elements is to print them with luminescent inks. In addition, luminescent pigments with a short-afterglow are applied to security offset printing ink that is suitable for fluorescent crack detection. The use of pigments is not only

due to their coloristic properties. They also protect the coating from the effects of solar light (UV, VIS and IC light). The ceramic pigments with a particle size on the nano scale have a massive potential market due to their high surface area, which assures higher surface coverage (Venkatachalaiah, Nagabhushana et al. 2017). In paint formulations, the small particle size allows for uniform dispersion by homogeneous mixing with binders, which enhances the mechanical strength of the paint after drying (Yen, Shionoya et al. 2007, Andres, Hersch et al. 2014). An enormous number of host/activator combinations have been studied for luminescence with a fair degree of success. However, the development of new materials will most likely require an improved understanding of the relationship between the host crystal structure and the energy levels of the dopant ions. The properties of these materials arise from complex interactions among the host structure, activators, and defects, which are strongly dependent on the composition (Darshan, Premkumar et al. 2016, Kumar, Singh et al. 2016).

2.4 $CaAl_2O_4$ characteristics

$CaAl_2O_4$ is the spinel oxide that is most promising ceramics for a lot of application. The special structure of this ceramic provides unique properties such as high strength, high toughness and high temperature resistance (Shiri, Abbasi et al. 2014). In the luminescence application, it have excellent properties such as high initial luminescence intensity, long afterglow time, suitable emitting color, and chemical stability when it doped with rare earth metals (Massiot, Trumeau et al. 1995, Shiri, Abbasi et al. 2014, Yuan, Jian et al. 2017, Yang, Xiao et al. 2018, Yang, Xiao et al. 2018). Figure 2.5 shows crystal structure of $CaAl_2O_4$.

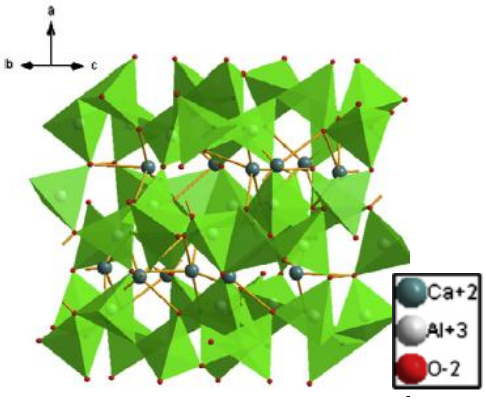

Figure 2.5. $CaAl_2O_4$ structure (Cao, Zhang et al. 2014)

In the previous research, there are several activators that are doped with $CaAl_2O_4$. Table 2.2 shows some research that is used some impurities to emit visible light.

Table 2.2 Several types of activator doped $CaAl_2O_4$ as a hosting material

No	Activator	Method	Temperature (^oC)	Holding time (h)	Atmosphere	λem (nm)	λex (nm)	Colour Emission	Ref.
1	La Tb	Sol-gel	900	2	Air	395, 535	800	Green, blue	(Freeda and Subash 2017)
2	Ce^{3+}, Mn^{2+}	Mixing	1200	5	95% N_2 + 5% H_2	520	448	Green	(Wang, Jia et al. 2003)
3	Eu^{2+}, Dy^{3+}	Laser sintering	600	5	Air	440	335, 280	Blue	(Souza, Silva et al. 2017)
4	Dy	Sol-gel	900	2	Air	390, 520	360	Blue, green	(Freeda and Subash 2017)
5	Tb	Sol-gel	900	2	Air	395, 535	800	Blue, green	(Freeda and Subash 2017)
6	Pr	Sol-gel	900	2	Air	390, 520, 790	360	Blue, green	(Freeda and Subash 2017)
7	Tb^{3+}	Sol-gel	300	-	Air	-	-		(Satapathy, Mishra et al. 2015)
8	Tb^{3+}	Self propagating combution sythesis (SPCS)	850	10	Air	545	275	Green	(Fu, Dong et al. 2010)
9	La, Eu	Solid sintering	1380	3	98.5% N_2 + 1.5% H_2	440	324	Blue	(Lin, Li et al. 2007)
10	Eu	Sol-gel	900	2	Air	390, 520, 790	360	Blue, green	(Freeda and Suresh 2017)
11	Eu^{2+}, Mn^{2+}	Solid state	1400	3	95% N_2 + 5% H_2	440, 550	340, 412	Blue, green	(Xu, Yu et al. 2013)
12	Ce^{3+}, Tb^{3+}	Laser heated pedestal-growth	1300	10	95% N_2 + 5% H_2	400, 543	280	Green	(Jia, Meltzer et al. 2002)

2.5 Activator characteristics

In this study, cerium (Ce) and manganese (Mn) were used as activators in the $CaAl_2O_4$ material. This following section will discused more about Ce and Mn properties.

2.5.1 Cerium

Cerium is a lanthanide ion that associated with rich oxygen vacancies and higher redox ability between Ce^{3+} and Ce^{4+}. In this case, Ce^{4+} is a very strong oxidizing agent ($E^o/Ce^{4+}/Ce^{3+}$)= 1.44V in H_2SO_4 0.5 M medium, and to avoid partial reduction of Ce^{4+} in Ce^{3+}, inert material such as teflon, kapton, or carbon has been used exclusively for all equipment in contact with the Ce^{4+} solutions. Inert gas also can be used to reduce the Ce^{4+} valance to become Ce^{3+} (Briois, Williams et al. 1993, Lin and Chowdhury 2010, Wu, Hu et al. 2011). In addition, the energy gap from the $5d^1$ states to the nearest level ($_2F^{7/2}$) below is so large that the 5d level serves as an efficient light emitting state. However, among the lanthanide ions, the 4f→5d transition energy is the lowest in Ce^{3+}. So, its need the best hosting material for the crystal field splitting of the 5d state and varies from near-ultraviolet to the green region. The other option to increase the transition energy is using sensitizer to enhance energy transfer. Ce is often used for sensitization of Tb^{3+} and combined with the other activator to produce white light (Zhang, Hou et al. 2016, Cui, Chen et al. 2017, Fan, Gou et al. 2017, Meng, Qiu et al. 2017, Park, Koh et al. 2017, Zhang, Hua et al. 2017, Zhang, Li et al. 2017, Zhang, Zhong et al. 2017). Furthermore, the decay time of the Ce^{3+} emission is 10^{-7} to 10^{-8}s, the shortest in observed lanthanide ions. This is due to two reasons: the d→f transition is both parity allowed and spin allowed and $4f^1$ states are spin doublets (Yen, Shionoya et al. 2007).

2.5.2 Manganese

Manganese is transition metal that has several oxidation states. The common oxidation states are +2, +4, and +7. For luminescence application, Mn^{2+} and Mn^{4+} are the common valence for the transition energy in hosting material. It can emmit several color, which depend on the hosting material, such as blue, green, red, and

deep red (Cao, Zhang et al. 2014, Cao, Zhang et al. 2016, Wang, Wang et al. 2016, Cao, Wang et al. 2017, Cao, Ye et al. 2017, Rong, Zhou et al. 2017, Bian and Zhang 2018, Sun, He et al. 2018). Luminescence bands due to Mn^{4+} ($3d^3$) exist at 620 to 700 nm in most host material. The spectrum has a structure consisting of several broad line (Yen, Shionoya et al. 2007). The other hand, luminescence due to Mn^{2+} is known to occur in more than 500 inorganic compounds. The luminescence spectrums consist of a structure less band with a half width of 1000 to 2500 cm^{-1} at peak wavelength of 490 to 750 nm. In phosphors, Mn^{2+} ions are located in the weak crystal field of Dq/B=1, and the luminescence corresponds to the $^4T_1(^4G) \rightarrow {}^6A_1(^6S)$ transition (Yen, Shionoya et al. 2007, Cao, Liu et al. 2016). Lamp phosphors must absorb the mercury ultraviolet (UV) line at 254 nm. In most cases, Mn^{2+} does not have strong absorption bands in this region. To counter the problem, energy transfer mechanisms are utilized to sensitize Mn^{2+}. This transfer mechanism are effected through the host or via several ions, such as Sb^{3+}, Pb^{2+}, Sn^{2+}, Ce^{3+}, and Eu^{2+}, which absorb the UV efficiently through allowed transition. Table 2.3 shows some combination activator between Ce^{3+} and Mn^{2+} in several types of hosting materials. According to the Table 2.3, most of the hosting material would emit two peaks around violet or blue and green or red region, if we combine Ce^{3+} and Mn^{2+}.

Table 2.3 Combination of Ce^{3+} and Mn^{2+} as activator in several type of hosting material

No	Hosting Material	Method	Temperature (^oC)	Holding time (h)	Atmosphere	λem (nm)	λex (nm)	Colour Emission	Ref.
1	$CaAl_2O_4$	Mixing	1200	5	95% N_2 + 5% H_2	520	448	Green	(Wang, Jia et al. 2003)
2	$SrAl_2O_4$	Solid state	1350	4	95% N_2 + 5% H_2	370, 515	273	Blue, green	(Xu, Wang et al. 2011)
3	$RbCaGd(PO_4)_2$	Sol-gel	1100	5	CO	408, 556	334	Blue, green	(Chen, Lv et al. 2016)
4	$Sr_3Y(PO_4)_3$	Solid state	1250	5	95% N_2 + 5% H_2	355, 627	270	violet, red	(Lin, Hu et al. 2016)
5	CaO	Solid state	1300	3	active Carbon	245, 600	243	red	(Liu, Yin et al. 2016)
7	$CaZrSi_2O_7$	High temperature solid state	1250	6	H_2	384, 550	271	green	(Wang, Wang et al. 2016)
8	$Y_7O_6F_9$	Flux assisted solid state	1000	2	96% Ar + 4% H_2	500, 580	260, 312	Green, yellow	(Yang, Kim et al. 2016)
9	$NaAlSiO_4$	High temperature solid state	1200	4	95% N_2 + 5% H_2	430, 590	350	Blue, yellow	(Zhou, Wang et al. 2016)
10	$CaAl_2B_2O_7$	Solid state	1000	8	Vacuum	680	310	Red	(Puchalska and Zych 2017)

2.6 Spray pyrolysis method

Spray pyrolysis method is the solution to produce the phosphor material with low temperature process, rapid, and continuous process(Chen, Tseng et al. 2008, Shih, Wu et al. 2012). Spray pyrolysis offers continuous production process that is advantageous for mass production for commercial product (Shih, Wu et al. 2012). The equipment of spray pyrolysis are mainly divided into 4 parts, it can be seen in Figure 2.6. The equipment are ultrasonic humidifier, horizontal tube furnace with 3 heating zones, electrostatic deposition collector, and pumping system.

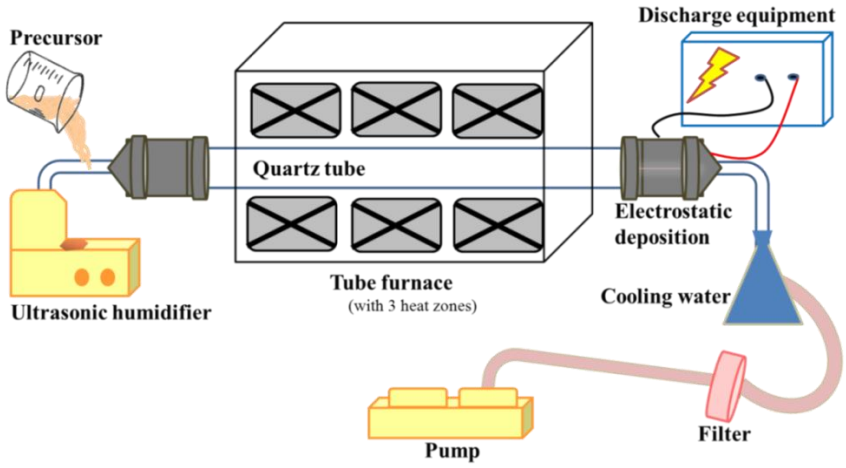

Figure 2.6 Spray Pyrolysis (Kusriantoko 2015)

The raw material for spray pyrolysis solution which is made from desire precursors. The precursors solution will be atomized using ultrasonic humidifier and result in formation of small droplets of precursor solution. The humidifier will also produce air that will carry the small droplets into the heating zone inside tube. There are 3 heating zones inside the reactor, which are evaporation, calcination, and cooling zone. Within, the heating zones, the solution in the form of small droplets undergoes solvent evaporation, solute precipitation, and precursor decomposition. Powder resulted from the spray pyrolysis then collected by using dust collector applied with high voltage. Dust collector is induced by 16kV and able to create electric field that will attract the powder.

There is two particle formation mechanism for spray pyrolysis method. There are gas-to-particle conversion and one-particle-per-drop mechanism (Shih,

Wu et al. 2011, Shih and Huang 2013, Kusriantoko 2015). From Figure 2.7 (a), gas-to-particle conversion process occurs when the droplets are very small (less than 100 nm), then oxide particles are formed directly from the gas phase. The gas-to-particle conversion mechanism will lead to rapid solvent evaporation and then will form solid particle in high temperature or small agglomerated particle in low temperature (Messing, Zhang et al. 1993). According to Figure 2.7 (b), one-particle-per-droplet, occurs when the droplets are in the range 100 nm- 1μm. There are four stages for precursor droplets to form particles in one-particle-per-droplet mechanism. Figure 2.7 (b) shows that each droplet will undergo atomization, solvent evaporation, solute decomposition, and particle calcination. In this mechanism, precursor solubility, solvent evaporation rate and precursors melting temperature play important role in controlling particle morphologies (Shih, Wu et al. 2011).

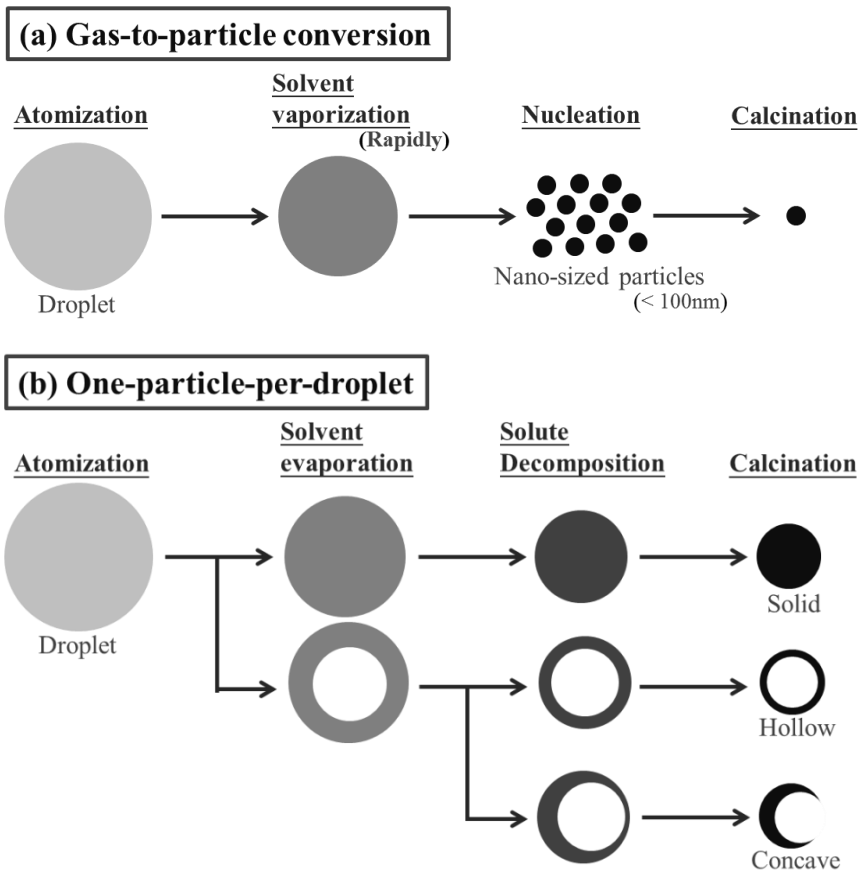

Figure 2.7 Different particle formation mechanism prepared by spray pyrolysis; (a) Gas-to-particle conversion and (b) One-particle-per-droplet mechanism (Shih, Wu et al. 2011)

CHAPTER 3
EXPERIMENTAL METHOD

3.1 Chemicals

Some chemical will be used to synthesize $Ce^{3+}$and Mn^{2+} doped with $CaAl_2O_4$ particles in this study. The details are listed in Table 3.1.

Table 3.1 List of experimental chemical

Precursor name	Chemical formula	Brand	Purity (%)
Calcium Nitrate Tetrahydrate (CaN)	$Ca(NO_3)_2.4H_2O$	SHOWA	98.50
Aluminium Nitrate	$Al(NO_3)_3.9H_2O$	SHOWA	98.00
Cerium Nitrate	$Ce(NO_3)_3.6H_2O$	AENCORE	98.00
Manganese Nitrate hydrate	$Mn(NO_3)_2 \cdot xH_2O$	ALDRICH	≥99.00
De-Ionized Water	H_2O	-	-

3.2 Experimental procedure

Some experimental equipment will use in this study. The details of equipment are listed in Table 3.2.

Table 3.2 List of experimental equipment

Equipment name	Brand	Model	Country
Ultrasonic Humidifier	K-Sonic	KT-100A	Taiwan
Horizontal furnace with tube	Dengyng	D110	Taiwan
Horizontal Furnace	-	-	-
Drying Machine	-	-	-
XRD	Bruker	D2 Phaser	Germany
SEM-EDX	ThermoFisher	FEI-QUANTA	USA
Spectrofluorometer		F-8500-PL	-
BET	Quantachrome	Nova touch surface area and pore size analyser	-

3.3 Material preparation

In this following section, the experiment was divided into four section. First, adjusting temperature was used to know the maximum temperature for the amorphous phase and high intensity for the photoluminescence properties. Second, adjusting atmosphere was used to know the best atmosphere for increasing photoluminescence properties. Then, variation composition of Ce and Mn were used to know the maximum composition for amorphous phase and photoluminescence properties.

3.3.1 Adjusting annealing temperature

Experimental flowchart for this research was divided into three step. First, adjusting temperature was needed to know the right temperature for the amorphous phase. It is showed in the Figure 3.1.

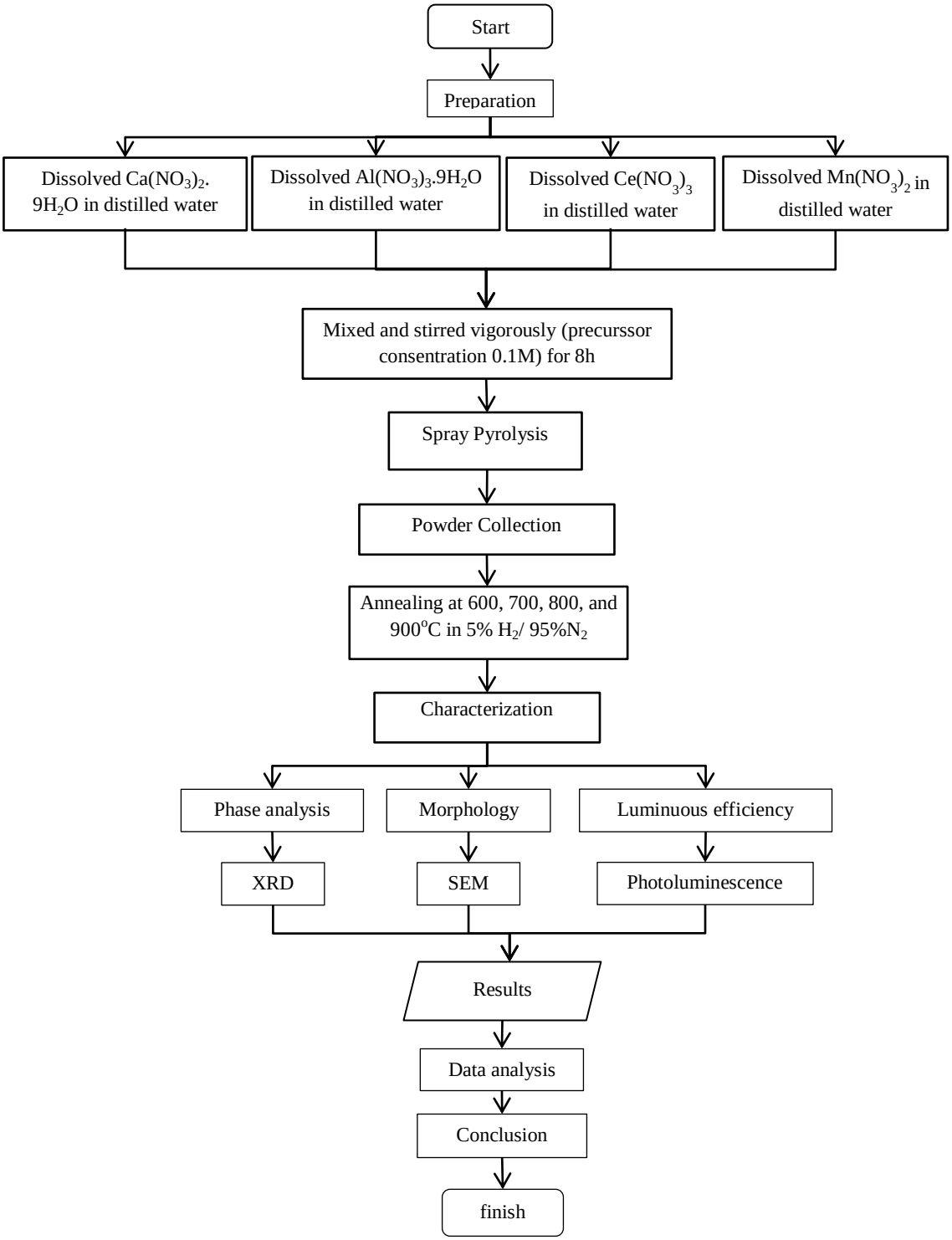

Figure 3.1 Experimental flowchart of adjusting annealing temperature

$CaAl_2O_4$ material were synthesized using cerium and manganese as activator with spray pyrolysis method. In this research, cerium and manganese composition were 0.5 mol % and 1 mol %, respectively. $Ce^{3+}$and Mn^{2+} -doped $CaAl_2O_4$ were synthesized using 23.261 gr of calcium nitrate tetrahydrate (CaN) (($Ca(NO_3)_2 \cdot 4H_2O$, 99%, Showa, Japan), 75.026 gr aluminium nitrate enneahydrate (AlN) ($Al(NO_3)_3 \cdot 9H_2O$,99%, Showa, Japan), 0.217 gr cerium nitrate ($Ce(NO_3)_3.6H_2O$, 98%, Aencore, US), and 0.178 gr manganese nitrate hydrate ($Mn(NO_3)_2$, 99%, Aldrich, US) as the source of Ca, Al, Ce, and Mn, respectively. Four precursor solutions of Ca, Al, Ce, and Mn were prepared by dissolution of the respective reagents in diluted 1000 mL deionized water. The molar concentration of the precursor was 0.1M. The precursors were stirred for 8 h in room temperature with magnetic stirrer. These solutions were poured into the tank of an ultrasonic atomizer system (KT-100A, King Ultrasonic, Taiwan) that was operated at an ultrasonic frequency of 1.7MHz. Droplets generated by the ultra sound process were injected into an electric furnace with a quartz tube and three heating zones (D-80, Dengyng Co.,Taiwan). In the first zone, the temperature was set to 250 °C to evaporate the solvent. In the second zone, which was pre-heated to 1000 °C, calcinated. In the last zone, which was pre-sett 350 °C, the product was cooled down. These spray pyrolysis temperatures also according to the previous study that has been done before(Shih, Lin et al. 2016). The calcination zone is where the calcination process take place (Shih, Wu et al. 2012). At the end of the quartz tube, the powder product was collected in a stainless steel cylinder that was electrically charged at 14kV. The schematic route for spray pyrolysis is explained in chapter 2.

After powder collection in spray pyrolysis process, it would continue with annealing process. In this step, $95\%N_2/5\%H_2$ gasses was used for reduction atmosphere. This gasses would reduce Ce^{4+} valence which formed into Ce^{3+} and Mn^{4+} to Mn^{2+}. The temperature which were used for adjusting amorphous phase, were 600, 700, 800, and 900^oC. From the phase diagram in Figure 3.2, the $CaAl_2O_4$ would be formed above temperature at 400^oC.

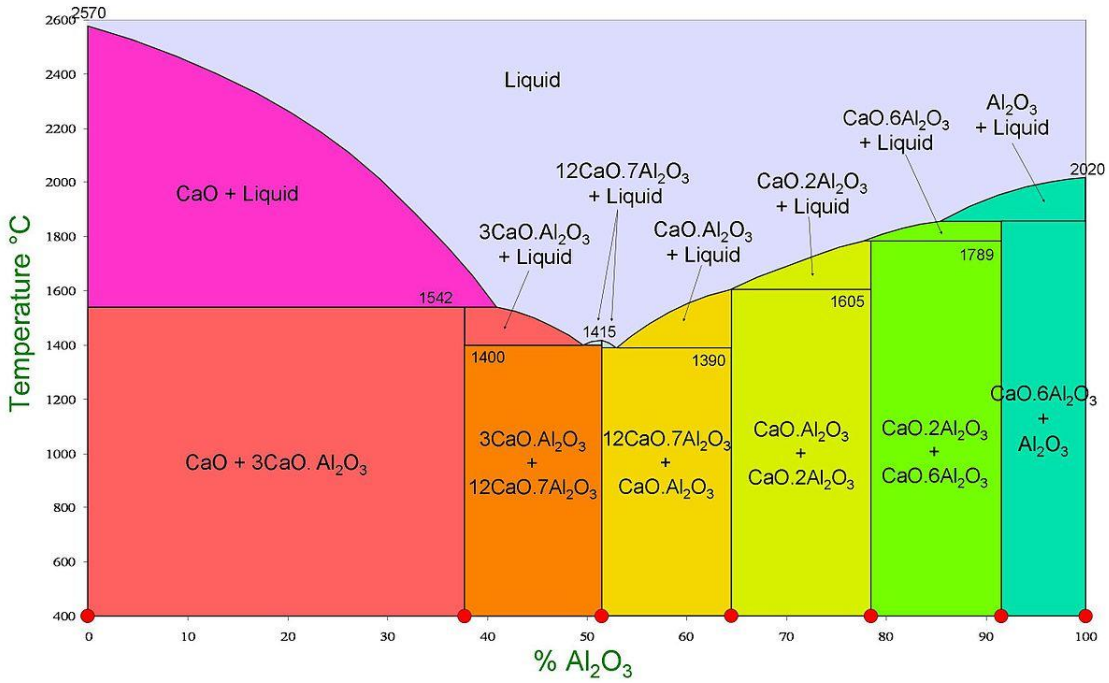

Figure 3.2 Phase Diagram of calcium aluminate

3.3.2 Adjusting atmospheric gases condition

Variation of the atmosphere was used to obtain the maximum atmosphere that can be used to enhance reduction process. It is showed in Figure 3.3.

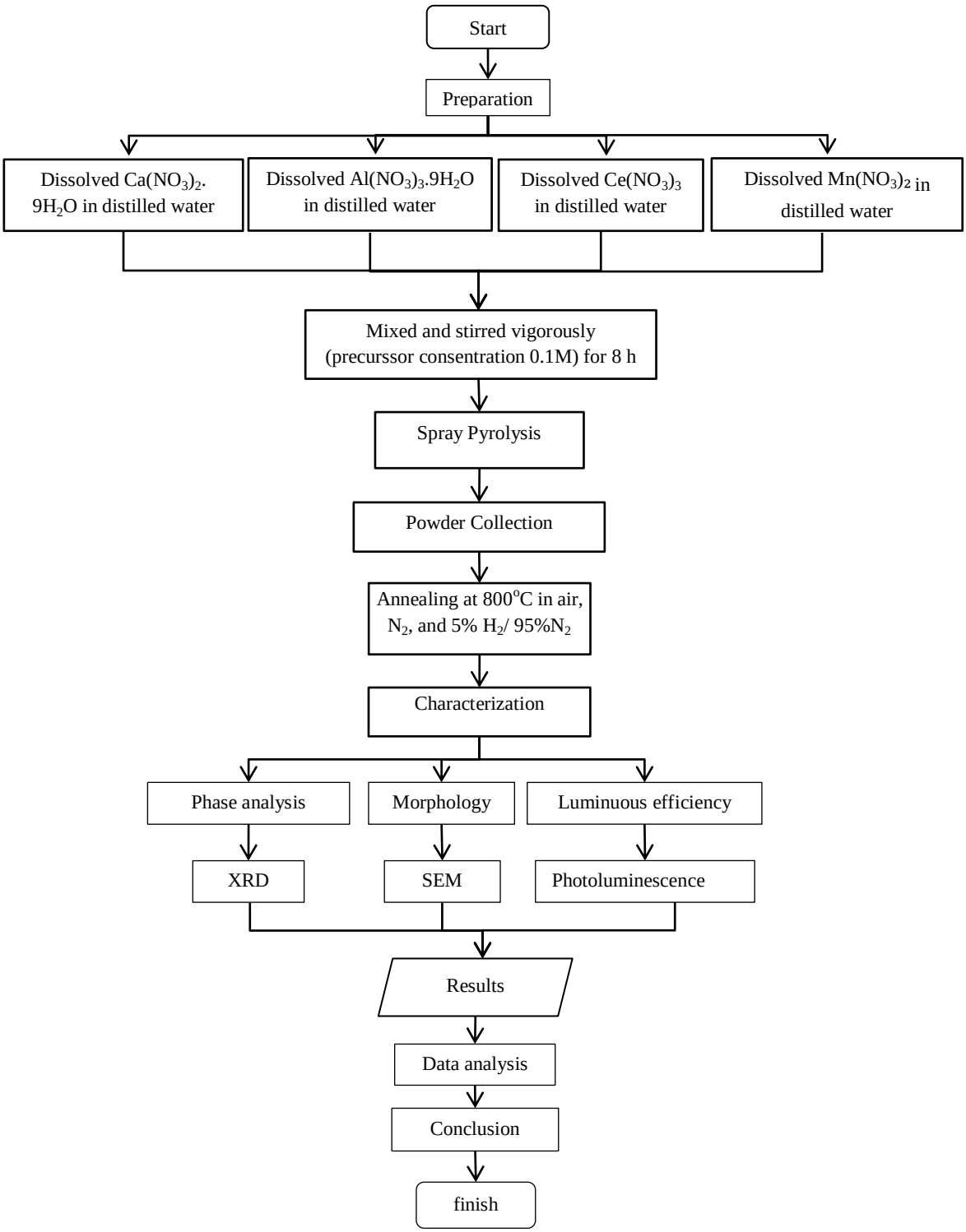

Figure 3.3 Experimental flowchart adjusting atmospheric gases condition

$CaAl_2O_4$ material was synthesized using cerium and manganese as activator with spray pyrolysis method. In this research, cerium and manganese composition were 0.5 mol% and 1 mol% respectively. Ce^{3+} and Mn^{2+} in $CaAl_2O_4$

were synthesized using 23.060 gr of calcium nitrate tetrahydrate (CaN) ($(Ca(NO_3)_2 \cdot 4H_2O$, 99%, Showa, Japan), 75.026 gr of aluminium nitrate enneahydrate (AlN) ($Al(NO_3)_3 \cdot 9H_2O$,99%, Showa, Japan), 0.217 gr of cerium nitrate ($Ce(NO_3)_3.6H_2O$, 98%, Aencore, US), and 0.178 gr of manganese nitrate hydrate ($Mn(NO_3)_2$, 99%, Aldrich, US) as the source of Ca, Al, Ce, and Mn, respectively. Four precursor solutions of Ca, Al, Ce, and Mn were prepared by dissolution in 1000 mL diluted deionized water. The molar concentration of the precursor was 0.1 M. The precursors were stirred for 8 h in room temperature with magnetic stirrer. These solutions were poured into the tank of an ultrasonic atomizer system (KT-100A, King Ultrasonic, Taiwan) that was operated at an ultrasonic frequency of 1.7MHz. Droplets generated by the ultra sound process were injected into an electric furnace with a quartz tube and three heating zones (D-80, Dengyng Co.,Taiwan). In the first zone, the temperature was set to 250 °C to evaporate the solvent. In the second zone, which was pre-heated to 1000 °C, calcinated. In the last zone, which was pre-sett 350 °C, the product was cooled down. These spray pyrolysis temperatures also according to the previous study that has been done before [1] . The calcination zone is where the calcination process take place [64]. At the end of the quartz tube, the powder product was collected in a stainless steel cylinder that was electrically charged at 14kV. The schematic route for spray pyrolysis is explained in chapter 2. Furthermore, after collecting process, powders were annealed at 800^oC using differences atmosphere condition, such as air, Nitrogen (N_2), and $5\%H_2$/ $95\%N_2$ for 1h.

3.3.3 Variation of cerium and manganese composition

Variation of the activators were used to obtain maximum composition that can be used to enhance photoluminescence material. It is showed in Figure 3.4.

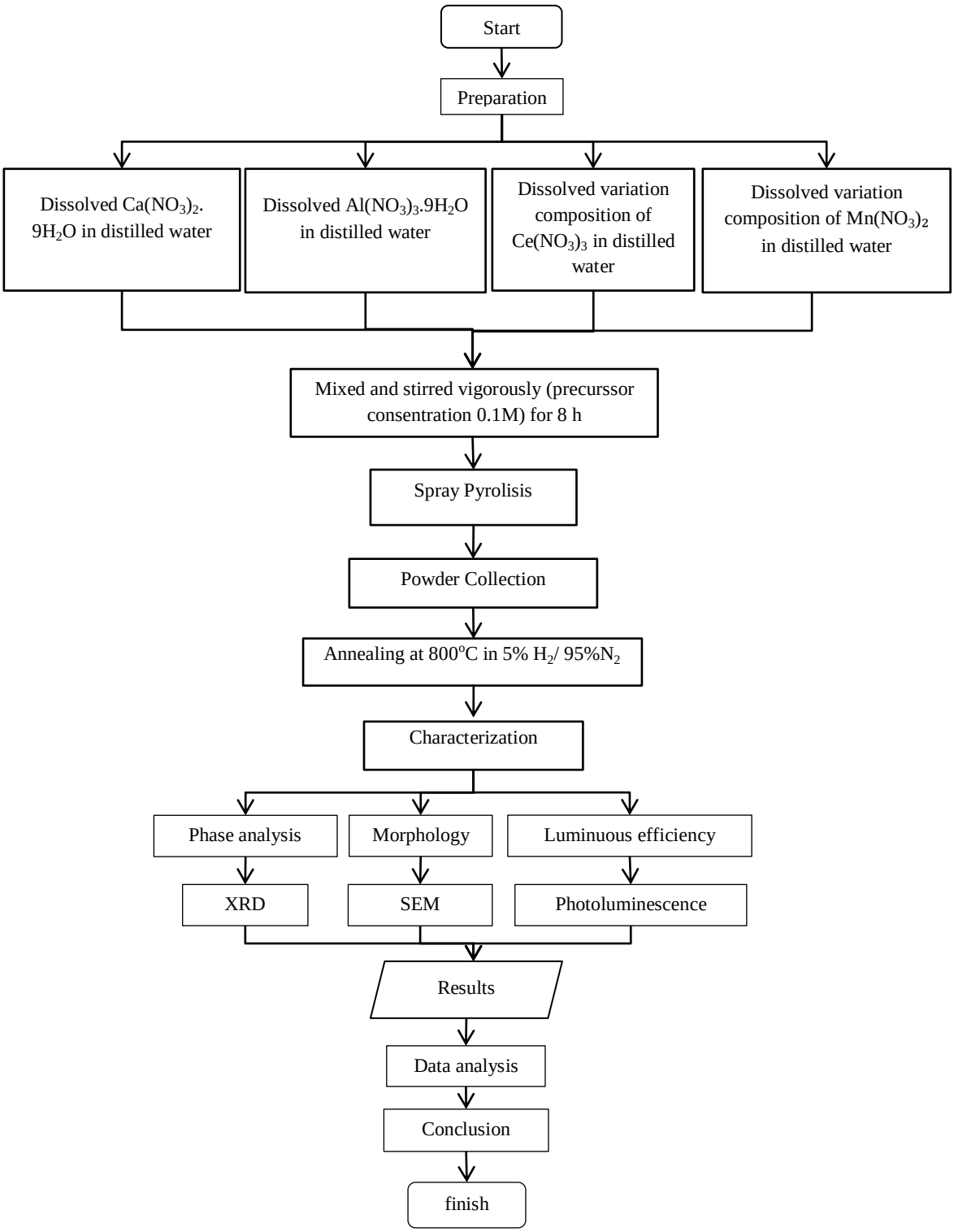

Figure 3.4 Experimental flowchart variation of Ce and Mn composition

Table 3.3. Variation composition of Ce, Mn –doped $CaAl_2O_4$

Sample name	Variation composition of cerium (% mol)	Variation composition of Manganese (%mol)
Sample 1	0	1
Sample 2	0.5	1
Sample 3	1	1
Sample 4	0.5	0
Sample 5	0.5	3
Sample 6	0.5	5

$CaAl_2O_4$ material were synthesized using cerium and manganese as activator with spray pyrolysis method. In this research, cerium and manganese composition, which was used, is showed in Table 3.1. Ce^{3+}, Mn^{2+}-doped $CaAl_2O_4$ were synthesized using calcium nitrate tetrahydrate (CaN) (($Ca(NO_3)_2 \cdot 4H_2O$, 99%, Showa, Japan), aluminium nitrate enneahydrate (AlN) ($Al(NO_3)_3 \cdot 9H_2O$,99%, Showa, Japan), cerium nitrate ($Ce(NO_3)_3.6H_2O$, 98%, Aencore, US), manganese nitrate hydrate ($Mn(NO_3)_2$, 99%, Aldrich, US) as the source of Ca, Al, Ce, and Mn, respectively. Four precursor solutions of Ca, Al, Ce, and Mn were prepared by dissolution of the respective reagents in diluted deionized water. The molar concentration of the used reagent was 0.1 M. The precursors were stirred for 8 h in room temperature with magnetic stirrer. These solutions were poured into the tank of an ultrasonic atomizer system (KT-100A, King Ultrasonic, Taiwan) that was operated at an ultrasonic frequency of 1.7MHz. Droplets generated by the ultra sound process were injected into an electric furnace with a quartz tube and three heating zones (D-80,DengyngCo.,Taiwan). In the first zone, the temperature was set to 250 °C to evaporate the solvent. In the second zone, this was pre-heated to1000 °C, calcinated. In the last zone, which was pre-sett 350 °C, the product was cooled down. These spray pyrolysis temperatures also according to the previous study that has been done before [2]. The calcination zone is where the calcination process takes place [1]. At the end of the quartz tube, the powder product was collected in a stainless steel cylinder that was electrically charged at 14kV. The schematic route for spray pyrolysis is explained in chapter 2. Furthermore, after collecting process, powders were annealed at 800^oC using $95\%N_2$:$5\%H_2$ atmosphere for 1h.

3.4 Materials characterization

Some material characterization techniques have been used in order to know the properties of Ce^{3+}, Mn^{2+} doped- $CaAl_2O_4$. The explanation of each characterization technique is described below.

3.4.1 X-ray diffraction

X-ray diffraction analysis is the most powerful technique to know the phase of certain material. In this research, XRD (D2 Phaser, Bruker, Germany) was used to investigate the glass crystallization behaviour. The operation condition of XRD was 30kV with operating current of 10 mA, the scan range of 20° - 80° (following the Bragg's law) and increment 0.05. Furthermore, data from XRD was analysed using Eva Diffraction software to identify each peak that appeared in the samples. The phase composition of Ce^{3+}, Mn^{2+} doped- $CaAl_2O_4$ powder was identified using an X-ray diffractometer (D2Phaser, Bruker,Germany) with Cu Kα radiation.

3.4.2 Scanning electron microscope

Field emission scanning electron microscope FEI QUANTA 3D, ThermoFisher, USA) was used to investigate the surface morphology and particle size of the Ce^{3+}, Mn^{2+} doped- $CaAl_2O_4$. The images were taken with top view orientation of Ce^{3+}, Mn^{2+} doped- $CaAl_2O_4$ samples. The operating condition for SEM was 15kV with operating current was 2mA. From SEM images, particle size can be calculated using more than 300 particles. The particle size distribution can be obtained by this method.

3.4.3 Spectrofluorometer

The photoluminescence spectra were measured using the spectrofluorometer (FP-8500,Jasco,Japan) equipped with a 150W Xenon lamp source. Fluorescence spectrophotometers are utilized to detect intensity of Ce^{3+}, Mn^{2+} -doped $CaAl_2O_4$. These are fluorescent molecules that, when exposed to light in a fluorescence spectrophotometer, absorb photons at a characteristic wavelength. Subsequently, they then emit photons at a different and slightly longer characteristic wavelength. The excitation and emission wavelength, which

was used, were 273 and 546 nm. The powder samples were compacted and excited under 45° incidence. The emitted luminescence was detected by a detector positioned perpendicular to the excitation beam with excitation and emission slits of 2.5 and 2.5 nm, successively.

(*This page intentionally left blank*)

CHAPTER 4
RESULTS

4.1 Adjusting temperature

This following section will discuss about several characterization that have been done in order to know the condition of Ce^{3+} and Mn^{2+} –doped $CaAl_2O_4$ powder after spray pyrolysis process and after annealed in several temperature. This information will greatly help to conduct the further experiments. The several characterization techniques that been used is including compositional analysis by XRD, morphological analysis using SEM, and also for the photoluminescence analysis using Spectrofluorometer.

4.1.1 Phases analysis

The XRD patterns of 0.5 mol%Ce^{3+} and 1 mol%Mn^{2+} –doped $CaAl_2O_4$ after spray pyrolysis is showed in black line in Figure 4.1. Before annealing, 0.5mol%Ce^{3+} and 1 mol%Mn^{2+} –doped $CaAl_2O_4$ is in amorphous phase. However, heat treatment using 95%N_2 :5%H_2 atmosphere should be applied in this experiment in order to reduce Ce^{4+} valence which formed into Ce^{3+} and Mn^{4+} to Mn^{2+}. Some observation about the phase transformation of 0.5 mol%Ce^{3+} and 1 mol%Mn^{2+} –doped $CaAl_2O_4$ at several temperature have been conducted. The 0.5 mol%Ce^{3+} and 1 mol%Mn^{2+} –doped $CaAl_2O_4$ powder was annealed at 600, 700, 800, and 900^{o}C for 1 h holding time with 5^{o}C/min heating rate. Figure 4.1 shows the XRD patterns of 0.5 mol%Ce^{3+} and 1 mol%Mn^{2+} –doped $CaAl_2O_4$ with several annealing temperatures. From these XRD patterns it can be seen that 0.5 mol%Ce^{3+} and 1 mol%Mn^{2+} –doped $CaAl_2O_4$ had amorphous phase until 800^{o}C. It starts to crystalize at 900^{o}C, however only small amount of peak appears in the sample. According to $CaAl_2O_4$ phase (PDF 53-0191), some peak indexed at 30.073^o [123], 35.742^o [303], 37.456^o [313], 47.261^o [226], 60.352^o [129], and 63.868^o [309]. In this observation, it can be concluded that the maximum temperature for amorphous phase of 0.5 mol%Ce^{3+} and 1 mol%Mn^{2+} –doped $CaAl_2O_4$ is 800^{o}C. This result will compare to the photoluminescence data to get the highest intensity.

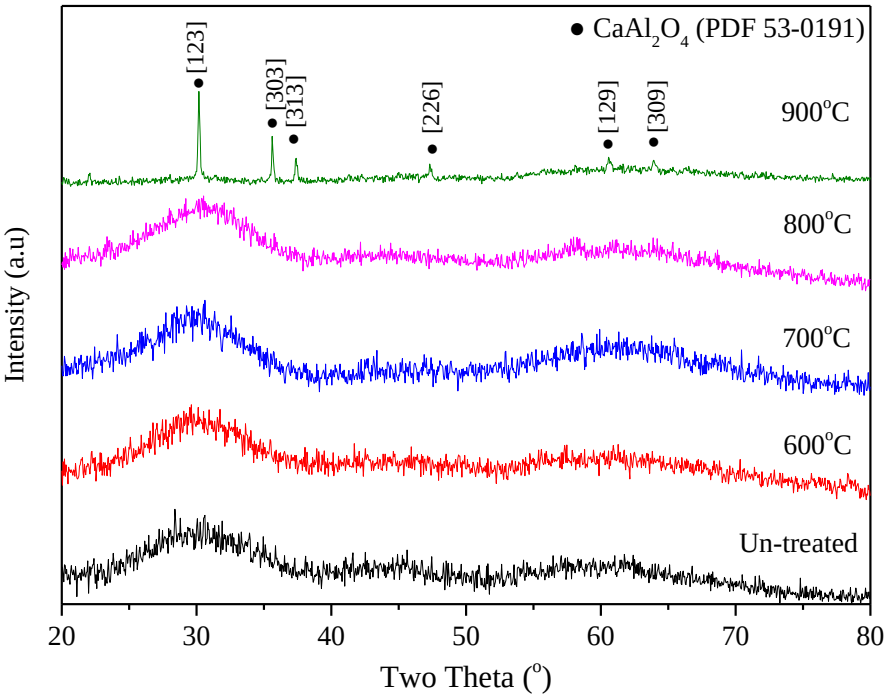

Figure 4.1. XRD patterns of 0.5 mol% Ce^{3+}, 1 mol% Mn^{2+}- doped $CaAl_2O_4$ un-treated and annealed at 600, 700, 800, and 900°C in 95%N_2 :5%H_2 with the heating rate of 5°C/min and the holding time of 1 h

4.1.2 Morphology analysis

The SEM images of 0.5 mol%Ce^{3+} and 1 mol%Mn^{2+} –doped $CaAl_2O_4$ powder are shown in Figure 4.2. It can be seen that the spherical morphology of 0.5 mol%Ce^{3+} and 1 mol%Mn^{2+} –doped $CaAl_2O_4$ were produced by spray pyrolysis. After particles annealed at 600, 700, 800, and 900°C for 1 h, it still had spherical morphology. It means there is no different morphology between before and after annealed at several temperatures.

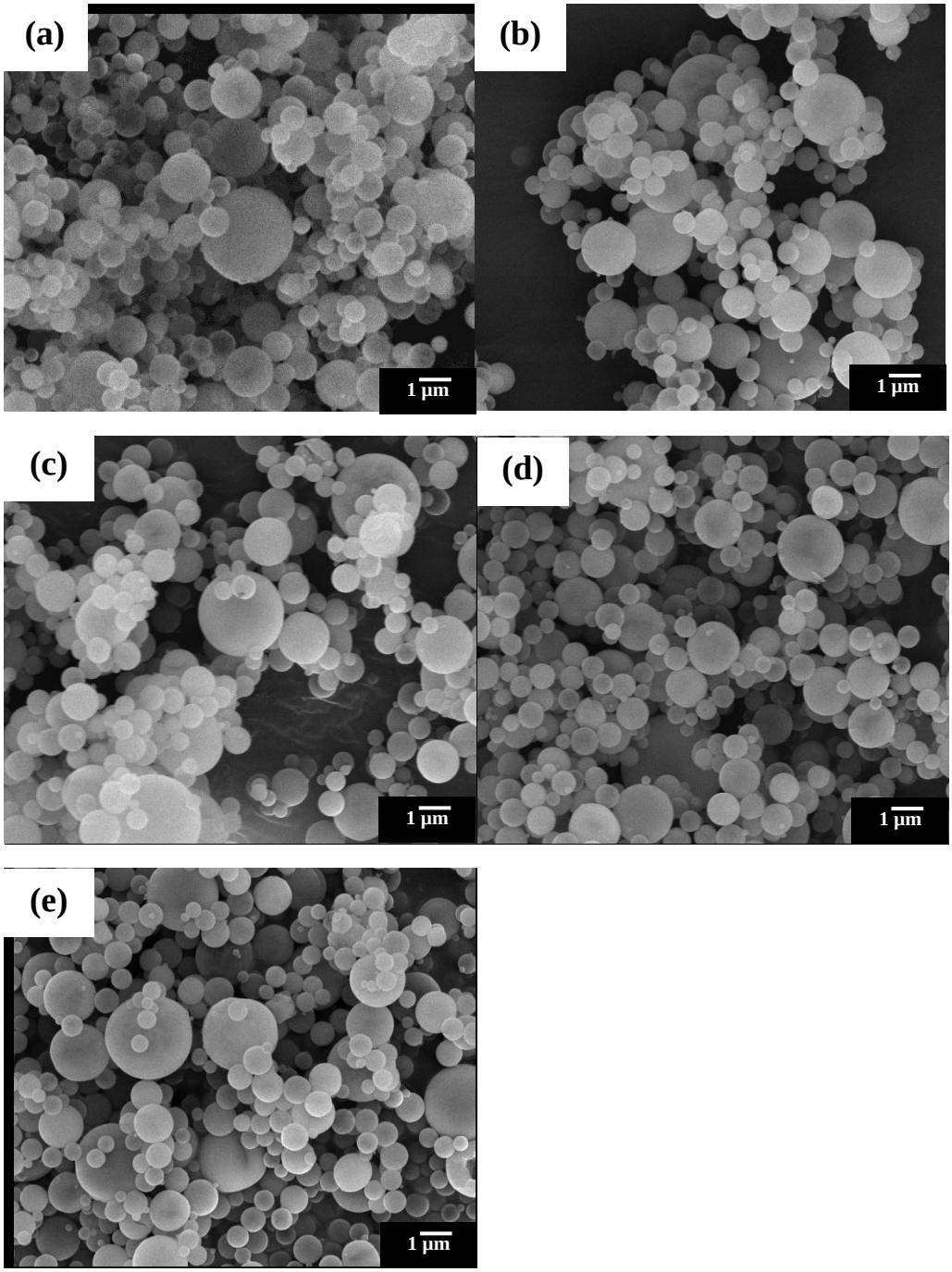

Figure 4.2 SEM images of 0.5 mol% Ce^{3+} and 1 mol% Mn^{2+}- doped $CaAl_2O_4$ (a) un-treated and annealed at (b) 600, (c) 700, (d) 800, and (e) 900^oC in 95%N_2 :5%H_2 atmosphere condition with the heating rate of 5^oC/min and the holding time of 1 h

The particle size distribution before and after annealed is shown in Figure 4.3. It can be clearly seen that there is almost no different in particle size. The particle size in spray pyrolysis is related to the droplet size and the type of droplet-to-particle mechanism. As already mentioned in chapter 2, that spray

pyrolysis would have two droplet-to-particle mechanisms, which are gas-to-particle conversion and one droplet-one-particle (Shih, Wu et al. 2012). The particle size of 0.5 mol%Ce^{3+} and 1 mol%Mn^{2+} –doped $CaAl_2O_4$ for un-treated, annealed at 600, 700, 800, and 900^oC are 977 ± 377, 801 ± 373, 836 ± 402, 852 ± 322, and 792 ± 453 nm, respectively.

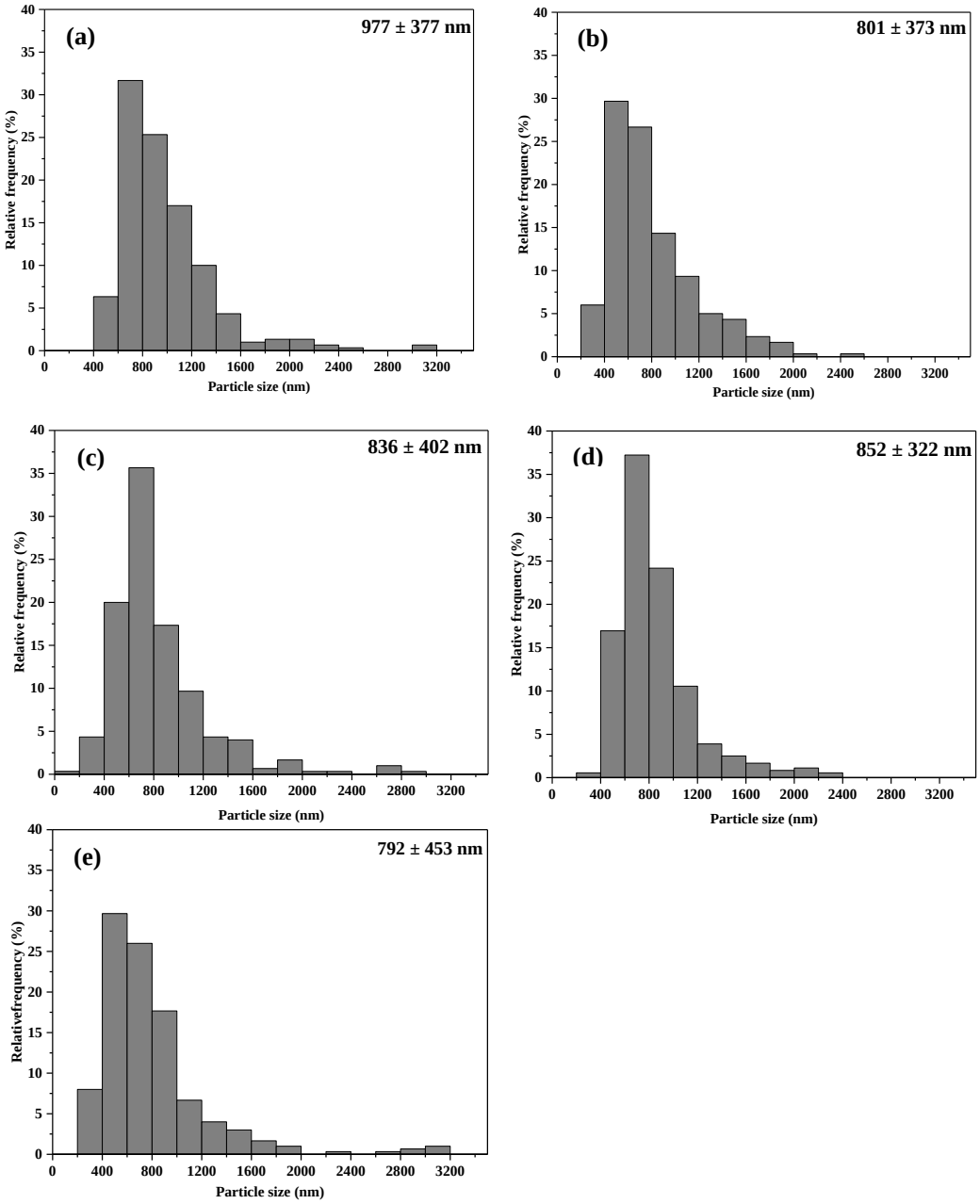

Figure 4.3 Particle size distribution of 0.5 mol% Ce^{3+} and 1 mol% Mn^{2+}- doped $CaAl_2O_4$ (a) un-treated, annealed at (b) 600, (c) 700, (d) 800, and (e) 900^oC in 95%N_2 : 5%H_2 with 5^oC/min of heating rate and 1 h holding time

4.1.3 Photoluminescence analysis

According to the Figure 4.4, in the emission spectra of 0.5 mol% Ce^{3+} and 1 mol% Mn^{2+}- doped $CaAl_2O_4$ un-treated shows the small peak in the wavelength around 450-475nm. It had a same result for the specimen that annealed at 600^{o}C. For the specimens that annealed at 700, 800, and 900^{o}C, it shows one broad peak in the ~408 nm. The highest intensity is for the crystalline phase, which is using 900^{o}C for annealing temperature. For the amorphous phase, the specimen that is using 800^{o}C for the annealing temperature has the highest intensity than the other amorphous phase.

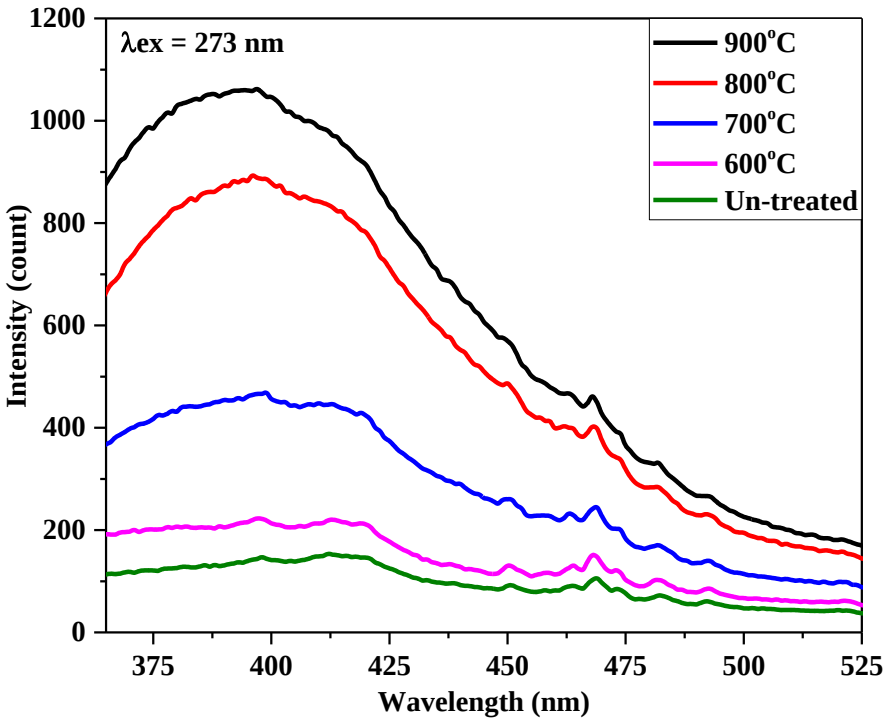

Figure 4.4 Emission spectra of 0.5 mol% $Ce^{3+}$and 1 mol% Mn^{2+}- doped $CaAl_2O_4$ un-treated and annealed at several temperature in 95%N_2 : 5%H_2 with the heating rate of 5^{o}C/min and the holding time of 1h

Figure 4.5 shows the excitation spectra, which means the ability of material to absorb energy in several wavelengths. It can be obtained that the specimen before and after annealed at several temperatures can strongly absorb energy at 273 nm. For the specimen that is annealed at 700, 800, and 900^{o}C, it show the

other broad band peak in the ~360nm. In addition, there is peak shift for the specimen that annealed at 900^{o}C with crystalline phase to the left side.

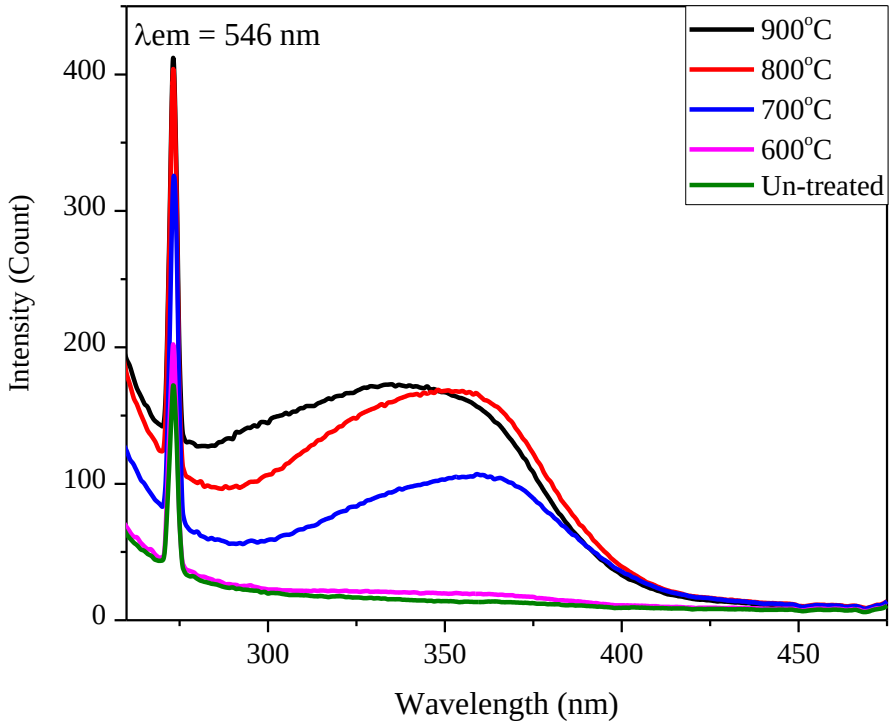

Figure 4.5 Excitation spectra of 0.5 mol% Ce^{3+} and 1 mol% Mn^{2+}- doped $CaAl_2O_4$ un-treated and annealed at several temperature in 95%N_2 : 5%H_2 with the heating rate of 5^{o}C/min and the holding time of 1h

4.2 Adjusting atmospheric gases

This following section will discuss about several characterization that have been done in order to know the condition of $Ce^{3+}$and Mn^{2+} –doped $CaAl_2O_4$ powder after spray pyrolysis process and after annealed in different atmosphere. This information will greatly help to conduct the further experiments. The several characterization techniques that had been used is including compositional analysis by XRD, morphological analysis using SEM, and also for the photoluminescence analysis using Spectrofluorometer.

4.2.1 Phases analysis

Figure 4.6 shows the XRD pattern of 0.5 mol%Ce^{3+} and 1 mol%Mn^{2+} – doped $CaAl_2O_4$ for un-treated and annealed at 800^oC in different atmosphere condition. It can be observed that un-treated and annealed specimens using different atmosphere had amorphous phase. This result will compare to the photoluminescence data to get the highest intensity.

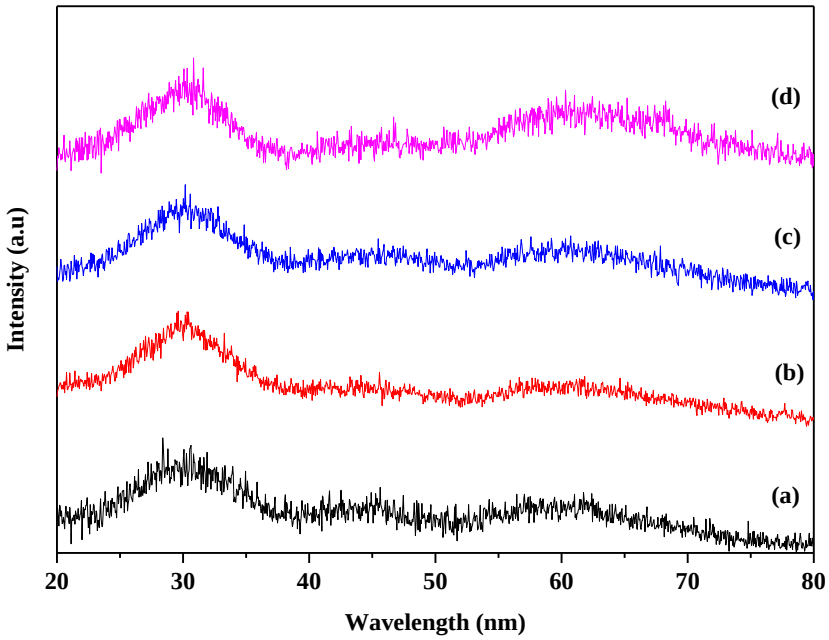

Figure 4.6 XRD patterns of 0.5 mol% $Ce^{3+}$and 1 mol% Mn^{2+}- doped $CaAl_2O_4$ un-treated and annealed at 800^oC in (b) air, (c) N_2, and (d) 95%N_2 : 5%H_2 with the heating rate of 5^oC/min and the holding time of 1h

4.2.2 Morphology analysis

The SEM image of 0.5 mol%Ce^{3+} and 1 mol%Mn^{2+} –doped $CaAl_2O_4$ powder are shown in Figure 4.7. It can be seen that the spherical morphology of 0.5 mol% Ce^{3+} and 1 mol% Mn^{2+} –doped $CaAl_2O_4$ were produced by spray pyrolysis. After particles annealed at 800^{o}C for 1 h in the different atmosphere, it still had spherical morphology same as un-treated specimen.

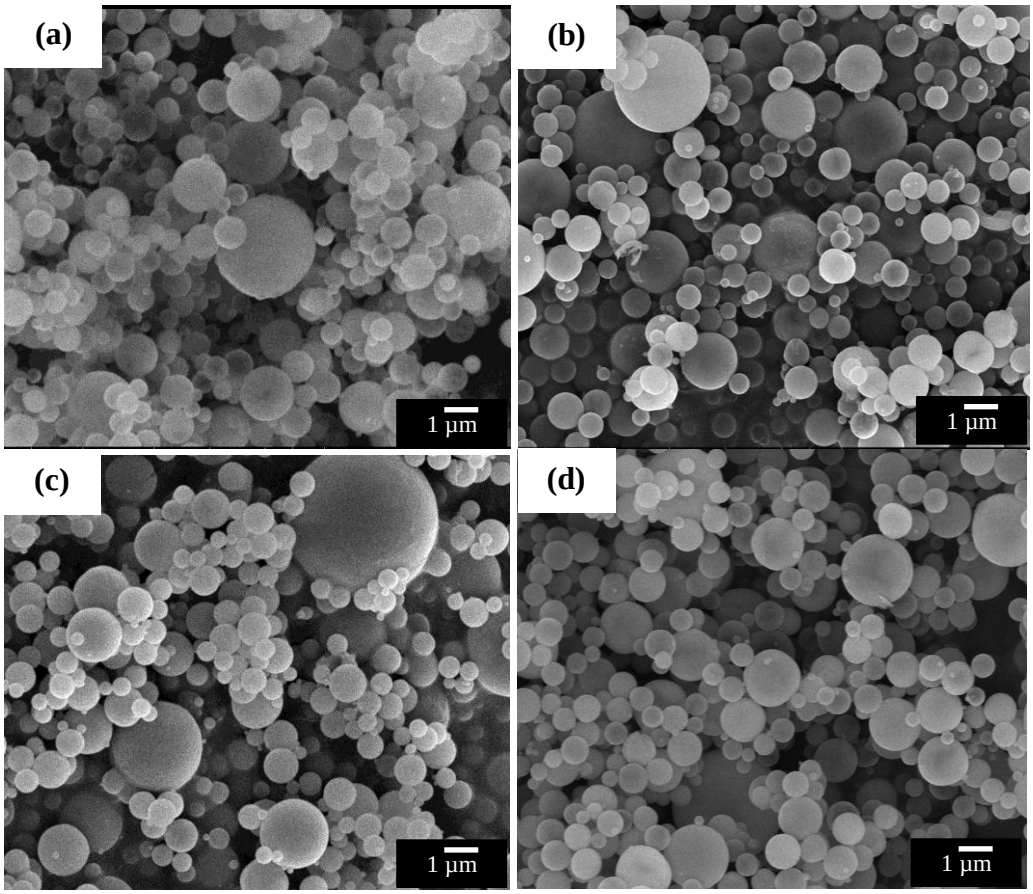

Figure 4.7 SEM images of 0.5 mol% $Ce^{3+}$and 1 mol% Mn^{2+}- doped $CaAl_2O_4$ (a) un-treated, and annealed at 800^{o}C in (b) air, (c) N_2, and (d) 95%N_2 :5%H_2 with the heating rate of 5^{o}C/min and the holding time of 1h

The particle size distribution un-treated and annealed is shown in Figure 4.8. It can be clearly seen that there is almost no different in particle size. The particle size in spray pyrolysis is related to the droplet size and the type of droplet-to-particle mechanism, as already mentioned in chapter 2 [64]. The particle size of 0.5 mol%Ce^{3+} and 1 mol%Mn^{2+} –doped $CaAl_2O_4$ for un-treated, annealed at 800^{o}C in air, N_2, and 95%N_2 :5%H_2 are 977 ± 377, 757 ± 355, 913 ± 352, and 852 ± 322 nm, respectively.

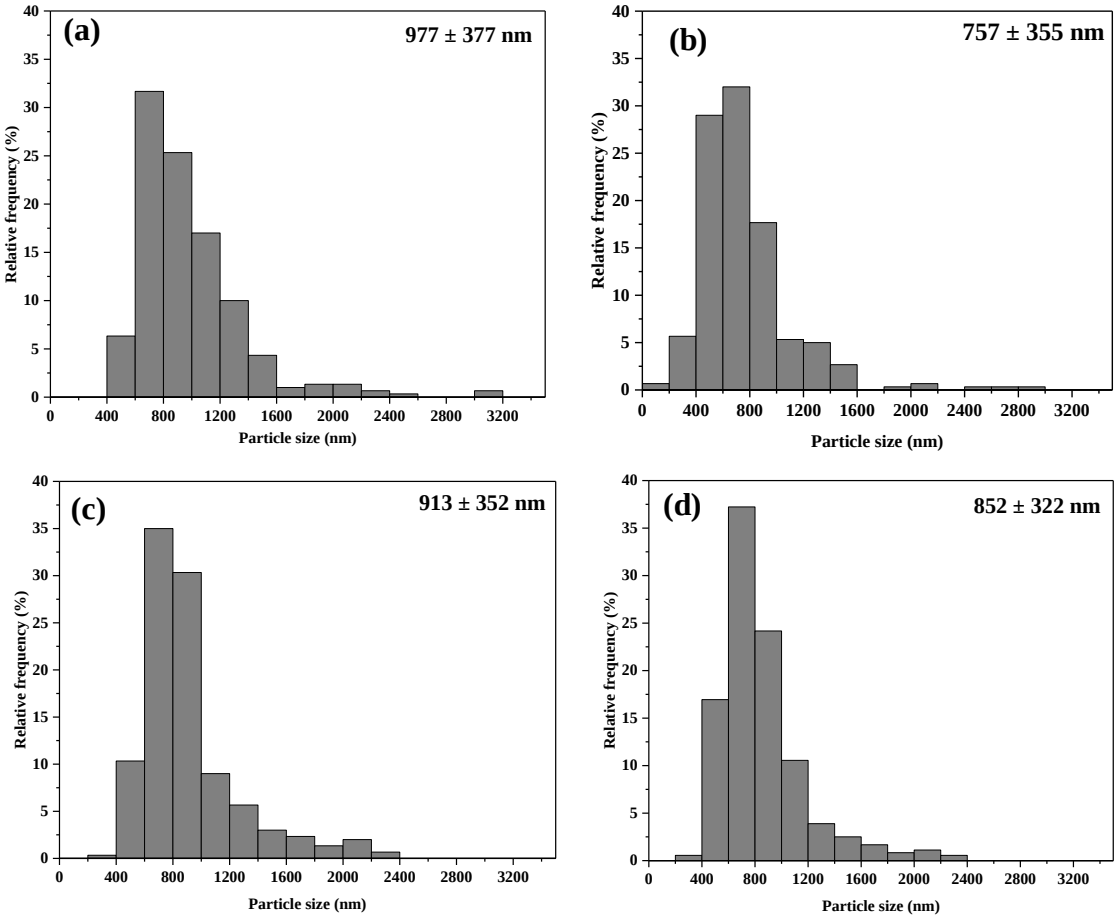

Figure 4.8 Particle size distribution of 0.5 mol% Ce^{3+}, 1 mol% Mn^{2+}- doped $CaAl_2O_4$ (a) un-treated, and annealed at 800^{o}C in (b) air, (c) N_2, and (d) 95%N_2 :5%H_2 with the heating rate of 5^{o}C/min and the holding time of 1h

4.2.3 Photoluminescence analysis

Figure 4.8 shows the low emission spectra for un-treated and annealed at 800^{o}C in air and N_2. In contrast to 95%N_2:5%H_2, it had one broad of peak and also small peak around wavelength 450-475 nm. The first one is the broad peak that had intensity more than 800 in the ~408nm and the other is the small peak around 450-475 nm..

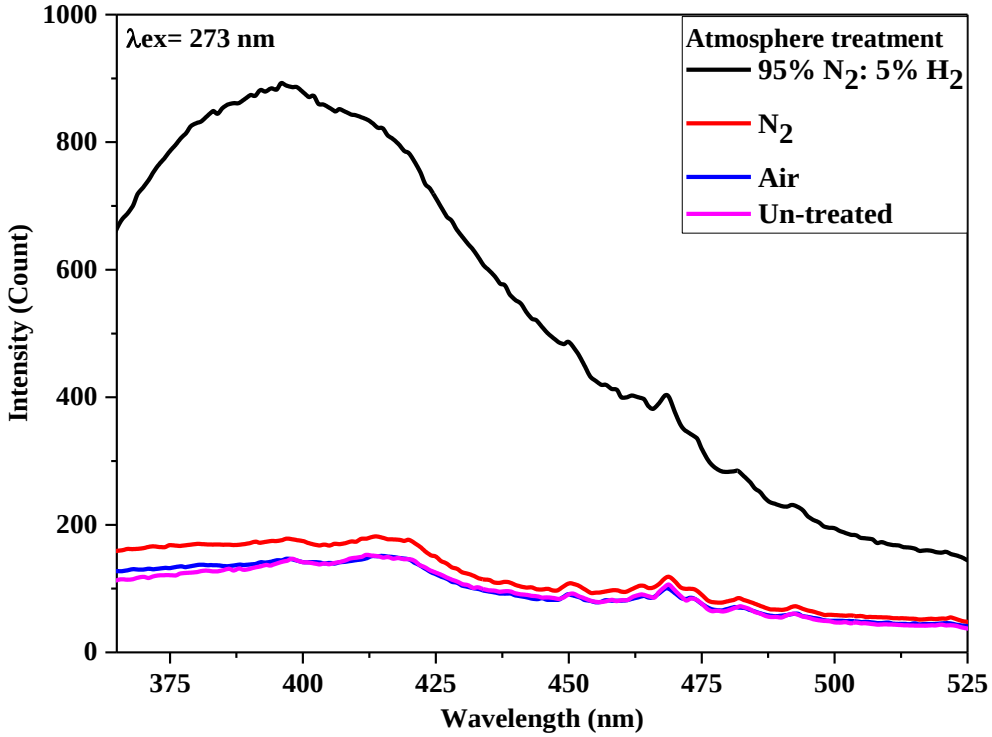

Figure 4.9 Emission spectra of 0.5 mol% Ce^{3+} and 1 mol% Mn^{2+}- doped $CaAl_2O_4$ un-treated and annealed at 800^{o}C in 95% N_2: 5%H_2, N_2, and air with the heating rate of 5^{o}C/min and the holding time of 1h

In accordance with Figure 4.9, the exitation spectra of 0.5 mol% $Ce^{3+}$and 1 mol% Mn^{2+}- doped $CaAl_2O_4$ annealed at 800^{o}C in 95%N_2:5%H_2 had the highest intensity in the ~273 nm if it compared to the other speciment. In the ~360 nm region, it also had a broad peak. It can be conclude that the atmosphere can change the intensity of emission and excitation spectra.

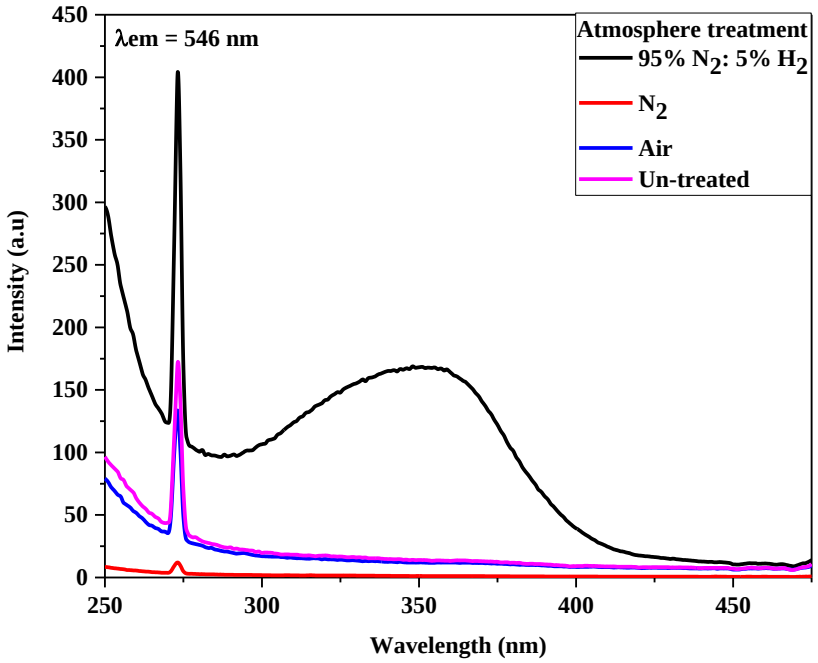

Figure 4.10 Excitation spectra of 0.5 mol% Ce^{3+} and 1 mol% Mn^{2+}- doped $CaAl_2O_4$ un-treated and annealed at 800^oC in 95%N_2: 5%H_2 with the heating rate of 5^oC/min and the holding time of 1h

4.3 Variation of cerium

This section will discuss about the effect variation of cerium to the material properties of Ce^{3+} and Mn^{2+} –doped $CaAl_2O_4$ using several characterization. In this section, 1 mol% Mn^{2+} was added to $CaAl_2O_4$ and combined with percentage variation of Ce^{3+}. Ce^{3+} variations that were used are 0, 0.5, and 1 mol% respectively. This information will greatly help to conduct the further experiments. The several characterization techniques that had been used, is including compositional analysis by XRD, morphological analysis using SEM, and also for the photoluminescence analysis using Spectrofluorometer.

4.3.1 Phases analysis

According to the Figure 4.11, it can explain about XRD pattern of Ce^{3+} and Mn^{2+} –doped $CaAl_2O_4$ after spray pyrolysis process. It can be showed that the maximum mol percentage of Ce^{3+} to get amorphous phase is 0.5 mol%. If the Ce^{3+} composition was increased until 1 mol%, the small peak of $CaAl_2O_4$ would appear. In this case, It can be concluded that the maximum composition of Ce^{3+}

for doping in the $CaAl_2O_4$ is 0.5 mol%. This result will compare to the XRD data after annealed and photoluminescence data to get the highest composition for the further experiment.

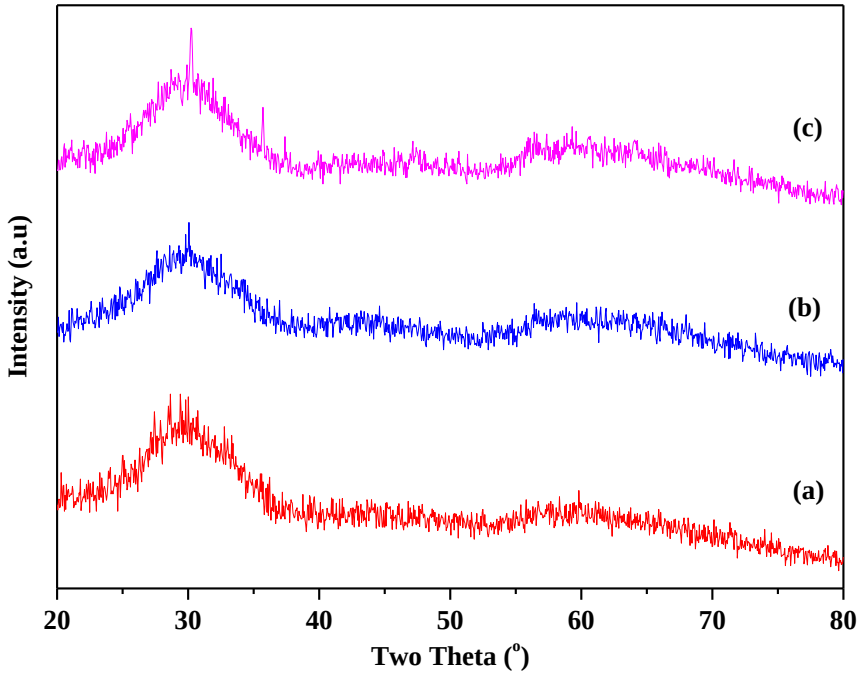

Figure 4.11 XRD patterns of as-prepared (a) 1 mol% Mn^{2+}- doped $CaAl_2O_4$, (b) 0.5 mol% Ce^{3+} and 1 mol% Mn^{2+}- doped $CaAl_2O_4$, and (c) 1 mol%Ce^{3+} and 1mol% Mn^{2+}- doped $CaAl_2O_4$

Figure 4.12 shows the XRD patterns after annealed process at 800°C in 95%N_2: 5%H_2 atmosphere condition. This result almost have a same pattern with before annealed for the 1 mol% Ce^{3+} composition. The peak of $CaAl_2O_4$ was small formed. XRD patterns of 0 and 0.5 mol% Ce^{3+} show the amophous phase without any high noise. It can be conclude that increasing composition of Ce^{3+} can modify the phase of material.

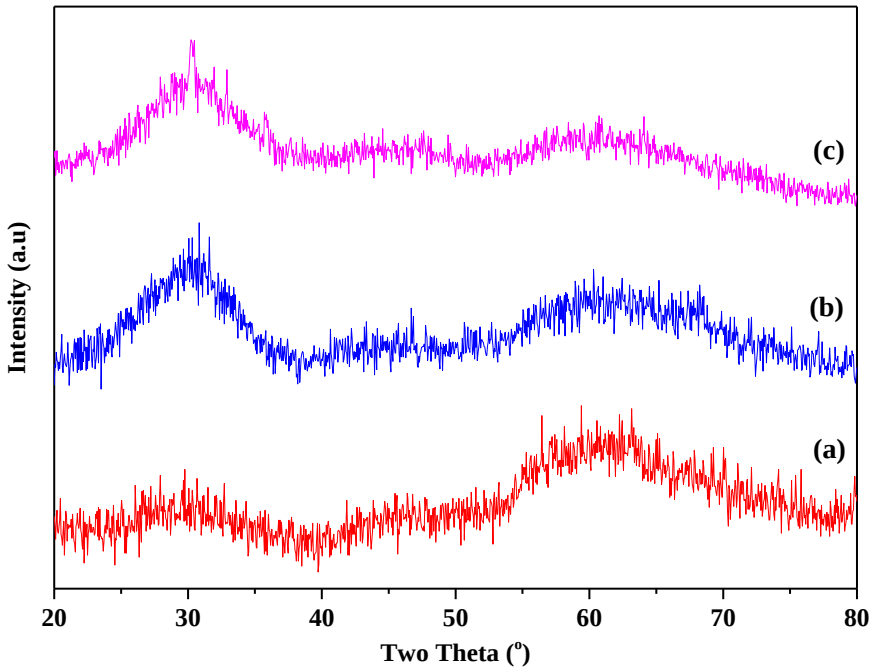

Figure 4.12 XRD patterns of (a) 1 mol% Mn^{2+}- doped $CaAl_2O_4$, (b) 0.5 mol% Ce^{3+} and 1 mol% Mn^{2+}- doped $CaAl_2O_4$, and (c) 1 mol%Ce^{3+} and 1mol% Mn^{2+}- doped $CaAl_2O_4$ annealed at 800°C in 95%N_2: 5%H_2 atmosphere condition with the heating rate of 5°C/min and the holding time of 1h

4.3.2 Morphology analysis

The SEM image of Ce^{3+} and Mn^{2+} –doped $CaAl_2O_4$ powder with different Ce^{3+} composition before annealed are shown in Figure 4.13. It can be seen that the spherical morphology of Ce^{3+} and Mn^{2+} –doped $CaAl_2O_4$ with different Ce^{3+} composition produced by spray pyrolysis. Nevertheless, the particle distribution is not homogeneous. It shows a small and large particle in un-doped and all Ce^{3+} composition. It can be caused by the spray pyrolysis mechanism as mentioned in chapter 2.

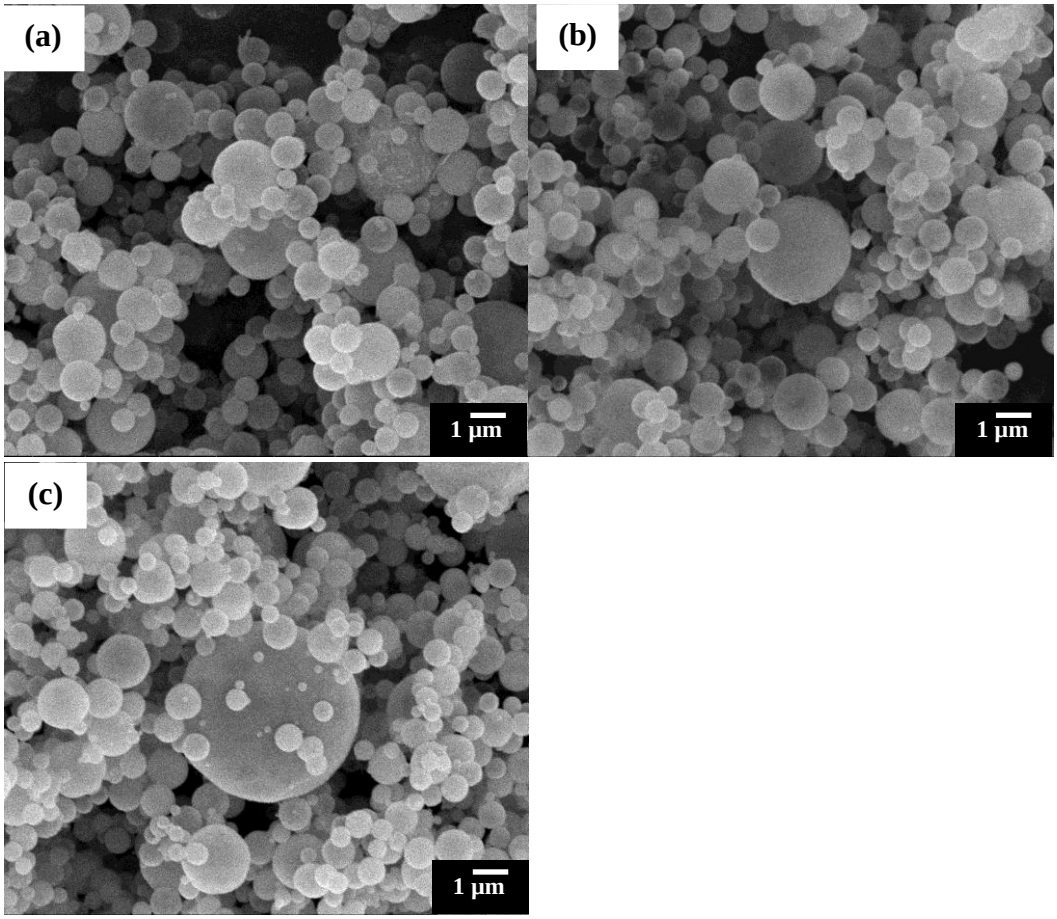

Figure 4.13 SEM images of as prepared (a) 1 mol% Mn^{2+}- doped $CaAl_2O_4$, (b) 0.5 mol% Ce^{3+} and 1 mol% Mn^{2+}- doped $CaAl_2O_4$, and (c) 1 mol% Ce^{3+} and 1 mol% Mn^{2+}- doped $CaAl_2O_4$

The particle size distribution before annealed is shown in Figure 4.13. It can be seen that the particle size cannot be affected significantly. The particle size of 1 mol% Mn^{2+}- doped $CaAl_2O_4$, 0.5 mol% Ce^{3+} and 1 mol% Mn^{2+}- doped $CaAl_2O_4$, and 1 mol% Ce^{3+} and 1 mol% Mn^{2+}- doped $CaAl_2O_4$ annealed at 800^{o}C in 95%N_2: 5%H_2 are 1145± 387, 9773± 377, and 1038 ± 374 nm, respectively.

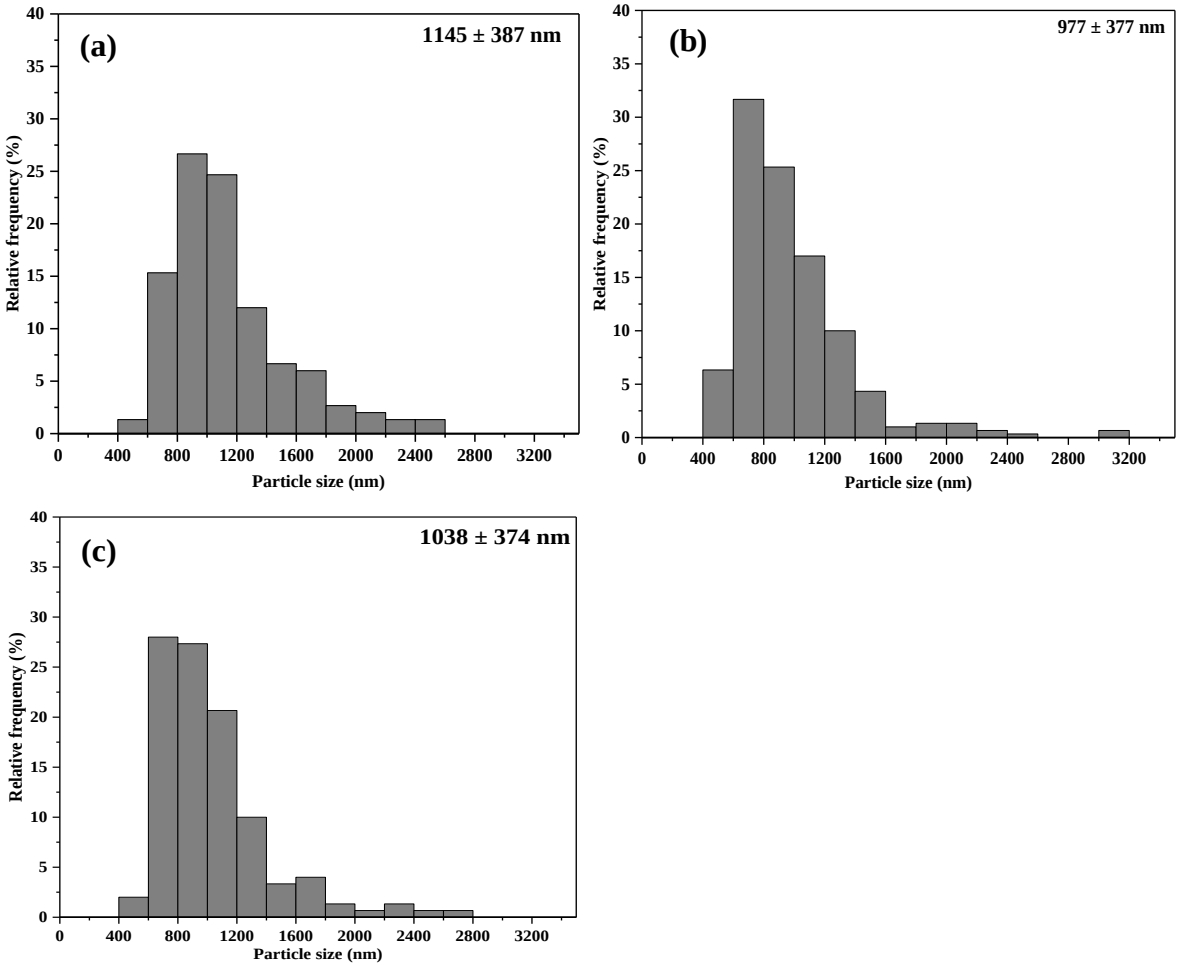

Figure 4.14 Particle size distribution of as-prepared (a)1 mol% Mn^{2+}- doped $CaAl_2O_4$, (b) 0.5 mol% Ce^{3+} and 1 mol% Mn^{2+}- doped $CaAl_2O_4$, and (c) 1 mol% Ce^{3+} and 1 mol% Mn^{2+}- doped $CaAl_2O_4$

Figure 4.15 shows SEM images of Ce^{3+} and Mn^{2+} –doped $CaAl_2O_4$ powder with different Ce^{3+} composition after annealed at 800^oC in 95%N_2: 5%H_2. The morphology of the all particle with different composition of Ce^{3+} is spherical. It had similar morphology with before annealing. It can be concluded that the variation Ce^{3+} composition had no effect for the particle morphology.

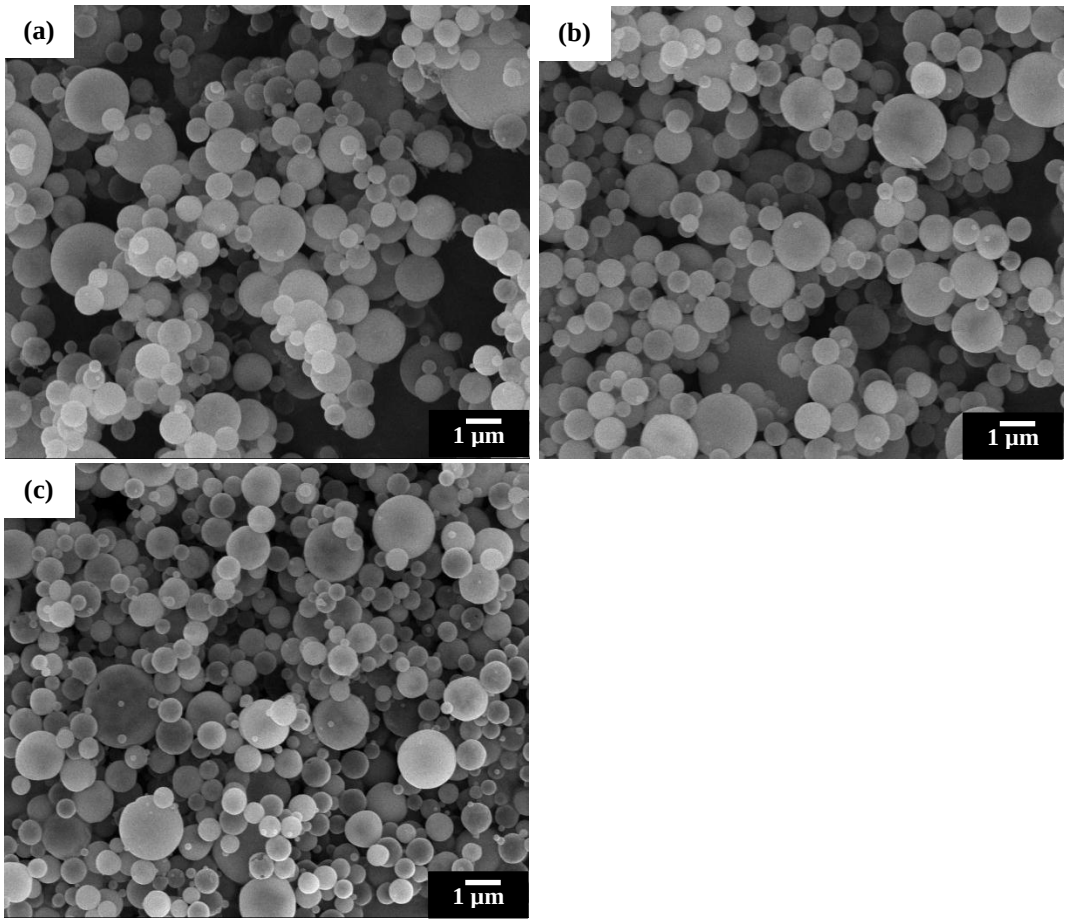

Figure 4.15 SEM images of (a)1 mol% Mn^{2+}- doped $CaAl_2O_4$, (b) 0.5 mol% Ce^{3+} and 1 mol% Mn^{2+}- doped $CaAl_2O_4$, and (c) 1 mol% Ce^{3+} and 1 mol% Mn^{2+}- doped $CaAl_2O_4$ annealed at 800^{o}C in 95%N_2: 5%H_2 with the heating rate of 5^{o}C/min and the holding time of 1h

The particle size distribution after annealed is shown in Figure 4.15. It can be seen that the particle size cannot affected significantly. The particle size of 1 mol% Mn^{2+}- doped $CaAl_2O_4$, 0.5 mol% Ce^{3+} and 1 mol% Mn^{2+}- doped $CaAl_2O_4$, and 1 mol% Ce^{3+} and 1 mol% Mn^{2+}- doped $CaAl_2O_4$ annealed at 800^{o}C in 95%N_2: 5%H_2 are 1083± 457, 852±322, and 1013±365 nm, respectively.

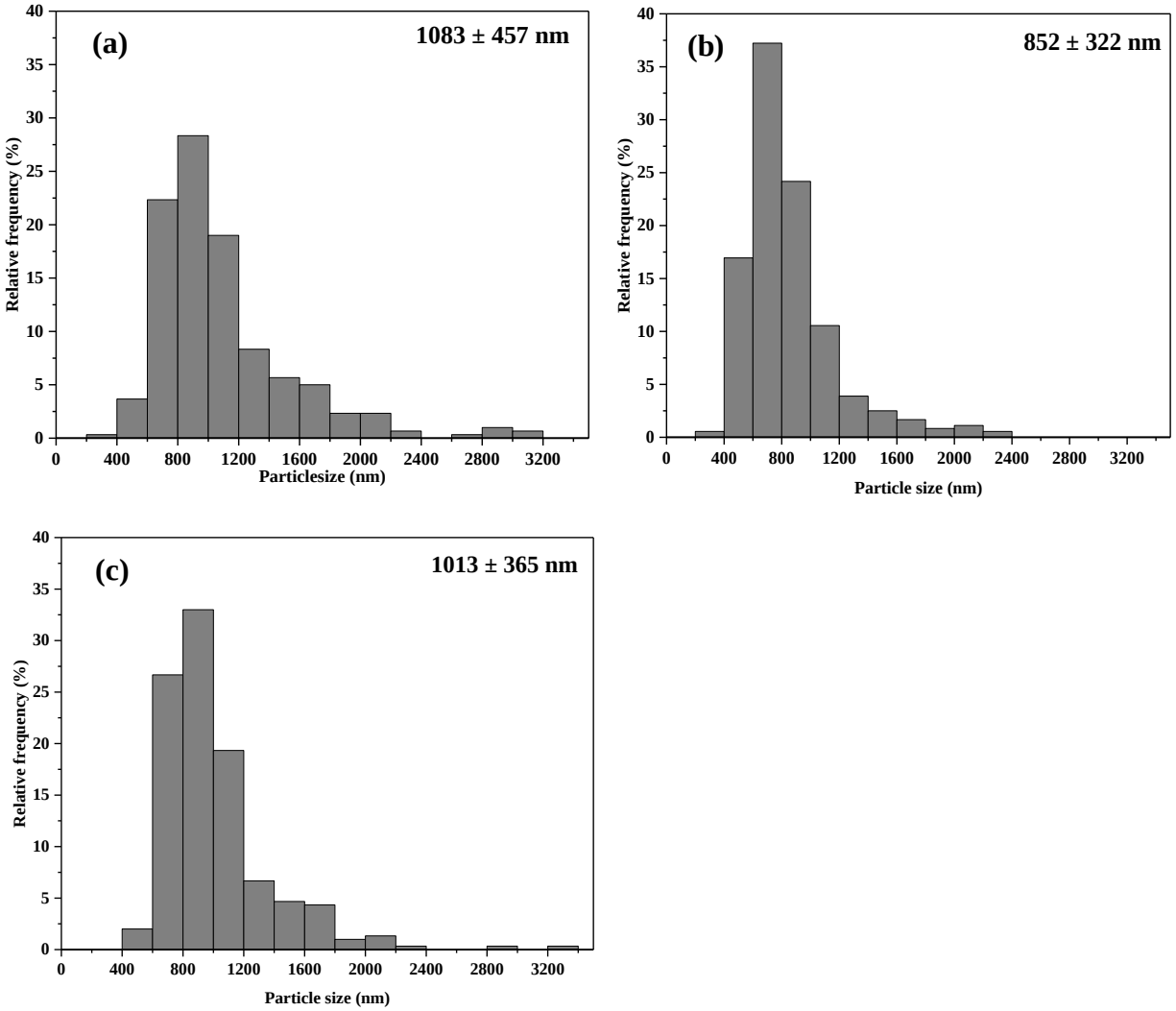

Figure 4.16 Particle size distribution of (a)1 mol% Mn^{2+}- doped $CaAl_2O_4$, (b) 0.5 mol% Ce^{3+} and 1 mol% Mn^{2+}- doped $CaAl_2O_4$, and (c) 1 mol% Ce^{3+} and 1 mol% Mn^{2+}- doped $CaAl_2O_4$ annealed at 800^{o}C in 95%N_2: 5%H_2 with the heating rate of 5^{o}C/min and the holding time of 1h

4.3.3 Photoluminescence analysis

Figure 4.16 shows the emission and excitation spectra of as-prepared Ce^{3+} and Mn^{2+}- doped $CaAl_2O_4$ in variation of Ce^{3+} composition. In this condition, it can be seen that the intensity is quite low if it is compared with emission or exitation spectra after annealed in 95%N_2 : 5%H_2. Nevertheless, for the highest emission at wavelength around 400-500 nm, the highest peak is 1% molCe^{3+} and 1 mol%Mn^{2+}- doped $CaAl_2O_4$. According to the 4.16 (b) the excitation spectra, the highest peak near ~273 nm is undoped and the smallest peak is 1 mol%Mn – doped $CaAl_2O_4$.

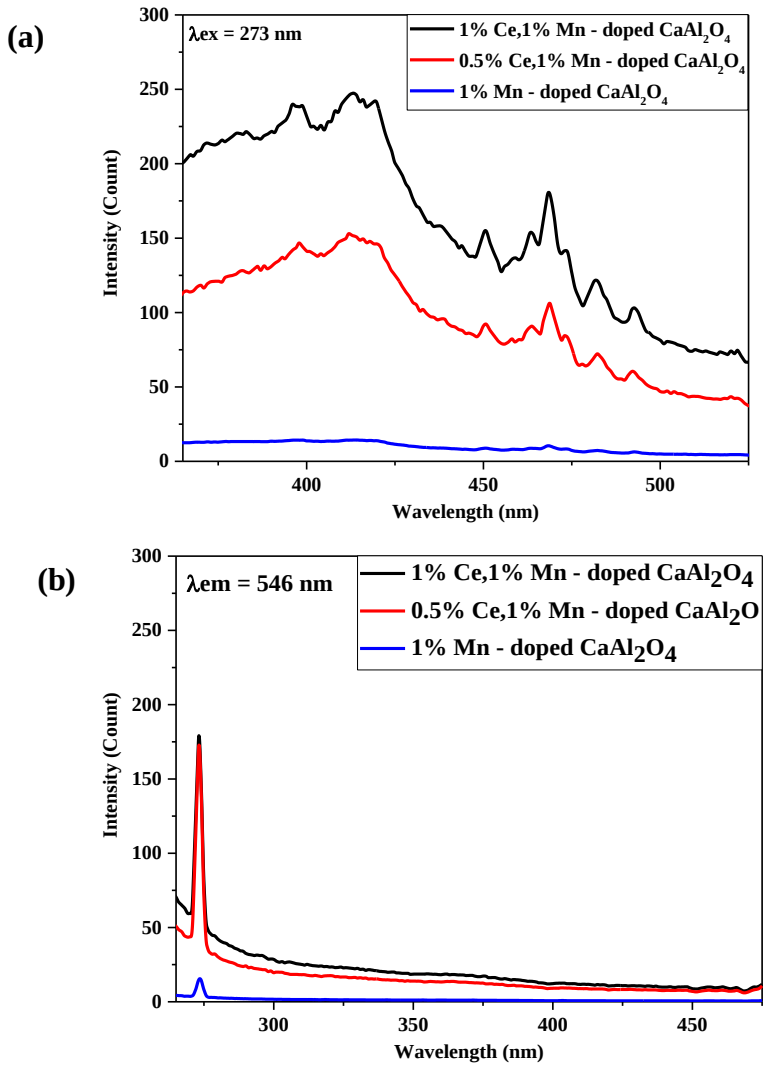

Figure 4.17 (a) Emission and (b) excitation spectra of as prepared 1 mol% Mn^{2+}- doped $CaAl_2O_4$, 0.5 mol% Ce^{3+} and 1 mol% Mn^{2+}- doped $CaAl_2O_4$, and 1 mol% Ce^{3+} and 1 mol% Mn^{2+}- doped $CaAl_2O_4$

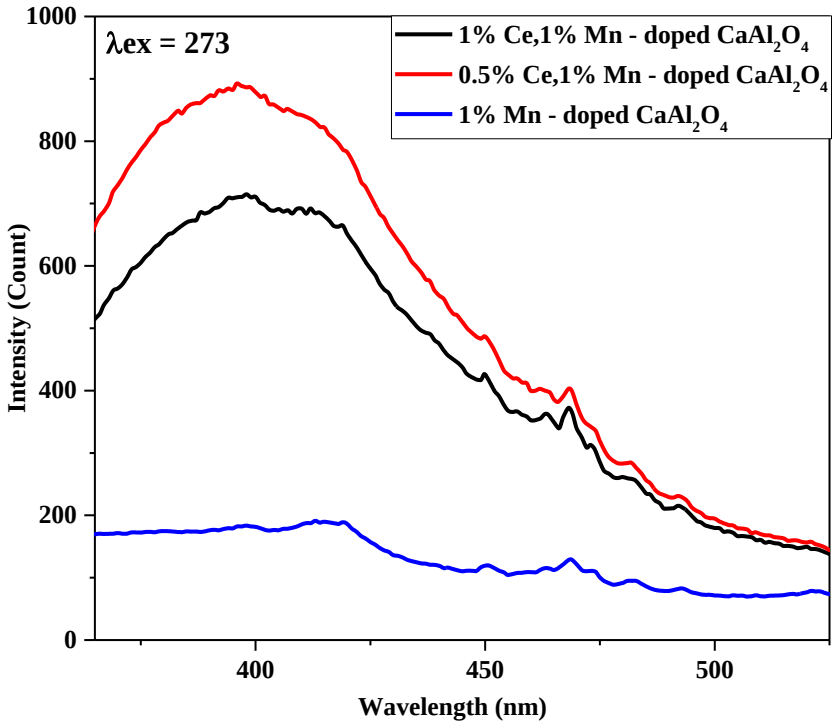

Figure 4.18 Emission spectra of 1 mol% Mn^{2+}- doped $CaAl_2O_4$, 0.5 mol% Ce^{3+} and 1 mol% Mn^{2+}- doped $CaAl_2O_4$, and 1 mol% Ce^{3+} and 1 mol% Mn^{2+}- doped $CaAl_2O_4$ annealed at 800^{o}C in 95%N_2: 5%H_2 with the heating rate of 5^{o}C/min and the holding time of 1h

In accordance with Figure 4.18, it can be seen one broad peak at wavelength ~408. The sequence for Ce^{3+} composition that had the highest to small intensity at wavelength ~408 are 0.5 mol%, 1 mol%, and 0 mol%. From the Figure 4.19, it shows the highest peak at wavelength ~273 nm for 0.5 mol%Ce^{3+} and 1 mol%Mn^{2+}- doped $CaAl_2O_4$. There is shifting peak for wavelength around 325 to 375 nm.

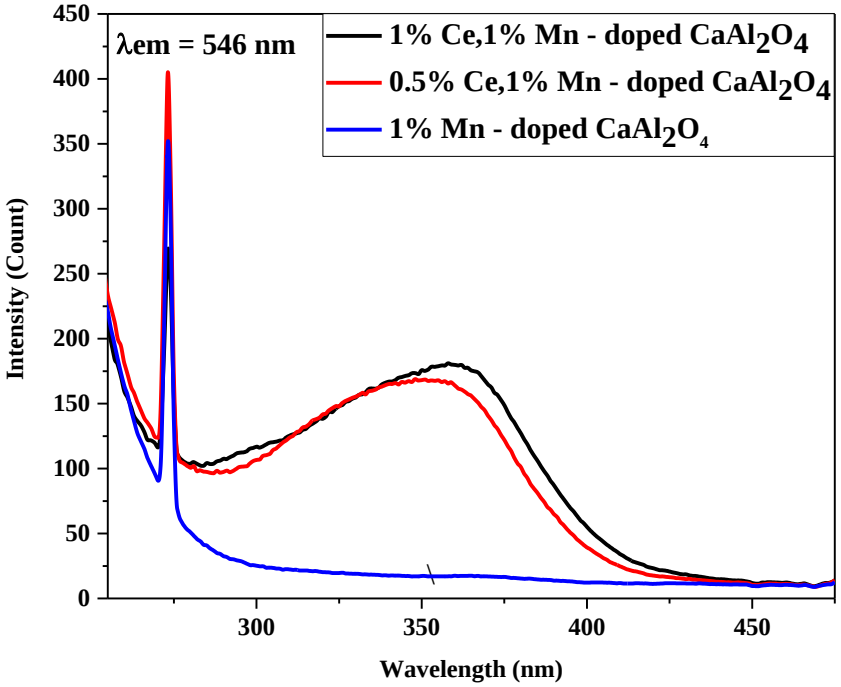

Figure 4.19 Excitation spectra of 1 mol% Mn^{2+}- doped $CaAl_2O_4$, 0.5 mol% Ce^{3+} and 1 mol% Mn^{2+}- doped $CaAl_2O_4$, and 1 mol% Ce^{3+} and 1 mol% Mn^{2+}- doped $CaAl_2O_4$ annealed at 800^{o}C in 95%N_2: 5%H_2 with the heating rate of 5^{o}C/min and the holding time of 1h

4.4 Variation of manganese

After know the highest intensity for Ce^{3+} composition from the previous section, this section will discuss about the effect variation of manganese to the material properties of Ce^{3+} and Mn^{2+} –doped $CaAl_2O_4$ using several characterization. 0.5 mol% Ce^{3+} was added to $CaAl_2O_4$ as the best composition according the previous section. Furthermore, Mn^{2+} variation would be combined with Ce^{3+}. This information will greatly help to conduct the further experiments. The several characterization techniques that had been used, is including compositional analysis by XRD, morphological analysis using SEM, and also for the photoluminescence analysis using Spectrofluorometer.

4.4.1 Phases analysis

According to the Figure 4.20, it can explain about XRD patterns of Ce^{3+} and Mn^{2+} –doped $CaAl_2O_4$ in different Mn^{2+} composition after spray pyrolysis process. It can be showed that the maximum Mn^{2+} composition to get amorphous phase is 3%. If the Mn^{2+} composition was increased to 5 mol%, the peak of $CaAl_2O_4$ would appear. In this case, it can be concluded that the maximum composition of Mn^{2+} for doping in the $CaAl_2O_4$ is 3 mol%. This result will compare to the XRD data after annealed and photoluminescence data to get the highest composition for the further experiment.

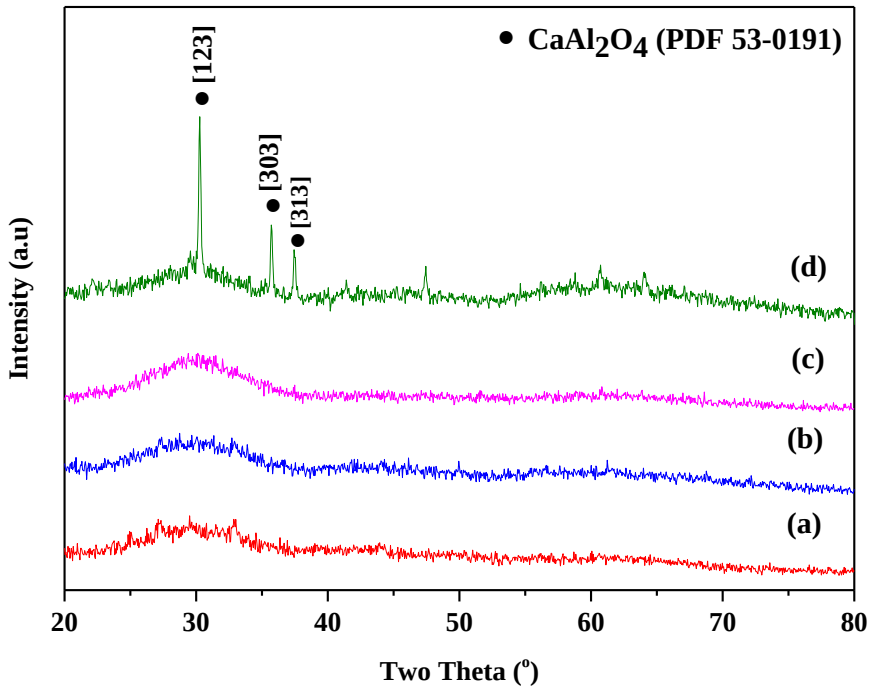

Figure 4.20 XRD patterns of as-prepared (a) 0.5 mol%Ce^{3+}- doped $CaAl_2O_4$,(b) 0.5 mol%$Ce^{3+}$and 1 mol% Mn^{2+}- doped $CaAl_2O_4$, (c) 0.5 mol% Ce^{3+} and 3 mol% Mn^{2+}- doped $CaAl_2O_4$, (d) 0.5 mol% Ce^{3+} and 5 mol% Mn^{2+}- doped $CaAl_2O_4$

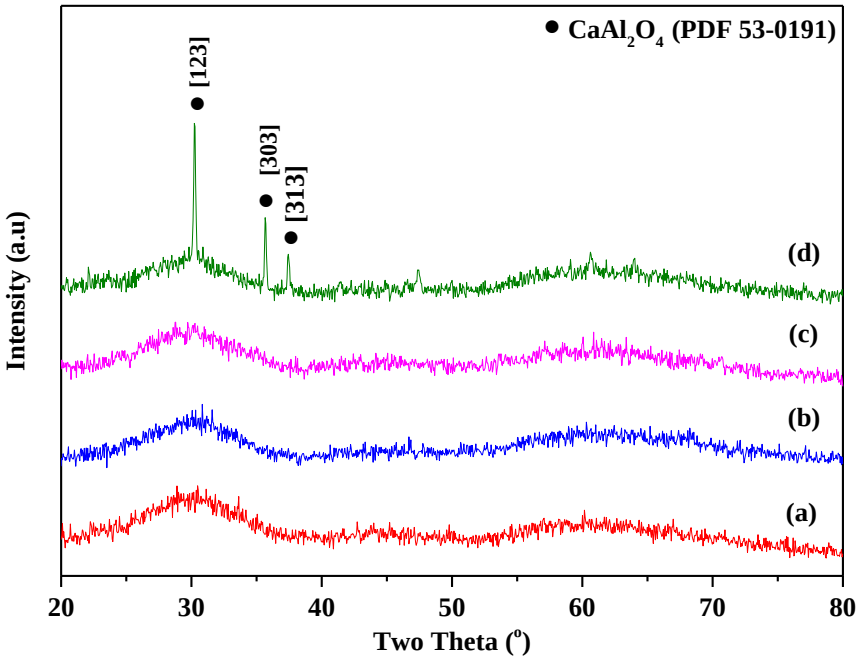

Figure 4.21 XRD patterns of (a) 0.5 mol%Ce^{3+}- doped $CaAl_2O_4$,(b) 0.5 mol%$Ce^{3+}$and 1 mol% Mn^{2+}- doped $CaAl_2O_4$, (c) 0.5 mol% Ce^{3+} and 3 mol% Mn^{2+}- doped $CaAl_2O_4$, (d) 0.5 mol% Ce^{3+} and 5 mol% Mn^{2+}- doped $CaAl_2O_4$ annealed at 800°C 95%N_2: 5%H_2 atmosphere condition with the heating rate of 5°C/min and the holding time of 1h

4.4.2 Morphology analysis

The SEM image of Ce^{3+} and Mn^{2+} –doped $CaAl_2O_4$ powder with different Mn^{2+} composition before annealed are shown in Figure 4.22. It can be seen that the spherical morphology of Ce^{3+} and Mn^{2+} –doped $CaAl_2O_4$ produced by spray pyrolysis. Nevertheless, the particle distribution is not homogeneous. It shows a small and large particle in all Mn^{2+} composition. It can be caused by the spray pyrolysis mechanism as mentioned in chapter 2.

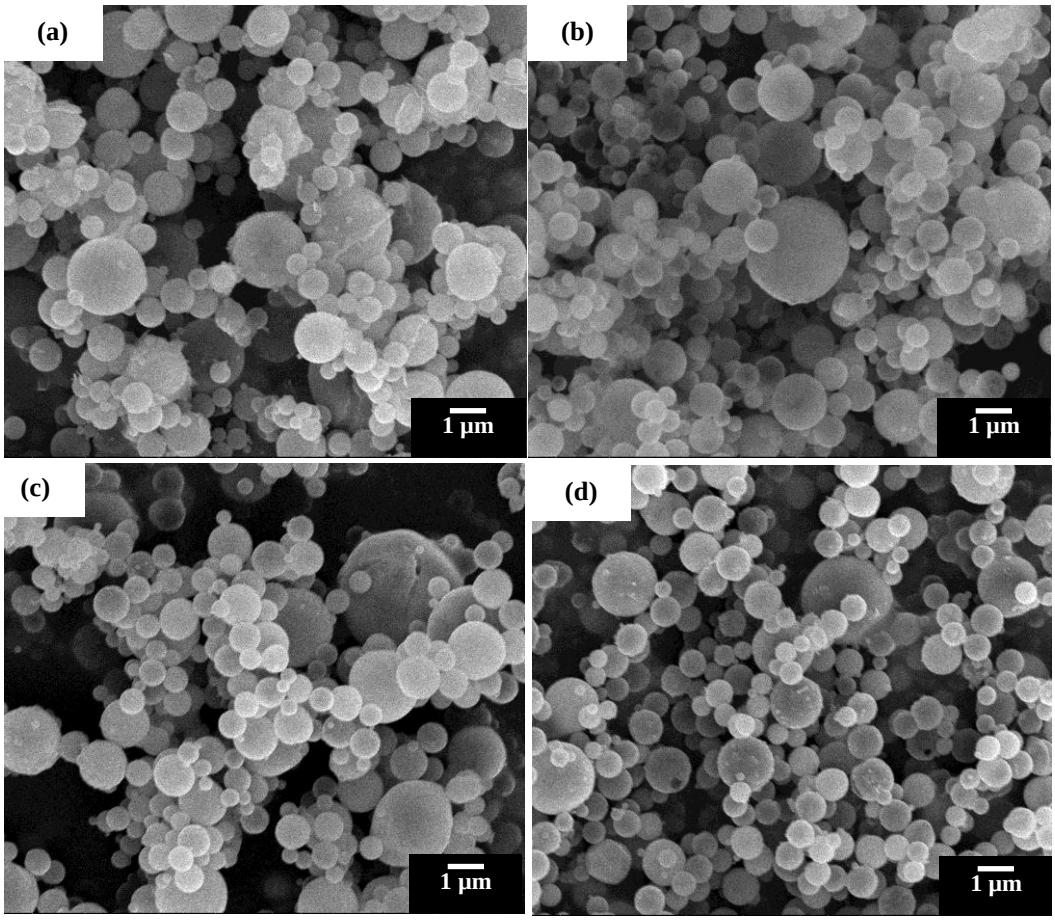

Figure 4.22 SEM images of as-prepared (a) 0.5 mol%Ce^{3+}- doped $CaAl_2O_4$,(b) 0.5 mol%$Ce^{3+}$and 1 mol% Mn^{2+}- doped $CaAl_2O_4$, (c) 0.5 mol% Ce^{3+} and 3 mol% Mn^{2+}- doped $CaAl_2O_4$, (d) 0.5 mol% Ce^{3+} and 5 mol% Mn^{2+}- doped $CaAl_2O_4$

The particle size distribution before annealed is shown in Figure 4.22. It can be seen that the particle size cannot be affected significantly. The particle size of 0.5 mol%Ce^{3+}- doped $CaAl_2O_4$,0.5 mol%$Ce^{3+}$and 1 mol% Mn^{2+}- doped $CaAl_2O_4$, 0.5 mol% Ce^{3+} and 3 mol% Mn^{2+}- doped $CaAl_2O_4$, and 0.5 mol% Ce^{3+} and 5 mol% Mn^{2+}- doped $CaAl_2O_4$ annealed at 800^{o}C are 1158± 430, 977± 377, 992± and 1038 ± 374 nm, respectively.

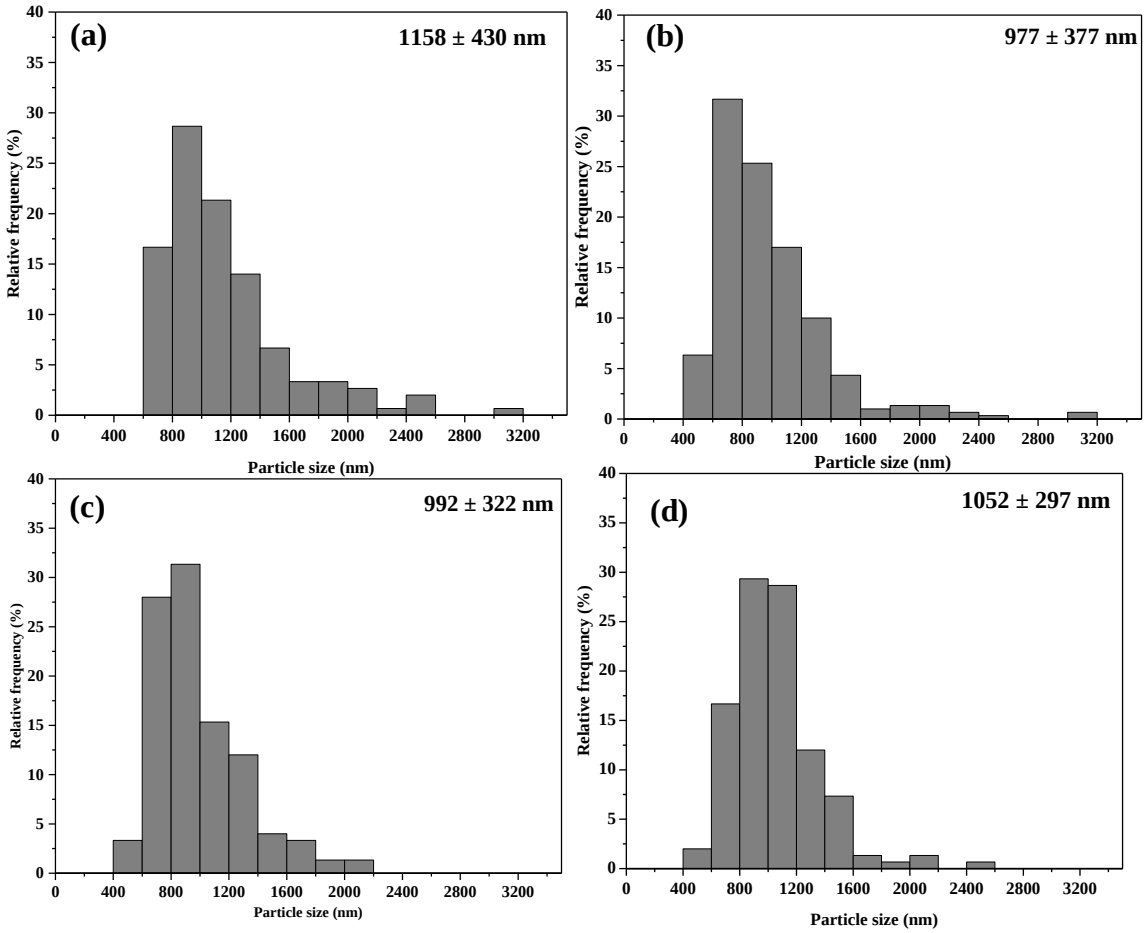

Figure 4.23 Particle size distribution of as-prepared (a) 0.5 mol%Ce^{3+}- doped $CaAl_2O_4$,(b) 0.5 mol%$Ce^{3+}$and 1 mol% Mn^{2+}- doped $CaAl_2O_4$, (c) 0.5 mol% Ce^{3+} and 3 mol% Mn^{2+}- doped $CaAl_2O_4$, (d) 0.5 mol% Ce^{3+} and 5 mol% Mn^{2+}- doped $CaAl_2O_4$

Figure 4.24 shows SEM image of (a) 0.5 mol%Ce^{3+}- doped $CaAl_2O_4$,(b) 0.5 mol%$Ce^{3+}$and 1 mol% Mn^{2+}- doped $CaAl_2O_4$, (c) 0.5 mol% Ce^{3+} and 3 mol% Mn^{2+}- doped $CaAl_2O_4$, (d) 0.5 mol% Ce^{3+} and 5 mol% Mn^{2+}- doped $CaAl_2O_4$ after annealed at 800^{o}C in 95%N_2: 5%H_2 atmosphere. The morphology of the all particle with different composition of Mn^{2+} is spherical. It had similar

morphology with before annealing. It can be conclude that the composition of Mn^{2+} had no effect for the particle morphology.

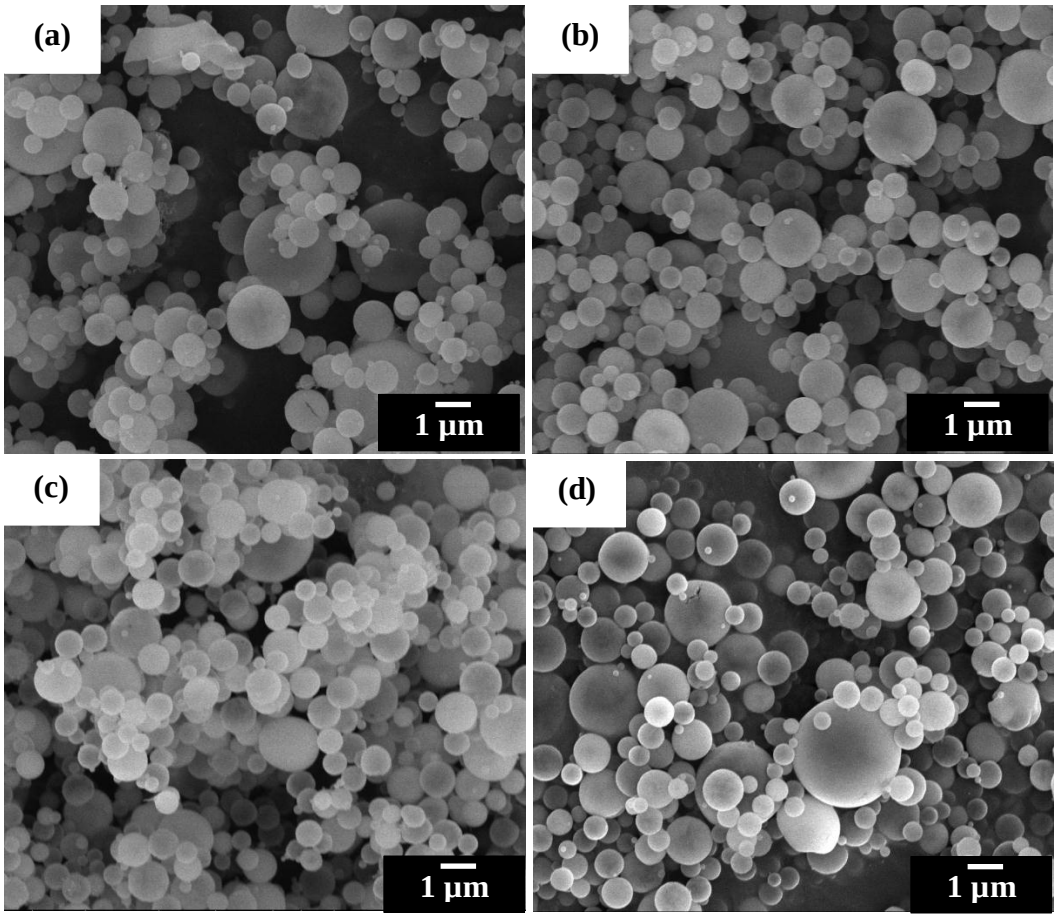

Figure 4.24 SEM images of (a) 0.5 mol%Ce^{3+}- doped $CaAl_2O_4$,(b) 0.5 mol%$Ce^{3+}$and 1 mol% Mn^{2+}- doped $CaAl_2O_4$, (c) 0.5 mol% Ce^{3+} and 3 mol% Mn^{2+}- doped $CaAl_2O_4$, (d) 0.5 mol% Ce^{3+} and 5 mol% Mn^{2+}- doped $CaAl_2O_4$ annealed at 800^{o}C in 95%N_2: 5%H_2 with the heating rate of 5^{o}C/min and the holding time of 1h

The particle size distribution after annealed is shown in Figure 4.24. It can be seen that the particle size cannot affected significantly. The particle size of 0.5 mol%Ce^{3+}- doped $CaAl_2O_4$, 0.5 mol%$Ce^{3+}$and 1 mol% Mn^{2+}- doped $CaAl_2O_4$, 0.5 mol% Ce^{3+} and 3 mol% Mn^{2+}- doped $CaAl_2O_4$, and 0.5 mol% Ce^{3+} and 5 mol% Mn^{2+}- doped $CaAl_2O_4$ annealed at 800^{o}C are 966 ± 385, 852 ± 322, 1131±355, and 940±390 nm, respectively.

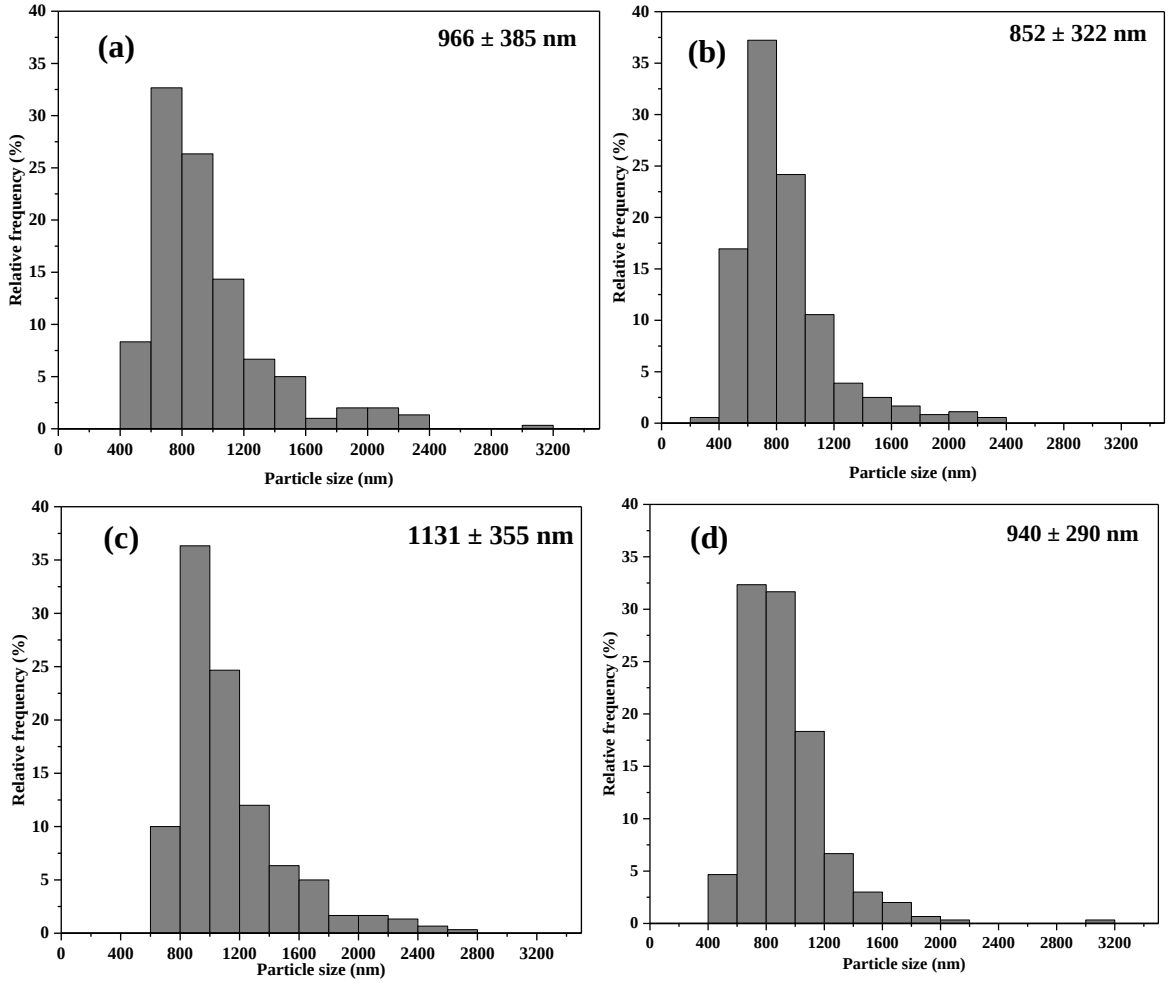

Figure 4.25 Particle size distribution of (a) 0.5 mol%Ce^{3+}- doped $CaAl_2O_4$,(b) 0.5 mol%$Ce^{3+}$and 1 mol% Mn^{2+}- doped $CaAl_2O_4$, (c) 0.5 mol% Ce^{3+} and 3 mol% Mn^{2+}- doped $CaAl_2O_4$, (d) 0.5 mol% Ce^{3+} and 5 mol% Mn^{2+}- doped $CaAl_2O_4$ annealed at 800^{o}C in 95%N_2: 5%H_2 with the heating rate of 5^{o}C/min and the holding time of 1h

4.4.3 Photoluminescence analysis

Figure 4.26 shows the emission and excitation spectra of Ce^{3+} and Mn^{2+}-doped $CaAl_2O_4$ in different Mn^{2+} composition before annealed. In this condition, it can be seen that the intensity is quite low if it is compared with emission or exitation spectra after annealed in 95%N_2:5%H_2. According to the Figure 4.26 (b) the exitation spectra, the highest peak near ~273 nm is 0.5 mol%Ce^{3+} -doped $CaAl_2O_4$ and the smallest peak is 0.5 mol %Ce^{3+} and 3 mol%Mn^{2+} -doped $CaAl_2O_4$.

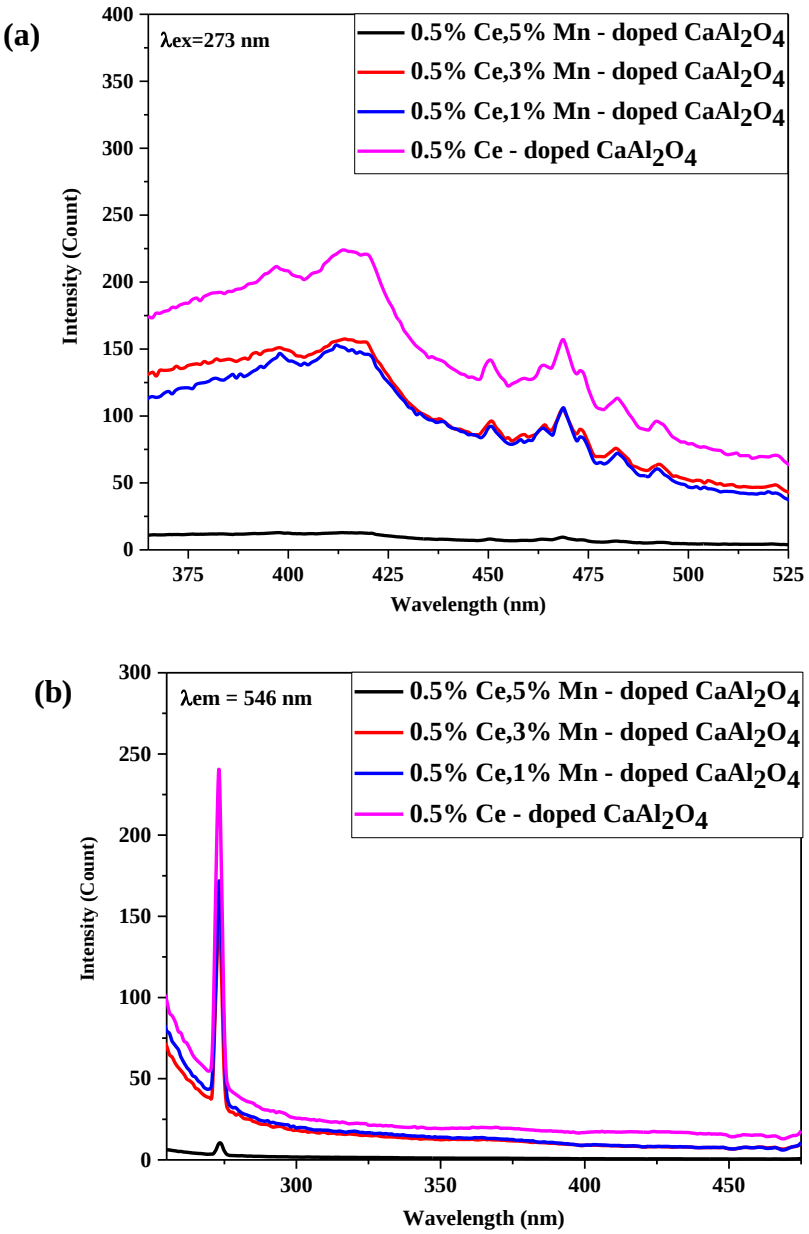

Figure 4.26 (a) Emission and (b) excitation spectra of as-prepared Ce^{3+} and Mn^{2+}-doped $CaAl_2O_4$ with different Mn^{2+} composition

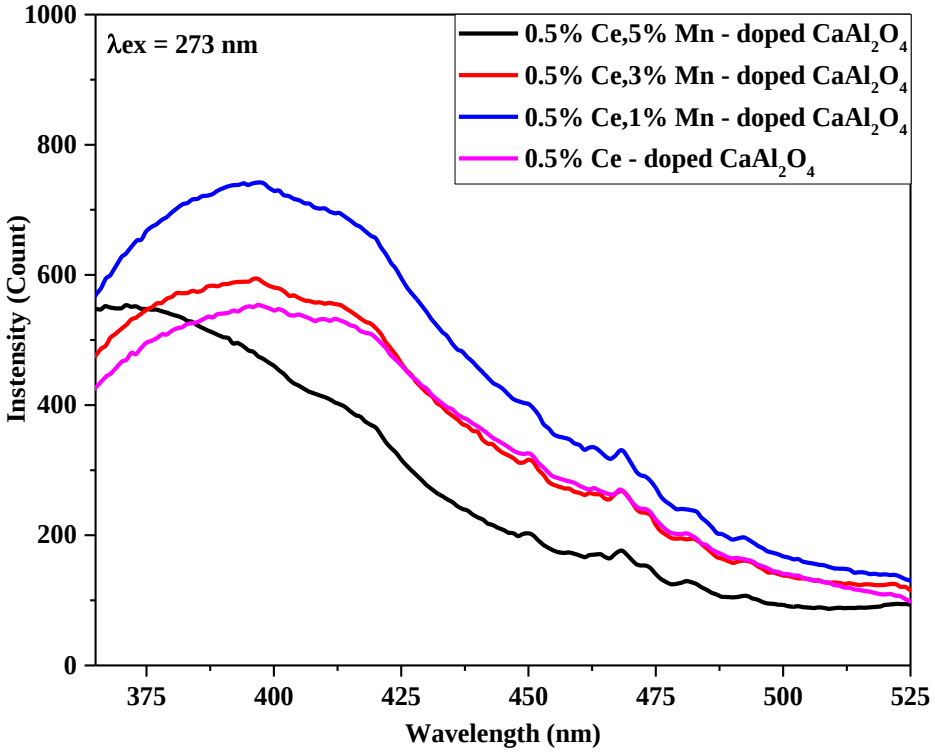

Figure 4.27 Emission spectra of Ce^{3+} and Mn^{2+}- doped $CaAl_2O_4$ with different Mn^{2+} composition annealed at 800^{o}C in 95%N_2: 5%H_2 with the heating rate of 5^{o}C/min and the holding time of 1h

In accordance with Figure 4.27, it can be seen one broad peak at wavelength ~408 nm. The sequence for specimens with different Mn^{2+} composition from the highest to small intensity at wavelength ~408 nm are 1 mol%, 3mol%, 0 mol%, and 5 mol%. In contrast to excitation spectra, it had several wavelength at ~273 and ~360 nm. The sequence for specimen with different Mn^{2+} composition from the highest to small intensity at wavelength ~360 nm 5 mol%, 1 mol%, 3 mol%, and 0 mol%.

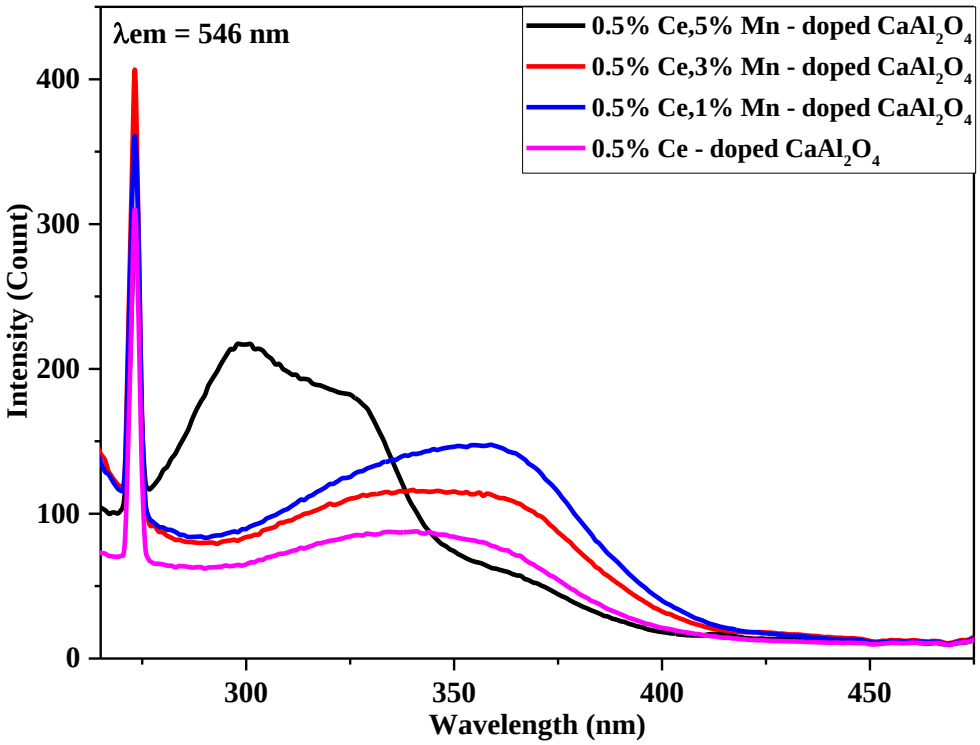

Figure 4.28 Excitation spectra of Ce^{3+} and Mn^{2+}- doped $CaAl_2O_4$ with different Mn^{2+} composition annealed at 800^{o}C in 95%N_2: 5%H_2 with the heating rate of 5^{o}C/min and the holding time of 1h

(*This page intentionally left blank*)

CHAPTER 5
DISCUSSION

5.1 Adjusting the temperature

The correlation between annealing temperature and material properties of 0.5 mol%Ce^{3+} and 1 mol%Mn^{2+} -doped $CaAl_2O_4$ will be discussed in this following section. As it already shown in previous section, the initial characterization of 0.5 mol%Ce^{3+} and 1 mol%Mn^{2+} -doped $CaAl_2O_4$ had been conducted using several characterization such as, XRD, SEM, and Spectrofluorocence.

5.1.1 Crystallization of as received Ce^{3+} and Mn^{2+}-doped $CaAl_2O_4$ powder

The XRD analysis of Ce^{3+} and Mn^{2+}-doped $CaAl_2O_4$ in different annealing temperature have been shown amorphous phase at 800^{o}C for the maximum temperature. In this experiment, the amorphous phase is an important thing that needs to be achieved, especially for the application that need amorphous phase for example fluorescent ink for security label. Guo explained that amorphous samples usually give different optical response compared to the crystalline because of the short range order to crystalline domain. It will affect with electronic level which is probably reflected by photoluminescence spectra (Guo, Huang et al. 2012). In the previous research, amorphous $CaAl_2O_4$ were successfully synthesized using spray drying method (Douy and Gervais 2000). After spray drying process, it was followed by calcination temperature to decompose the salt. These can produce homogeneous calcium aluminates powder. According to the Douy TGA result, the decomposition process of aluminium nitrate started around 200^{o}C and for the calcium nitrate started from 490^{o}C. Then, the temperature that used for the initial crystallite phase was 900^{o}C after annealed in 1 h. Fumo defined that the key to synthesized single phase $CaAl_2O_4$ is using rapid decomposition of mixture of nitrates (Fumo, Morelli et al. 1996).The other preparation report that pure $CaAl_2O_4$ can be achieved after calcination at 900^{o}C (Desai, Xu et al. 1995).

In the present work, Ce^{3+} and Mn^{2+} were used to occupy the Ca^{2+} site. The phase of Ce^{3+} and Mn^{2+} were not appeared in the crystallite and amorphous phase

$CaAl_2O_4$, it indicated that the Ce^{3+} and Mn^{2+} successfully occupied the Ca^{2+} sites. It is caused by the ionic radii of Ce^{3+} and Mn^{2+} almost close to Ca^{2+}. The ionic radii of Ca^{2+}, Ce^{3+} and Mn^{2+} are 0.98, 1.07 and 0.8^{o}A, respectively. For the decomposition temperature already reached in the spray pyrolysis process. Because in the spray pyrolysis, the temperature that were used for heating, calcination, and cooling process are 250, 1000, and 350^{o}C, respectively. According to the XRD result (see Figure 4.1), crystallite phase of $CaAl_2O_4$ showed for the annealed at 900^{o}C. For the temperature bellow 900^{o}C, which was 600, 700, and 800^{o}C, it showed amorphous phase. It can be concluded that the highest temperature for the amorphous phase are 800^{o}C.

5.1.2 Morphological analysis

According to SEM result, 0.5 mol%Ce^{3+} and 1 mol%Mn^{2+}-doped $CaAl_2O_4$ show only one type of morphology spherical. Spray pyrolysis process contributed to form the particle morphology to become spherical. For spray pyrolysis, the particle size depends on the size of the precursor droplets, precursor concentration, and the frequency of the ultrasonic nebulizer (Messing, Zhang et al. 1993). Another important factor is the droplet to particle conversion mechanism in spray pyrolysis would have two droplet-to-particle mechanisms, which are gas-to-particle conversion and one-droplet-one particle. In this present study, the mechanism of converting droplet to particle belongs to one-droplet-one-particle mechanism (Messing, Zhang et al. 1993, Chen, Tseng et al. 2008, Shih, Wu et al. 2012, Shih, Wu et al. 2012). Due to, this mechanism will lead to the precipitation of homogeneous particle size. When the solutions atomized into tube furnace, each of droplets can be seen as a micro reactor. There precursors will undergo solvent evaporation, solute precipitation, pyrolysis of precipitated particles and calcination to form a dense particle(Messing, Zhang et al. 1993). The particle morphologies depend on how the solute is precipitated. There are two mechanism of precipitation in spray pyrolysis which are volume precipitation and surface precipitation. Volume precipitation will lead to the formation of solid particle, otherwise surface precipitation will lead to the formation of hollow particle. In

this present study, Ce^{3+} and Mn^{2+}-doped $CaAl_2O_4$ have no hollow structure, only solid microstructure.

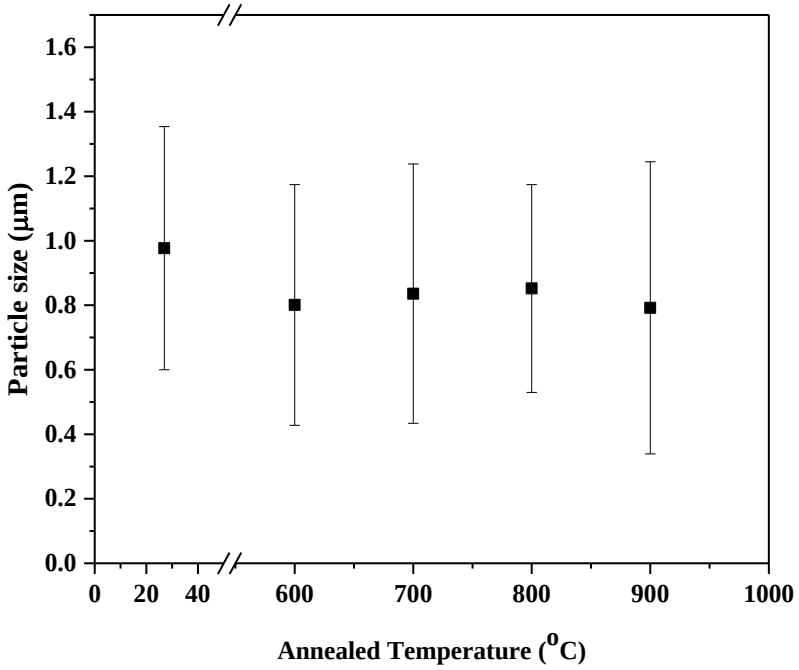

Figure 5.1 Correlation between annealed temperature and particle size of 0.5 mol%Ce^{3+} and 1 mol %Mn^{2+} -doped $CaAl_2O_4$ powder

5.1.3 Photoluminescence analysis

According to the emission and excitation spectra (Figure 4.4 and 4.5), it show different intensity for the variation of the annealing temperature. The broad peak with wavelength at ~408 nm in the specimens that annealed at 700, 800, and 900^{o}C show the strong intensity than the narrow peak. It similar as strong crystal field dependence of the 5d levels in Ce^{3+}, the emission of Ce^{3+} usually exhibits strong site dependence. Therefore, Ce^{3+} are doped into a host that has multiple cation sites, it often results in multiple Ce^{3+} emission centres in this host. Ce^{3+} have two emission peak that are due to terminating levels, $^2F_{5/2}$ and $^2F_{7/2}$, of the 4f configuration of Ce^{3+}. Furthermore, color of the powder has some effect for the emission light. Figure 5.2 show about the powder color of the 0.5 mol%Ce^{3+} and 1 mol%Mn^{2+} –doped $CaAl_2O_4$.

Figure 5.2 The photos of 0.5 mol%Ce^{2+} and 1 mol%Mn^{2+} -doped $CaAl_2O_4$ powder (a) un-treated and with different anneling temperature (b) 600, (c) 700, (d) 800, and (e) 900^{o}C for 1 h in 95%N_2: 5%H_2

Teixeira defined that the darker color is undesirable for application as phosphor because the self-absorption will dominate and reduce the light yield of material(Teixeira, Montes et al. 2014). In the previous research, it explained that the dark color may be attributed to absorption by products (Iso, Takeshita et al. 2014). In this study, for the specimen that un-treated, annealed at 600^{o}C had a light orange color. So, these specimens cannot absorb the UV light as in Figure 4.5. This specimens had no broad peak for the excitation spectra at wavelength ~350 nm. In contrast, for the specimen annealed at 700 and 800^{o}C, it had a bright white powder than specimen annealed at 900^{o}C. However, specimen annealed at 900^{o}C had a crystallite structure, so the arrangement of the ion site already fit in the crystal structure. Bernando defined the differences intensity of glassy and crystallite phase it was caused by presence of high energy phonons in host matrix. In the glassy material, the activator site is in the disordered glassy matrix

(Bernardo, Fiocco et al. 2014). So, for the crystallite phase, it had a high intensity than the amorphous. However, there are the other factor that can be used to increase the intensity of phosphor material.

For the small peak around wavelength 450-475 nm. it can be attributed to $^4T_1$-$^6A_1$ transition of Mn^{2+}. Mn^{2+} also occupied Ca^{2+} site. Suryamurthy defined that the d-d transition in Mn^{2+} is both spin and parity forbidden. That is caused by the luminescence observe from Mn^{2+} is due to the admixture of parity between 3d and 4p configuration lifting the spin selection rule and also possible electron-phonon coupling(Suriyamurthy and Panigrahi 2007). The Mn^{2+} ion have probability to emit green and red light. It can emit green light if it is tetrahedral coordinated (CN=4) in the lattice and red light in the octahedral coordination (CN=6) (Yen, Shionoya et al. 2007). In this present case, observation of blue-green emission around wavelength 450-475 nm suggests that Mn^{2+} probably occupies a tetrahedral site in $CaAl_2O_4$ matrix. It can be conclude that the material that can absorb and emit the highest intensity is annealed at 800^{o}C in 95%N_2: 5%H_2.

5.2 Adjusting atmospheric gases

This following section will discuss about correlation between atmosphere effect and photoluminescence properties. As it already shown in previous section, the initial characterization of 0.5 mol%Ce^{3+} and 1 mol%Mn^{2+}-doped $CaAl_2O_4$ had been conducted using several characterization such as, XRD, SEM, and Spectrofluorocence.

5.2.1 Crystallization of as received Ce^{3+} and Mn^{2+}-doped $CaAl_2O_4$ powder

According to the XRD pattern in Figure 4.6, it shows amorphous pattern in un-treated and all atmosphere condition. But there is a small shifting to the right in the broad peak. Figure 5.3 show the shifting of the XRD pattern result.

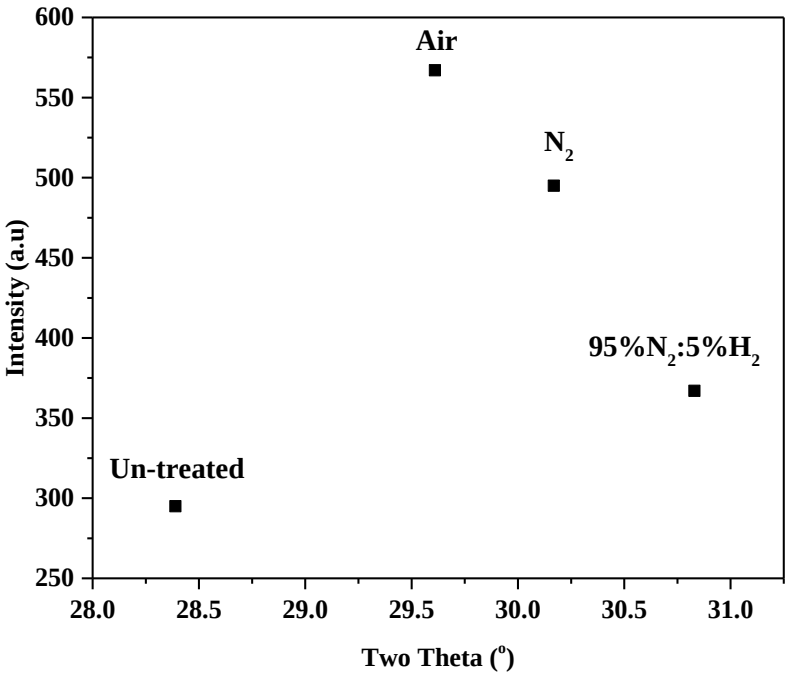

Figure 5.3 Comparison between shifting XRD peaks and different atmosphere treatment condition of 0.5 mol%Ce, 1%Mn^{2+} -doped $CaAl_2O_4$ powder

Anwar defined that the atmosphere treatment had an effect to the inducing structural change (Anwar, Li et al. 2016). The XRD peak will shift to the higher angle if the unit cell or lattice parameter is decreasing. In this study, reducing atmosphere was needed to change the Ce valence from 4+ to 3+ and Mn^{3+} to Mn^{2+}. Ce^{4+} and Ce^{3+} valence had different ionic radii and also for the Mn^{3+} and Mn^{2+}. Ce^{3+}, Ce^{4+}, Mn^{3+}, and Mn^{2+} had ion radii 1.07, 0.87, 1.04, and 0.8^{o}A. It means in the un-treated, air, and also in N_2 the valence cannot reduce. Because air composed with any variation of gas, so it could be assured that reduce the valence of Ce and Mn. Furthermore, N_2 gases is the inert gases which does not undergo chemical reactions under a set of given conditions. When 95%N_2: 5%H_2 was used for the reducing agent, the H_2 gas contributed to the reducing process. Then, the peak will shift to the higher angle, it almost fit with the highest intensity for the crystallite phase of $CaAl_2O_4$ in plane (123).

5.2.2 Morphological analysis

Figure 4.7 in the previous section show the spherical morphology when the specimen annealed in different atmosphere. If it is compared with particle size result (see Figure 5.4), the particle had typical size. The correlation between particle size and atmosphere treatment had been explained by Lin for the gehlenite material (Lin, Shi et al. 2017). In his research, Lin defined that difference atmosphere condition in the annealing process is no significant effect for the particle size.

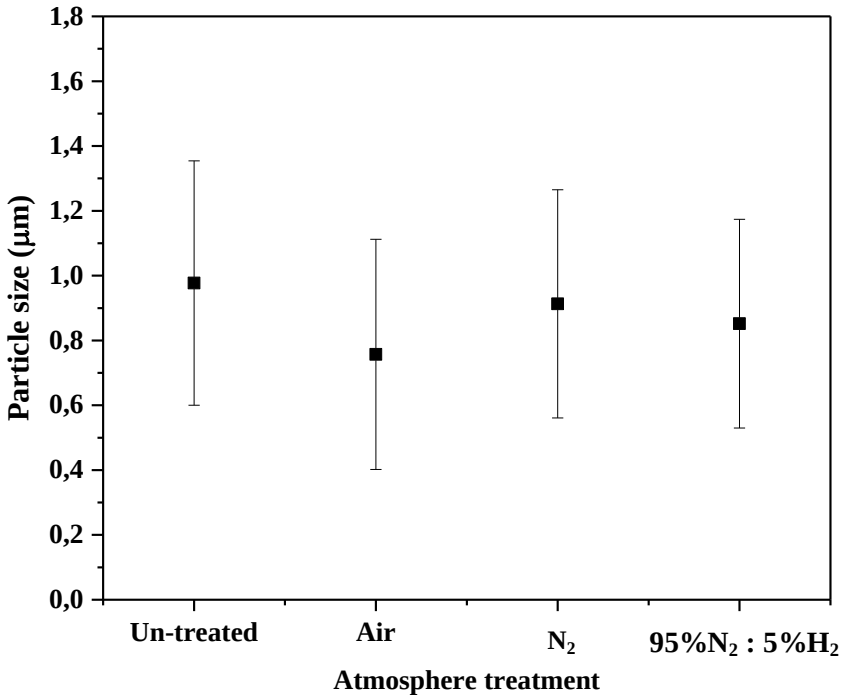

Figure 5.4 Correlation between atmosphere treatment and particle size of 0.5 mol%Ce and 1 mol%Mn^{2+} -doped $CaAl_2O_4$ powder

5.2.3 Photoluminescence analysis

Figure 4.8 and 4.9 show the emission and excitation spectra of 0.5 mol% Ce^{3+} and 1 mol% Mn^{2+}- doped $CaAl_2O_4$ annealed at 800^{o}C in different atmosphere with 5^{o}C/min of heating rate and 1 h holding time. The highest intensity for the peak, which are broad and small peak is the specimen that annealed in 95%N_2:5%H_2. For the un-treated and annealed in air and N_2

specimens, it had a small intensity for the small peak around 450-475nm. The broad peak is correlated with Ce^{3+} in $5d^1$-$4f^1$ transition, and the small peak for the Mn^{2+} which is d-d transition. It means that the reduction process using $95\%N_2$:$5\%H_2$ is more effective than using air and N_2.

Furthermore, as it was mentioned in the previous section, the emission and excitation can be affected by the powder color. The dark color can be due to Mn in higher oxidation states were partially adsorbed by the Mn ions instead of the exciting the Ce ions lowering the emission. The second possibility is that the oxidizing atmosphere, during the annealing step converted part of the Ce^{3+} to Ce^{4+}. Ce ions in tetravalent charge state show no luminescence (Teixeira, Montes et al. 2014). Thus, the excitation spectrum is lower than the other specimen, although the nominal concentration of Ce is the same as in the other co-doped samples.

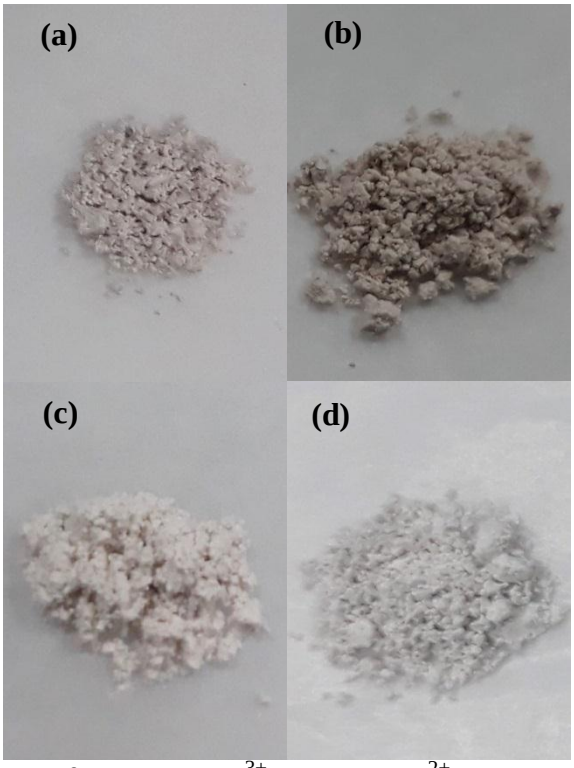

Figure 5.5 The photos of 0.5 mol%Ce^{3+}, 1 mol%Mn^{2+} -doped $CaAl_2O_4$ powder (a) un-treated and with different anneling atmosphere (b) air, (c) N_2, (d) $95\%N_2$:$5\%H_2$ at 800^oC for 1 h

According to the Figure 5.5, for the un-treated and annealed specimen in N_2 has light orange color. Then for the specimen that annealed at air, the color is

darker than the other specimen. It has correlation with excitation and emission intensity, so it cannot had high intensity. In contrast to the powder using 95%N_2:5%H_2 as the annealing atmosphere, it has a white color. So, it can absorb the UV light and emit more efficient that the other specimen.

5.3 Variation of Ce composition

In this section, the effect of Ce^{3+} composition in the 1 mol%Mn^{2+}-doped $CaAl_2O_4$ to the photoluminescence properties will be discussed. The variation of Ce^{3+} that used in this study are 0 mol%, 0.5 mol%, and 1 mol% . As it already shown in previous section, the initial characterization of Ce^{3+} and Mn^{2+}-doped $CaAl_2O_4$ had been conducted using several characterization such as, XRD, SEM, and Spectrofluorocence.

5.3.1 Crystallization of as received Ce^{3+} and Mn^{2+}-doped $CaAl_2O_4$ powder

Based on XRD result of Ce^{3+}, Mn^{2+} -doped $CaAl_2O_4$ with different composition of Ce^{3+}, the maximum composition that allowed for amorphous phase had been known. When 1 mol%Mn doped in $CaAl_2O_4$ and annealed it at 800^{o}C in 95%N_2:5%H_2 the phase is amorphous. This Mn^{2+} will occupy Ca^{2+} site to make unstable condition in hosting material. So, if the energy is given to the material, the electron will be excited to the other layer then it can emit the color. Furthermore, from the Figure 4.6, it can be seen that small amount of Ce^{3+} will not change amorphous phase, but if the composition of Ce^{3+} increase until 1 mol%, the small peak will appear in the broad peak. That peak is belonged to $CaAl_2O_4$. According to the Li, $CaAlSiN_3$: Ce^{3+} was successfully synthesized for WLED application. In his research, Li defined the maximum composition of Ce^{3+} to occupy Ca^{2+} sites are below 1 mol%. It is due to the 1 mol% composition of Ce^{3+} will make second phase or the impurities peak in the XRD pattern (Anwar, Li et al. 2016). In the other research, Cerium phases were found in agreement at higher dopant concentration >4% in the YAG as hosting material (Borlaf, Kubrin et al. 2017). In this study, it can be concluded that the maximum solubility Ce^{3+} in $CaAl_2O_4$ is 0.5 mol%.

5.3.2 Morphological analysis

In the previous section, it already mentioned the morphology of the particle. Spray pyrolysis method had a big contribution to produce the spherical particle. Increasing composition of Ce^{3+} has no effect to the particle shape. For the particle size as is shown in Figure 5.6, there is no significant effect for increasing Ce^{3+} composition until 1 mol%. It is caused by the ion radii of Ce^{3+} has similar size with Ca, 0.107 and 0.98^{o}A. And also for the small amount of Ce^{3+} that was added in the 1%Mn-doped $CaAl_2O_4$.

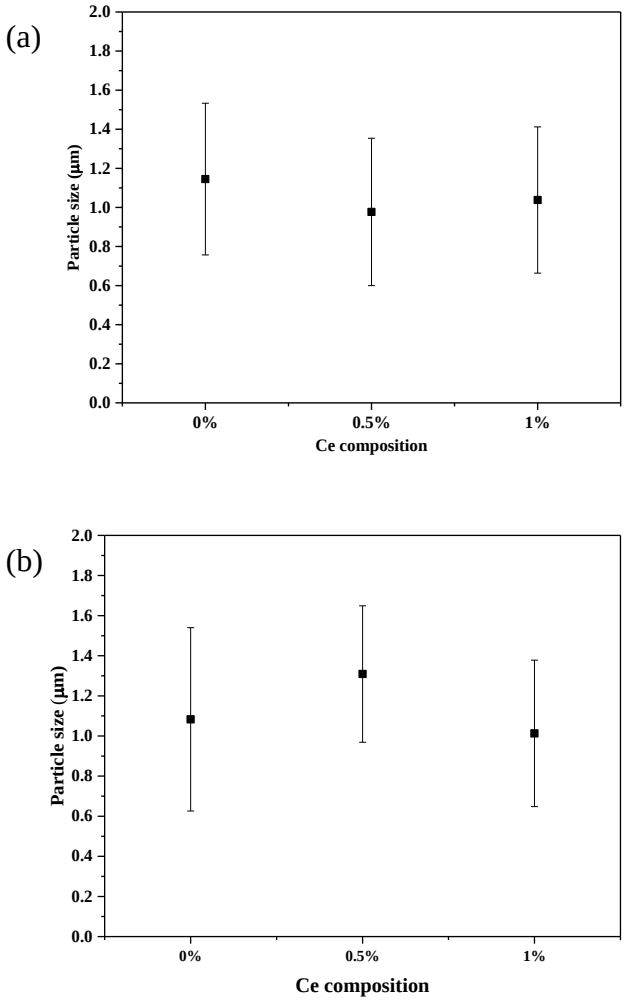

Figure 5.6 Correlation between Ce^{3+} concentration and particle size (a) as-prepared and (b) after annealing

5.3.3 Photoluminescence analysis

There is several factors that affect the photoluminescence properties, one of the factor is the amount of impurities, in this study various composition of Ce^{3+} was used to occupy Ca^{2+} sites in $CaAl_2O_4$. According to Figure 4.17 and 4.18 there is two possibilities to explain the difference intensity of the specimen. First, Mn^{2+} have a lower capability to absorb the UV light [3]. When the specimen only using Mn^{2+} as an activator, it have not strong absorption band. Since every excited level of d^5 is a spin quartet or a doublet, all transition from the ground sextet to them are spin-forbidden. Optical absorption intensity is weak, and the phosphors have no color (although the powder body is white, see Figure 5.7). The $_4A^1$ and $_4E(_4G)$ levels have the same energy and are parallel to the ground level $_6A^1$. The absorption band corresponding to $_6A^1 \rightarrow {}_4A^1$, $_4E(_4G)$ therefore has a narrow bandwidth, lying at ~425 nm, irrespective of the kind of host material. One notices that this band splits into more than one line when carefully investigated. The splitting is considered to reflect the reduction of the crystal field symmetry [3]. In contrast with the other specimen with 0.5 mol% and 1 mol% of Ce^{3+}, it shows the high intensity for broad and narrow peak. The specimens can absorb effectively the UV light and the Mn^{2+} ions transfer the electron through Ce^{3+} ions. Ce^{3+} ion is called sensitizers for the Mn^{2+} luminescence [3].

The second reason is the quenching effect of the Ce^{3+} ions. Each type of hosting material had their own maximum composition for the Ce^{3+} composition. Comparing with the other researcher, Ce^{3+} 2% was used in $Ca_2Al_2SiO_7$ to get the maximum intensity in the crystallite phase [18]. Xu used 1% of Ce as a dopan and mix it with 1.25% Mn in $SrAl_2O_4$ to get the highest intensity in the crystallite phase(Xu, Wang et al. 2011). Lin defined that the hosting material has a saturated composition for the activator (Lin, Shi et al. 2017). Thus, adding a high amount of Ce^{3+} will decrease the emission spectra of specimen. In this study, the maximum composition to increase the emission spectra is 0.5 mol% Ce^{3+} and in 1 mol%Ce^{3+} the emission light start to decrease in the broad peak. In addition, for the shifting in the excitation spectra for 1 mol%Ce^{3+} and 1 mol%Mn^{2+}- doped $CaAl_2O_4$, the possible reason is the highest composition of Ce^{3+} and the other phase in the XRD pattern.

Table 5.1 Comparison powder color before and after annealing of $Ce^{3+}$and Mn^{2+} –doped $CaAl_2O_4$ in different Ce^{3+} composition

Specimen Name	Before Annealing	After Annealing
1 mol%Mn^{2+} –doped $CaAl_2O_4$		
0.5 mol%Ce^{3+} and 1 mol%Mn^{2+} $CaAl_2O_4$		
1 mol%Ce^{3+} and 1 mol%Mn^{2+} $CaAl_2O_4$		

5.4 Variation of Mn composition

In this following section, the effect of Mn^{2+} composition in the 0.5 mol%Ce^{3+}-doped $CaAl_2O_4$ to the photoluminescence properties will be discussed. The variation of Mn^{2+} that used in this study are 0 mol%, 1 mol%, 3 mol%, and 5 mol%. As it already shown in previous section, the initial characterization of Ce^{3+} and Mn^{2+}-doped $CaAl_2O_4$ with different Mn^{2+} composition had been conducted using several characterization such as, XRD, SEM, and Spectrofluorocence.

5.4.1 Crystallization of as received Ce^{3+} and Mn^{2+}-doped $CaAl_2O_4$ powder

Based on XRD result of Ce^{3+} and Mn^{2+} -doped $CaAl_2O_4$ with different composition of Mn^{2+}, the maximum composition of Mn^{2+} that allowed for amorphous phase is 3 mol%. The specimen that has no Mn^{2+} composition show the amorphous phase. The uniform diffraction pattern show that the incorporation of Ce^{3+} and Mn^{2+} have dissolve completely in the $CaAl_2O_4$ host. However, when the Mn^{2+} was added to the 0.5 mol%Ce^{3+} –doped $CaAl_2O_4$ until 5 mol%, the phase changed to crystallite phase. Several peaks appear that belong to $CaAl_2O_4$. It means 5 mol% of Mn^{2+} is the saturated composition to add in the $CaAl_2O_4$ as a hosting material. Thus, the Mn^{2+} ions cannot occupy the Ca^{2+} sites and it makes a new phase. It also caused by changing the crystalline temperature when the composition of the specimen was changed.

5.4.2 Morphological analysis

In the previous section, it already mentioned the morphology of the particle. Spray pyrolysis method had a big contribution to produce the spherical particle. Increasing composition of Mn^{2+} have no effect to the particle shape. For the particle size as is shown in Figure 5.8 there is no significant effect for increasing Mn^{2+} composition until 5 mol%. It is caused by the ion radii of Mn^{2+} has similar size with Ca^{2+}, 0.8 and 0.98^{o}A.

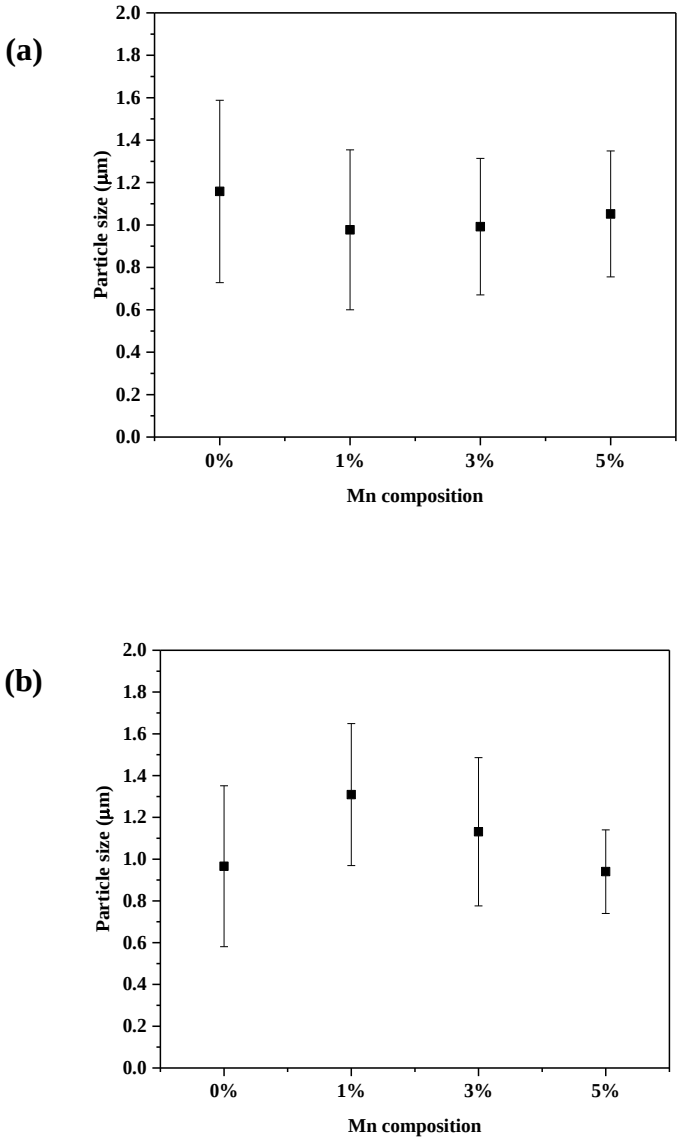

Figure 5.8 Correlation between Mn^{2+} composition and particle size (a) as-prepared and (b) after annealing

5.4.3 Photoluminescence analysis

According to the emission and excitation spectra Figure 4.20 and 4.21, the highest intensity for the blue-green region can be shown. In the emission spectra, the highest intensity for the green region at wavelength 450-475 nm is 0.5 mol%Ce^{3+} and 1 mol%Mn^{2+} –doped $CaAl_2O_4$. From the emission spectra the Ce^{3+} characteristic emission is observed at 325-425 nm (Xu, Wang et al. 2011, Teixeira, Montes et al. 2014, Chen, Lv et al. 2016, Lin, Hu et al. 2016, Liu, Yin et

al. 2016, Wang, Wang et al. 2016, Yang, Kim et al. 2016, Zhou, Wang et al. 2016, Puchalska and Zych 2017). In accordance Table 5.1 , there is a shifting peak to the left in the broad peak region at 325-425 nm due to increasing the Mn^{2+} composition. Beside this emission, a small band can be seen at 450-475 nm. There is a small shifting peak to the right, for the specimen with 0 mol%Mn^{2+} and the specimen that adding Mn^{2+} in different composition. This fact can be interpreted theoretically. Yen defined that at higher Nd, an excitation bound to a donor collides with other donors. Donor electrons can thus be virtually excited and can exert the screening effect on the bound excitation through changes of the dielectric constant. This brings about high energy shift of the emission peak. The asymmetry of the spectral shape with long tails is interpreted as being caused by the Stark effect due to ionized impurities, i.e, compensated donors and acceptors (Yen, Shionoya et al. 2007).

As shown in the emission spectra with increasing Mn^{2+} content, the PL intensity of Mn^{2+} increases systematically until the quenching composition in 5 mol%Mn^{2+}, whereas the intensity of the blue band was found to decrease proportionally. However, the intensity of 0.5 mol%Ce^{3+}-doped $CaAl_2O_4$ is not highest than 0.5 mol%Ce^{3+} and 1 mol%Mn^{2+} –doped $CaAl_2O_4$. It is caused by the powder color of 0.5 mol%Ce^{3+}-doped $CaAl_2O_4$ is quite dark than the other specimen. The possible reason is caused by impurities when it annealed at 800^{o}C in 95%N_2: 5%H_2 (see Figure 5.9).

Table 5.2 Shifting intensity broad peak at λex=273 nm

Mn Composition	**Wavelength (nm)**	**PL intensity**
0%	397	55383
1%	397	741.81
3%	396	593.71
5%	371	553.53

Table 5.3 Comparisom powder color before and after annealing of Ce^{3+} and Mn^{2+} –doped $CaAl_2O_4$ in different Mn^{2+} composition

Specimen name	Before Annealing	After Annealing
0.5 mol% Ce^{3+} - doped $CaAl_2O_4$		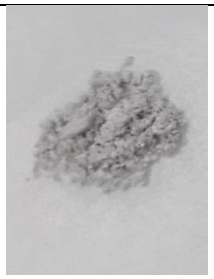
0.5 mol%Ce^{3+} and 1 mol%Mn^{2+} – doped $CaAl_2O_4$		
0.5 mol%Ce^{3+} and 3 mol%Mn^{2+} - doped $CaAl_2O_4$		
0.5 mol%Ce^{3+} and 5 mol%Mn^{2+} - doped $CaAl_2O_4$		

CHAPTER 6
CONCLUSIONS

The conclusions of this study are:

1. The Ce^{3+} and Mn^{2+} -doped $CaAl_2O_4$ glassy powder were successfully synthesized using spray pyrolysis method.
2. XRD patterns show that the amorphous phase was obtained by Ce, Mn doped $CaAl_2O_4$ phosphor powders with annealing in 600, 700, 800°C for 1h.
3. From SEM images, the particle shape is spherical after annealed at 600, 700, 800, and 900^oC in N_2:H_2 (95:5) atmosphere.
4. The maximum temperature for amorphous phase and high photoluminescence of Ce^{3+} and Mn^{2+} -doped $CaAl_2O_4$ powder is 800^oC.
5. XRD patterns show that the amorphous phase can be gotten by Ce, Mn doped $CaAl_2O_4$ powders with annealing at 800°C for 1h in air, N_2, and N_2:H_2 (95:5).
6. The best atmosphere to get the highest intensity of Ce^{3+} and Mn^{2+} -doped $CaAl_2O_4$ powder is 95%N_2: 5%H_2.
7. The various composition of Ce^{3+} and Mn^{2+} in the $CaAl_2O_4$ have different effect of photoluminescence.
8. The maximum composition of Ce in $CaAl_2O_4$ for amorphous phase and to enhance the photoluminescene properties is 0.5%.
9. The maximum composition of Mn in $CaAl_2O_4$ for amorphous phase and to enhance the photoluminescene properties is 1%.
10. The maximum composition to increase the intensity of the blue-green light is 0.5 mol%Ce^{3+} and 1 mol%Mn^{2+} in $CaAl_2O_4$.

(*This page intentionally left blank*)

CHAPTER 7
FUTURE WORKS

1. From this study, the best composition of Ce^{3+} and Mn^{2+} were investigated. Hence, the valence of Ce^{3+} and Mn^{2+} must be known to compare it with electron transfer phenomenon using XPS.
2. The other parameter can be used to increase the photoluminescence properties of the material, such us using different concentration of solution to know the best intensity.
3. The morphology of the material is spherical. The morphology can be design to become hollow or porous. Thus, the material can be easily to mix with binder in the security label application.

(*This page intentionally left blank*)

REFERENCES

Andres, J., R. D. Hersch, J. E. Moser and A. S. Chauvin (2014). "A New Anti-Counterfeiting Feature Relying on Invisible Luminescent Full Color Images Printed with Lanthanide-Based Inks." Advanced Functional Materials **24**(32): 5029-5036.

Anwar, T., W. Li, N. Hussain, W. Chen, R. U. R. Sagar and L. Tongxiang (2016). "Effect of annealing atmosphere induced crystallite size changes on the electrochemical properties of TiO_2 nanotubes arrays." Journal of Electrical Engineering **4**: 43-51.

Bernardo, E., L. Fiocco, A. Prnová, R. Klement and D. Galusek (2014). "Gehlenite: Eu^{3+} phosphors from a silicone resin and nano-sized fillers." Optical Materials **36**(7): 1243-1249.

Bharathan, J. and Y. Yang (1998). "Polymer electroluminescent devices processed by inkjet printing: I. Polymer light-emitting logo." Applied Physics Letters **72**(21): 2660-2662.

Bian, X. and J. Zhang (2018). "White-light emission in a single-phase $Ca_{9.3}Mg_{0.7}K(PO_4)_7$: Eu^{2+}, Tb^{3+}, Mn^{2+} phosphor for light-emitting diodes." Journal of Luminescence **194**: 334-340.

Borlaf, M., R. Kubrin, V. Aseev, A. Y. Petrov, N. Nikonorov and T. Graule (2017). "Deep submicrometer YAG: Ce phosphor particles with high photoluminescent quantum yield prepared by flame spray synthesis." Journal of the American Ceramic Society **100**(8): 3784-3793.

Briois, V., C. Williams, H. Dexpert, F. Villain, B. Cabane, F. Deneuve and C. Magnier (1993). "Formation of solid particles by hydrolysis of cerium (IV) sulphate." Journal of materials science **28**(18): 5019-5031.

Britannica, T. E. o. E. (2015). "Thermoluminescence." Retrieved June 26, 2018, from https://www.britannica.com/science/thermoluminescence.

Brito, V. R. S., R J dos Santos, P N M dos Anjos (2016). "Thermal and optical analysis of the dopan Cerium Calcium Aluminate obtained by the gel process using ethylenediamine tetraacetic acid." Biological and Chemical Research **3**: 5.

Cao, R., W. Wang, J. Zhang, S. Jiang, Z. Chen, W. Li and X. Yu (2017). "Synthesis and luminescence properties of Li_2SnO_3: Mn^{4+} red-emitting phosphor for solid-state lighting." Journal of Alloys and Compounds **704**: 124-130.

Cao, R., Y. Ye, Q. Peng, G. Zheng, H. Ao, J. Fu, Y. Guo and B. Guo (2017). "Synthesis and luminescence characteristics of novel red-emitting $Ba_2TiGe_2O_8$: Mn^{4+} phosphor." Dyes and Pigments **146**: 14-19.

Cao, R., F. Zhang, C. Cao, X. Yu, A. Liang, S. Guo and H. Xue (2014). "Synthesis and luminescence properties of $CaAl_2O_4$: Mn^{4+} phosphor." Optical Materials **38**: 53-56.

Cao, R., J. Zhang, W. Wang, Z. Hu, T. Chen, Y. Ye and X. Yu (2016). Preparation and photoluminescence characteristics of $Li_2Mg_3SnO_6:Mn^{4+}$ deep red phosphor.

Cao, Y., N. Liu, J. Tian and X. Zhang (2016). "Solid state synthesis and tunable luminescence of $LiSrPO_4$: $Eu^{2+}/Mn^{2+}/Tb^{3+}$ phosphors." Polyhedron **107**: 78-82.

Chen, C.-Y., T.-K. Tseng, C.-Y. Tsay and C.-K. Lin (2008). "Formation of irregular nanocrystalline CeO_2 particles from acetate-based precursor via spray pyrolysis." Journal of Materials Engineering and Performance **17**(1): 20-24.

Chen, X., F. Lv, P. Li and Y. Zhang (2016). "Synthesis and tunable luminescence of RbCaGd $(PO_4)_2$: Ce^{3+}, Mn^{2+} phosphors." Optical Materials **54**: 276-281.

Cui, B., Z. Chen, Q. Zhang, H. Wang and Y. Li (2017). "A single-composition $CaSi_2O_2N_2$: RE (RE= Ce^{3+}/Tb^{3+}, Eu^{2+}, Mn^{2+}) phosphor nanofiber mat: Energy transfer, luminescence and tunable color properties." Journal of Solid State Chemistry **253**: 263-269.

Darshan, G., H. Premkumar, H. Nagabhushana, S. Sharma, S. Prashantha, H. Nagaswarup and B. D. Prasad (2016). "Blue light emitting ceramic nano-pigments of Tm^{3+} doped $YAlO_3$: Applications in latent finger print, anti-counterfeiting and porcelain stoneware." Dyes and Pigments **131**: 268-281.

Desai, P. G., Z. Xu and J. A. Lewis (1995). "Synthesis and Properties of $CaAl_2O_4$-Coated AI_2O_3 Microcomposite Powders." Journal of the American Ceramic Society **78**(11): 2881-2888.

Douy, A. and M. Gervais (2000). "Crystallization of amorphous precursors in the calcia–alumina system: a differential scanning calorimetry study." Journal of the American Ceramic Society **83**(1): 70-76.

Fan, J., J. Gou, Y. Chen, B. Yu and S. Liu (2017). Enhanced luminescence and tunable color of $Sr_8CaSc(PO_4)_7$:Eu^{2+} , Ce^{3+} , Mn^{2+} phosphor by energy transfer between Ce^{3+} -Eu^{2+} -Mn^{2+}.

Freeda, M. and T. Subash (2017). "Comparision of Photoluminescence studies of Lanthanum, Terbium doped Calcium Aluminate nanophosphors ($CaAl_2O_4$: La, $CaAl_2O_4$: Tb) by sol-gel method." Materials Today: Proceedings **4**(2): 4302-4307.

Freeda, M. and T. Subash (2017). "Optical Characterization of Dysporsium doped Calcium Aluminate Nanophosphor ($CaAl_2O_4$: Dy) by sol-gel method." Materials Today: Proceedings **4**(2): 4290-4301.

Freeda, M. and T. Subash (2017). "Photoluminescence studies of Terbium doped Calcium Aluminate nanophosphors ($CaAl_2O_4$: Tb) synthesized by sol-gel method." Materials Today: Proceedings **4**(2): 4283-4289.

Freeda, M. and T. Subash (2017). "Preparation and Characterization of Praseodymium doped Calcium Aluminate nanophosphor ($CaAl_2O_4$: Pr) by sol-gel method." Materials Today: Proceedings **4**(2): 4266-4273.

Freeda, M. and G. Suresh (2017). "Structural and Luminescent properties of Eu-doped $CaAl_2O_4$ Nanophosphor by sol-gel method." Materials Today: Proceedings **4**(2): 4260-4265.

Fu, C., H. Dong, C. Liu and Y. Wang (2010). "Synthesis, structure and luminescence properties of phosphor $CaAl_2O_4$ activated by Tb_{3+}." Optoelectronics Adv. Materials Rapid Commun **4**: 73-76.

Fumo, D., M. Morelli and A. Segadaes (1996). "Combustion synthesis of calcium aluminates." Materials Research Bulletin **31**(10): 1243-1255.

Guilbault, G. G. (1967). Fluorescence: theory, instrumentation, and practice, E. Arnold.

Guo, K., M.-L. Huang, H.-H. Chen, X.-X. Yang and J.-T. Zhao (2012). "Comparative study on photoluminescence of amorphous and nano-crystalline YAG: Tb phosphors prepared by a combustion method." Journal of Non-Crystalline Solids **358**(1): 88-92.

Igarashi, T., M. Ihara, T. Kusunoki, K. Ohno, T. Isobe and M. Senna (2000). "Relationship between optical properties and crystallinity of nanometer Y_2O_3: Eu phosphor." Applied Physics Letters **76**(12): 1549-1551.

Iso, Y., S. Takeshita and T. Isobe (2014). "Effects of annealing on the photoluminescence properties of citrate-capped YVO_4: Bi^{3+}, Eu^{3+} nanophosphor." The Journal of Physical Chemistry C **118**(20): 11006-11013.

Jia, D., R. Meltzer, W. Yen, W. Jia and X. Wang (2002). "Green phosphorescence of $CaAl_2O_4$: Tb^{3+}, Ce^{3+} through persistence energy transfer." Applied physics letters **80**(9): 1535-1537.

Jin, L., L. Yuanyuan, Z. Zhiyong, Y. Junfeng, Z. Wu, Y. Jiangni and Z. Chunxue (2017). "Effect of Annealing Temperature on Photoluminescence of ZnO/Graphene Nano-films Deposited by Sol-gel Method." Rare Metal Materials and Engineering **46**(4): 888-892.

Katsumata, T., T. Nabae, K. Sasajima and T. Matsuzawa (1998). "Growth and characteristics of long persistent $SrAl_2O_4$-and $CaAl_2O_4$-based phosphor crystals by a floating zone technique." Journal of Crystal Growth **183**(3): 361-365.

Kubrin, R. (2014). "Nanophosphor coatings: Technology and applications, opportunities and challenges." KONA Powder and Particle Journal **31**: 22-52.

Kumar, P., S. Singh and B. K. Gupta (2016). "Future prospects of luminescent nanomaterial based security inks: from synthesis to anti-counterfeiting applications." Nanoscale **8**(30): 14297-14340.

Kusriantoko, P. (2015). Degradation behavior and bioactivity of various compositional mesoporous bioactive glasses. Master Degree, NTUST.

Ligler, F. S. and C. R. Taitt (2011). Optical biosensors: today and tomorrow, Elsevier.

Lin, J., Y. Hu, L. Chen, Z. Wang and S. Zhang (2016). "Luminescence and energy transfer properties of $Sr_3Y(PO_4)_3$: Ce^{3+}, Mn^{2+} phosphors." Physica B: Condensed Matter **485**: 39-44.

Lin, K.-S. and S. Chowdhury (2010). "Synthesis, characterization, and application of 1-D cerium oxide nanomaterials: a review." International journal of molecular sciences **11**(9): 3226-3251.

Lin, L., R. Shi, R. Zhou, Q. Peng, C. Liu, Y. Tao, Y. Huang, P. Dorenbos and H. Liang (2017). "The Effect of Sr^{2+} on Luminescence of Ce^{3+}-Doped (Ca, Sr)$_2Al_2SiO_7$." Inorganic chemistry **56**(20): 12476-12484.

Lin, Y. H., M. Li, C. W. Nan and Z. Zhang (2007). "Tunable Trap Levels Observed in La and Eu Codoped $CaAl_2O_4$-Based Phosphor." Journal of the American Ceramic Society **90**(9): 2992-2994.

Liu, Q., H. Yin, T. Liu, C. Wang, R. Liu, W. Lü and H. You (2016). "Luminescent properties and energy transfer of CaO: Ce^{3+}, Mn^{2+} phosphors for white LED." Journal of Luminescence **177**: 349-353.

Massiot, D., D. Trumeau, B. Touzo, I. Farnan, J.-C. Rifflet, A. Douy and J.-P. Coutures (1995). "Structure and dynamics of $CaAl_2O_4$ from liquid to glass: A high-temperature 27Al NMR time-resolved study." The Journal of Physical Chemistry **99**(44): 16455-16459.

Meng, X., K. Qiu, Z. Tian, X. Shi, J. You, Z. Wang, P. Li and Z. Yang (2017). "Tunable-emission single-phase phosphors $Ba_3Ca_2(PO4)_3F$: M (M= Ce^{3+}, Eu^{2+}, Mn^{2+}): Crystal structure, luminescence and energy transfer." Journal of Alloys and Compounds **719**: 322-330.

Mercury, J. R., A. De Aza and P. Pena (2005). "Synthesis of $CaAl_2O_4$ from powders: Particle size effect." Journal of the European Ceramic Society **25**(14): 3269-3279.

Messing, G. L., S. C. Zhang and G. V. Jayanthi (1993). "Ceramic powder synthesis by spray pyrolysis." Journal of the American Ceramic Society **76**(11): 2707-2726.

Mishra, G. C., K. K. Satapathy, S. J. Dhoble and R. S. Kher (2017). "Urea assisted self combustion synthesis of $CaAl_2O_4$: Eu phosphor and its mechanoluminescence characterization." New Journal of Chemistry **41**(5): 2193-2197.

Park, K., H. Kim and D. Hakeem (2017). "Effect of host composition and Eu3+ concentration on the photoluminescence of aluminosilicate (Ca, Sr)$_2Al_2SiO_7$: Eu^{3+} phosphors." Dyes and Pigments **136**: 70-77.

Park, S., S. Koh and H. Kim (2017). "Single-phase Ce^{3+}–Mn^{2+}–Tb^{3+} tri–codoped barium–yttrium–silicate phosphors." Displays **48**: 29-34.

Peng, M. and G. Hong (2007). "Reduction from Eu^{3+} to Eu^{2+} in $BaAl_2O_4$: Eu phosphor prepared in an oxidizing atmosphere and luminescent properties of BaAl2O4: Eu." Journal of Luminescence **127**(2): 735-740.

Penghui, Y., Y. Xue, Y. Hongling, T. Jiang, Z. Dacheng and Q. Jianbei (2012). "Effects of crystal field on photoluminescence properties of $Ca_2Al_2SiO_7$: Eu^{2+} phosphors." Journal of Rare Earths **30**(12): 1208-1212.

Puchalska, M. and E. Zych (2017). "Ce^{3+}-sensitized red Mn^{2+} luminescence in calcium aluminoborate phosphor material." Optical Materials **74**: 2-11.

Revupriya, M. R., P S Anjana, R Divya and N. Gopakumar (2017). "Synthesis and characterization of $CaAl_2O_4$ Dy^{3+} ceramic." International Journal of Advance in Science and Engineering **03**(6): 6.

Ronda, C. Luminescence: From Theory to Applications. 2008, Wiley-VCH.

Rong, M., X. Zhou, R. Xiong, N. Wang, Q. Wang and Z. Wang (2017). "Luminescent properties and application of Rb_2GeF_6: Mn^{4+} red phosphor." Materials Letters **207**: 206-208.

Sanguinetti, S., M. Guzzi and M. Gurioli (2008). Accessing structural and electronic properties of semiconductor nanostructures via photoluminescence. Characterization of Semiconductor Heterostructures and Nanostructures, Elsevier**:** 175-208.

Satapathy, K., G. Mishra, R. Kher and S. Dhoble (2015). "Mechanoluminescence and thermoluminescence characterization of Tb^{3+} doped $CaAl_2O_4$: A theoretical and experimental study." RSC Advances **5**(97): 79391-79396.

Sathaporn, T. and S. Niyomwas (2011). "Synthesis and characterization of MAl_2O_4 (M= Ba, Ca, Sr) phosphor by self-propagating high temperature synthesis." Energy Procedia **9**: 410-417.

Shashikala, B., H. Premkumar, G. Darshan, H. Nagabhushana, S. Sharma, S. Prashantha and H. Nagaswarupa (2017). "Synthesis and Photoluminescence Studies of an Orange Red Color Emitting novel $CaAl_2O_4$: Sm^{3+} nanophosphor for LED Applications." Materials Today: Proceedings **4**(11): 11820-11826.

Shih, S.-J., Y.-J. Chou, A. Hadush, S.-H. Lin and C.-W. Hsiao (2018). "Morphology Control of Eu-Doped Amorphous Gehlenite Phosphors Prepared by Spray Pyrolysis." Journal of nanoscience and nanotechnology **18**(8): 5849-5853.

Shih, S.-J., Y.-C. Lin, S.-H. Lin, P. Veteška, D. Galusek and W.-H. Tuan (2016). "Preparation and characterization of Eu-doped gehlenite glassy particles using spray pyrolysis." Ceramics International **42**(9): 11324-11329.

Shih, S.-J., Y.-Y. Wu and K. B. Borisenko (2011). "Control of morphology and dopant distribution in yttrium-doped ceria nanoparticles." Journal of Nanoparticle Research **13**(12): 7021-7028.

Shih, S.-J., Y.-Y. Wu, C.-Y. Chen and C.-Y. Yu (2012). "Morphology and formation mechanism of ceria nanoparticles by spray pyrolysis." Journal of Nanoparticle Research **14**(5): 879.

Shih, S.-J., Y.-Y. Wu, Y.-J. Chou and K. B. Borisenko (2012). "Nanoscale control of composition in cerium and zirconium mixed oxide nanoparticles." Materials Chemistry and Physics **135**(2-3): 749-754.

Shih, S. and J. Huang (2013). "Designing the morphology of ceria particles by precursor complexes." Ceramics International **39**(3): 2275-2281.

Shinde, K. N., S. Dhoble, H. Swart and K. Park (2012). Basic mechanisms of photoluminescence. Phosphate Phosphors for Solid-State Lighting, Springer**:** 41-59.

Shiri, S., M. Abbasi, A. Monshi and F. Karimzadeh (2014). "Synthesis of the $CaAl_2O_4$ nanoceramic compound using high-energy ball milling with subsequent annealing." Advanced Powder Technology **25**(1): 338-341.

Sohn, K.-S., B. Cho, H. D. Park, Y. G. Choi and K. H. Kim (2000). "Effect of heat treatment on photoluminescence behavior of Zn_2SiO_4: Mn phosphors." Journal of the European Ceramic Society **20**(8): 1043-1051.

Souza, N., D. Silva, D. Sampaio, M. Rezende, C. Kucera, A. Trofimov, L. Jacobsohn, J. Ballato and R. Silva (2017). "Laser sintering of persistent luminescent $CaAl_2O_4$: Eu^{2+} Dy^{3+} ceramics." Optical Materials **68**: 2-6.

Sun, X.-Y., Z. He and X. Gu (2018). "Synthesis, deep red emission and warm WLED applications of K_2SiF_6: Mn^{4+} phosphors." Journal of Photochemistry and Photobiology A: Chemistry **350**: 69-74.

Suriyamurthy, N. and B. Panigrahi (2007). "Luminescence of $BaAl_2O_4$: Mn^{2+}, Ce^{3+} phosphor." Journal of Luminescence **127**(2): 483-488.

Tang, C. W., S. A. VanSlyke and C. Chen (1989). "Electroluminescence of doped organic thin films." Journal of Applied Physics **65**(9): 3610-3616.

Teixeira, V., P. Montes and M. Valerio (2014). "Structural and optical characterizations of $Ca_2Al_2SiO_7$: Ce^{3+}, Mn^{2+} nanoparticles produced via a hybrid route." Optical Materials **36**(9): 1580-1590.

Venkatachalaiah, K., H. Nagabhushana, G. Darshan, R. Basavaraj and B. D. Prasad (2017). "Novel and highly efficient red luminescent sensor based $SiO_2@Y_2O_3$: Eu^{3+}, M^+ (M^+= Li, Na, K) composite core–shell fluorescent markers for latent fingerprint recognition, security ink and solid state lightning applications." Sensors and Actuators B: Chemical **251**: 310-325.

Wako, A. H. (2011). Preparation and Properties of Long Afterglow $CaAl_2O_4$ Phosphors Activated by Rare Earth Metal Ions, University of the Free State Republic of South Africa.

Wang, F., W. Wang and Y. Jin (2016). "Photoluminescence properties of Ce^{3+}/Mn^{2+} doped calcium zirconium silicate phosphors with energy transfer for white LEDs." Ceramics International **42**(15): 16626-16632.

Wang, X.-J., D. Jia and W. M. Yen (2003). "Mn^{2+} activated green, yellow, and red long persistent phosphors." Journal of Luminescence **102**: 34-37.

Wei, Y., Z. Wu, Y. Jia and Y. Liu (2015). "Piezoelectrically-induced stress-luminescence phenomenon in $CaAl_2O_4$: Eu^{2+}." Journal of Alloys and Compounds **646**: 86-89.

Wu, H., Y. Hu, G. Ju, L. Chen, X. Wang and Z. Yang (2011). "Photoluminescence and thermoluminescence of Ce^{3+} and Eu2+ in Ca2Al2SiO7 matrix." Journal of Luminescence **131**(12): 2441-2445.

Xu, H., L. Wang, X. Ma, R. Houzong, Q. Sun, D. Qu and J. Shi (2018). "A novel Mn (II)-based green phosphor and its self-reduction mechanism." Journal of Luminescence **194**: 303-310.

Xu, X., Y. Wang, X. Yu, Y. Li and Y. Gong (2011). "Investigation of Ce–Mn energy transfer in $SrAl_2O_4$: Ce^{3+}, Mn^{2+}." Journal of the American Ceramic Society **94**(1): 160-163.

Xu, X., X. Yu, D. Zhou and J. Qiu (2013). "A potential tunable blue-to-white-emitting phosphor CAO: Eu, Mn for ultraviolet light emitting diodes." Materials Research Bulletin **48**(6): 2390-2392.

Yang, S., G. Xiao, D. Ding, Y. Ren, L. Lv, P. Yang and J. Gao (2018). "Solid-phase combustion synthesis of calcium aluminate with $CaAl_2O_4$ nanofiber structures." Ceramics International **44**(6): 6186-6191.

Yang, S., G. Xiao, D. Ding, Y. Ren, L. Lv, P. Yang and J. Gao (2018). "Solid-phase combustion synthesis of calcium aluminate with $CaAl_2O_4$ nanofiber structures." Ceramics International.

Yang, W., S.-H. Kim and S. Park (2016). "Multi-color tunable Ce^{3+}–Mn^{2+} cooperative $Y_7O_6F_9$ vernier phosphors." Journal of Alloys and Compounds **673**: 1-7.

Yen, W., S. Shionoya and H. Yamamoto (2007). "Phosphor Handbook CRC Press." Boca Raton.

Yuan, Y., W. Jian, W. Jidong, L. Jing, Z. Yanan, L. Xiaoqiang, S. Xiaolei and G. Mingqiao (2017). "Structural characterization and optical properties of long-lasting $CaAl_2O_4$: Eu^{2+}, Nd^{3+} phosphors synthesized by microwave-assisted chemical co-precipitation." Journal of Rare Earths **35**(7): 652-657.

Zhang, J., Z. Hua and H. Jiao (2017). Investigation on photoluminescence of $Ca_2Gd_8(SiO_4)_6O_2$:Ce^{3+} ,Tb^{3+} ,Mn^{2+} phosphors.

Zhang, S., Y. Li, Y. Lv, L. Fan, Y. Hu and M. He (2017). "A full-color emitting phosphor $Ca_9Ce(PO_4)_7$: Mn^{2+}, Tb^{3+}: Efficient energy transfer, stable thermal stability and high quantum efficiency." Chemical Engineering Journal **322**: 314-327.

Zhang, Z.-w., J.-w. Hou, J. Li, X.-y. Wang, X.-y. Zhu, H.-x. Qi, R.-j. Lv and D.-j. Wang (2016). "Tunable luminescence and energy transfer properties of $LiSrPO_4$: Ce^{3+}, Tb^{3+}, Mn^{2+} phosphors." Journal of Alloys and Compounds **682**: 557-564.

Zhang, Z., H. Zhong, S. Yang and X. Chu (2017). "Tunable luminescence and energy transfer properties of $Ca_{19}Mg_2(PO_4)_{14}$: Ce^{3+}, Tb^{3+}, Mn^{2+} phosphors." Journal of Alloys and Compounds **708**: 671-677.

Zhou, J., T. Wang, X. Yu, D. Zhou and J. Qiu (2016). "The synthesis and photoluminescence of a single-phased white-emitting $NaAlSiO_4$: Ce^{3+}, Mn^{2+} phosphor for WLEDs." Materials Research Bulletin **73**: 1-5.

(*This page intentionally left blank*)

APPENDIXES

A. Decomposition of precurssor

The chemical reaction process for pure $CaAl_2O_4$

$$Ca(NO_3)_2 + 2Al(NO_3)_3 + 4H_2O \rightarrow CaAl_2O_4 + 8HNO_3$$

In 1000 mL DI water

gr $Ca(NO_3)_2$ = n x MW $Ca(NO_3)_2$ = 0.1 mol x 236.15 = 23.615 gr

gr $Al(NO_3)_3$ = n x MW $Al(NO_3)_3$ = 2 x 0.1 mol x 375.13= 75.026 gr

Ca in $CaAl_2O_4$ was substituted with 0.5 mol% Ce^{3+}

In 1000 mL DI water

gr $Ca(NO_3)_2$ = n x MW $Ca(NO_3)_2$ = 0.1 mol x 236.15 x 0.995 = 23.496 gr

gr $Al(NO_3)_3$ = n x MW $Al(NO_3)_3$ = 2 x 0.1 mol x 375.13 = 75.026 gr

gr $Ce(NO_3)_3$ = n x MW $Ce(NO_3)_3$ = 0.1 mol x 434.22 x 0.005 = 0.217 gr

Ca in $CaAl_2O_4$ was substituted with 1 mol% Mn^{2+}

In 1000 mL DI water

gr $Ca(NO_3)_2$ = n x MW $Ca(NO_3)_2$ = 0.1 mol x 236.15 x 0.99 = 23.378 gr

gr $Al(NO_3)_3$ = n x MW $Al(NO_3)_3$ = 2 x 0.1 mol x 375.13 = 75.026 gr

gr $Mn(NO_3)_2$ = n x MW $Mn(NO_3)_2$ = 0.1 mol x 178.95 x 0.01 = 0.178 gr

Ca in $CaAl_2O_4$ was substituted with 0.5 mol% Ce^{3+} and 1 mol% Mn^{2+}

gr $Ca(NO_3)_2$ = n x MW $Ca(NO_3)_2$ = 0.1 mol x 236.15 x 0.985 = 23.260 gr

gr $Al(NO_3)_3$ = n x MW $Al(NO_3)_3$ = 2 x 0.1 mol x 375.13 = 75.026 gr

gr $Ce(NO_3)_3$ = n x MW $Ce(NO_3)_3$ = 0.1 mol x 434.22 x 0.005 = 0.217 gr

gr $Mn(NO_3)_2$ = n x MW $Mn(NO_3)_2$ = 0.1 mol x 178.95 x 0.01 = 0.178 gr

Ca in $CaAl_2O_4$ was substituted with 1 mol% Ce^{3+} and 1 mol% Mn^{2+}

gr $Ca(NO_3)_2$ = n x MW $Ca(NO_3)_2$ = 0.1 mol x 236.15 x 0.98 = 23.142 gr

gr $Al(NO_3)_3$ = n x MW $Al(NO_3)_3$ = 2 x 0.1 mol x 375.13 = 75.026 gr

gr $Ce(NO_3)_3$ = n x MW $Ce(NO_3)_3$ = 0.1 mol x 434.22 x 0.01 = 0.434 gr

gr $Mn(NO_3)_2$ = n x MW $Mn(NO_3)_2$ = 0.1 mol x 178.95 x 0.01 = 0.178 gr

Ca in $CaAl_2O_4$ was substituted with 0.5 mol% Ce^{3+} and 3 mol% Mn^{2+}

gr $Ca(NO_3)_2$ = n x MW $Ca(NO_3)_2$ = 0.1 mol x 236.15 x 0.965 = 22.788 gr

gr $Al(NO_3)_3$ = n x MW $Al(NO_3)_3$ = 2 x 0.1 mol x 375.13 = 75.026 gr

gr $Ce(NO_3)_3$ = n x MW $Ce(NO_3)_3$ = 0.5 mol x 434.22 x 0.005 = 0.217 gr

gr $Mn(NO_3)_2$ = n x MW $Mn(NO_3)_2$ = 0.1 mol x 178.95 x 0.03 = 0.536 gr

Ca in $CaAl_2O_4$ was substituted with 0.5 mol% Ce^{3+} and 5 mol% Mn^{2+}

gr $Ca(NO_3)_2$ = n x MW $Ca(NO_3)_2$ = 0.1 mol x 236.15 x 0.945 = 22.316 gr

gr $Al(NO_3)_3$ = n x MW $Al(NO_3)_3$ = 2 x 0.1 mol x 375.13 = 75.026 gr

gr $Ce(NO_3)_3$ = n x MW $Ce(NO_3)_3$ = 0.5 mol x 434.22 x 0.005 = 0.217 gr

gr $Mn(NO_3)_2$ = n x MW $Mn(NO_3)_2$ = 0.1 mol x 178.95 x 0.05 = 0.894 gr

B. XRD data of $CaAl_2O_4$ for crystallite phase

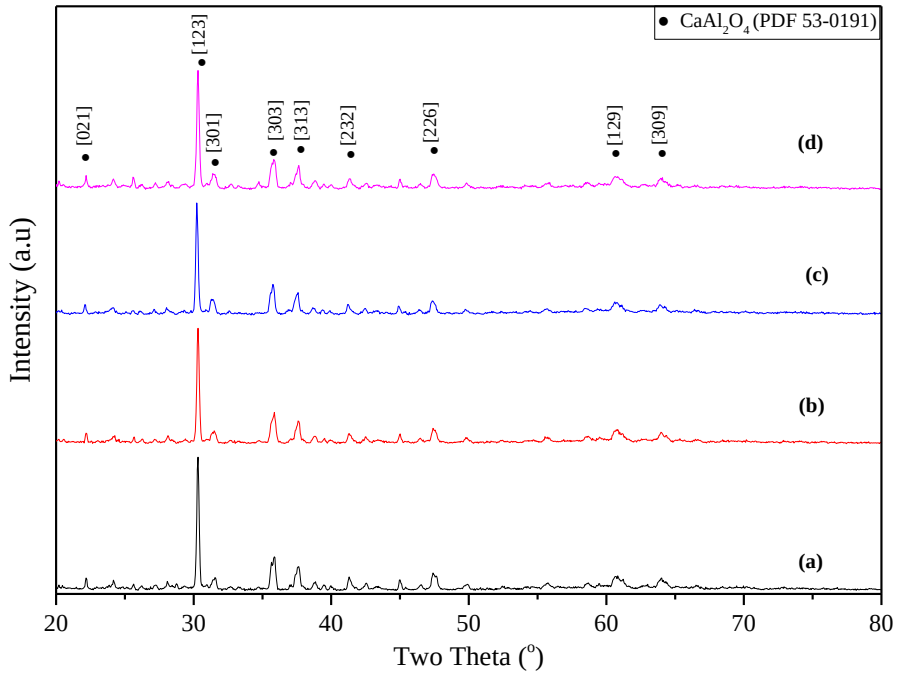

Figure XRD patterns of (a) pure $CaAl_2O_4$, (b) 0.5 mol% Ce^{3+} - doped $CaAl_2O_4$, (c) 0.5 mol% Ce^{3+} and 1mol% Mn^{2+} - doped $CaAl_2O_4$, and (d) 0.5 mol% Ce^{3+} and 5 mol% Mn^{2+} -doped $CaAl_2O_4$ annealed at 1350°C in 95%N_2: 5%H_2 with heating rate of 5°C/min and the holding time of 1h

C. Photoluminescence data

Table 1. Emission spectra with wavelength at 273 nm of 0.5 mol% Ce and 1 mol% Mn – doped $CaAl_2O_4$ un-treated and annealed at 600, 700, 800, and 900^oC in 95% N_2: 5% H_2 with the heating rate of 5^oC/min and the holding time of 1 h

Theta	900	800 -	700	600	Untreated
300	2082,96	2013,37	1557,26	1286,09	829,596
301	2101,18	2031,77	1573,05	1295,63	842,084
302	2085,41	2022,79	1561,07	1279	839,877
303	2042,29	1960,48	1518,39	1249,07	815,649
304	1988,94	1915,96	1476,74	1215,82	782,464
305	1952,94	1885,47	1444,85	1192,91	762,783
306	1899,45	1838,62	1414,22	1171,2	747,723
307	1867	1808,16	1383,46	1153,11	725,685
308	1841,93	1782,17	1362,86	1128,57	714,019
309	1778,5	1739,47	1327,61	1104,33	693,874
310	1743,25	1683,38	1292,59	1071,96	675,793
311	1699,1	1652,01	1255,02	1044,5	663,05
312	1636,04	1596,45	1219,01	1010,95	638,61
313	1587,08	1529,18	1174,35	979,676	615,511
314	1524,22	1465,01	1121,98	939,491	584,878
315	1471,78	1407,87	1086,67	910,268	560,722
316	1424,59	1343,42	1041,4	871,106	539,254
317	1366,27	1290,16	996,798	838,782	513,922
318	1321,9	1229,87	950,592	795,296	486,347
319	1257,88	1165,09	896,41	748,044	464,714
320	1210,56	1108,34	854,059	717,086	440,905
321	1179,71	1069,33	818,101	687,178	418,07
322	1125,85	1013,91	775,417	645,489	392,474
323	1060,91	943,118	715,634	598,856	366,215
324	974,644	860,574	655,351	545,572	329,231
325	908,01	787,534	598,314	495,889	300,217
326	847,569	733,041	554,264	461,836	279,178
327	814,463	694,357	534,943	437,703	267,047
328	783,283	662,071	506,023	414,857	250,852
329	755,75	628,03	484,643	391,252	235,728
330	735,59	602,927	465,435	372,122	227,418
331	717,754	588,385	447,675	360,363	220,416
332	710,195	575,351	438,001	351,62	213,166
333	706,948	574,386	435,081	344,418	207,857
334	710,23	567,274	430,882	339,015	208,275
335	709,878	562,256	426,59	334,775	201,464
336	710,019	564,34	425,802	332,12	200,393

337	717,096	566,911	427,535	326,626	199,798
338	731,176	576,3	427,547	326,862	199,689
339	734,972	582,873	435,288	330,687	200,292
340	750,327	589,375	432,993	329,193	199,277
341	764,905	604,403	438,215	328,468	199,75
342	773,345	613,867	441,581	331,126	199,808
343	789,272	621,042	448,338	331,29	201,759
344	803,674	626,763	452,056	330,962	202,06
345	820,757	648,072	456,749	332,491	204,497
346	843,89	663,248	459,474	334,311	202,773
347	860,944	673,787	470,344	336,363	205,174
348	877,65	692,386	477,358	339,35	209,846
349	902,39	707,207	484,069	343,113	209,679
350	921,03	726,087	498,056	350,591	211,802
351	947,979	744,908	503,709	349,032	214,489
352	970,046	761,225	511,791	354,846	217,671
353	995,226	779,932	523,731	357,687	218,841
354	1020,34	798,023	533,178	363,896	219,227
355	1040,59	816,278	541,048	368,852	223,333
356	1071,19	842,829	554,618	370,549	225,782
357	1084,11	860,506	561,454	378,183	227,35
358	1118,9	888,325	574,539	385,125	229,888
359	1139,5	915,65	588,625	388,967	237,412
360	1160,04	937,5	597,636	401,897	238,323
361	814,631	602,427	343,589	180,264	109,61
362	830,786	623,095	347,632	183,734	109,314
363	846,27	633,136	355,326	186,365	109,616
364	864,11	644,915	361,775	189,138	109,38
365	877,084	664,314	367,283	191,659	113,134
366	890,859	679,047	371,877	191,044	114,464
367	905,162	687,788	381,072	191,091	113,757
368	920,946	699,482	386,229	194,959	114,62
369	927,891	719,914	391,548	195,993	117,066
370	944,922	729,581	397,642	196,827	118,318
371	957,231	740,681	400,972	200,012	116,501
372	965,999	754,339	406,39	196,169	119,479
373	978,335	765,514	407,955	199,752	120,736
374	987,212	774,909	411,655	200,878	120,939
375	984,657	786,085	416,948	201,112	121,004
376	997,506	795,292	424,353	201,126	120,341
377	1006,9	805,619	423,661	201,834	123,683
378	1015,55	813,832	427,279	205,522	124,475
379	1014,43	825,497	432,687	203,944	124,899
380	1028,95	829,7	431,359	206,442	125,683

381	1032,77	833,174	439,814	205,114	127,512
382	1035,64	841,057	441,103	206,685	128,092
383	1039,1	848,365	441,872	204,796	127,038
384	1042,3	844,493	440,897	204,202	126,938
385	1041,31	854,228	441,702	205,122	128,899
386	1048,94	859,191	444,411	204,3	130,989
387	1051,24	860,935	445,769	204,809	128,299
388	1051,93	861,258	449,436	202,991	131,31
389	1047,58	867,266	450,569	207,255	129,385
390	1052,46	873,158	453,894	205,187	130,859
391	1054,63	872,423	452,839	206,878	133,02
392	1058,43	881,634	453,804	209,355	134,536
393	1058,24	879,454	457,845	212,67	136,961
394	1059,4	884,209	455,248	214,236	136,192
395	1058,97	882,139	460,733	215,349	139,264
396	1057,94	892,798	463,804	219,24	141,793
397	1061,78	888,32	465,825	222,408	143,463
398	1055,02	886,233	466,12	221,812	146,687
399	1046,95	885,714	467,794	218,183	143,789
400	1046,1	878,574	456,214	213,373	141,297
401	1039,97	871,26	451,849	210,429	140,895
402	1030,91	872,823	449,521	209,095	139,443
403	1018,18	859,162	449,475	205,92	137,844
404	1017,33	858,495	442,959	204,956	139,467
405	1008,4	853,628	443,338	205,418	138,275
406	1006,62	848,359	439,961	207,945	140,273
407	999,384	851,637	443,026	206,568	141,751
408	999,33	847,695	445,931	209,035	144,109
409	995,605	843,453	444,193	212,413	147,276
410	987,462	842,056	447,512	212,534	148,44
411	984,095	838,907	444,516	213,824	149,496
412	980,149	835,571	444,835	218,671	153,009
413	970,649	830,25	445,678	220,166	151,72
414	967,616	822,965	441,873	218,395	150,895
415	955,302	821,741	437,629	215,675	148,651
416	948,6	810,128	435,542	214,368	149,45
417	939,875	804,296	431,173	210,999	146,884
418	928,784	796,816	425,955	211,653	147,782
419	921,637	786,715	428,982	212,807	146,153
420	913,984	781,961	423,791	210,909	146,013
421	899,401	769,372	416,009	205,783	143,623
422	881	754,096	400,032	195,654	136,652
423	862,955	734,332	393,163	187,663	133,066
424	850,896	726,049	380,166	182,774	128,185

425	832,619	712,133	373,696	177,129	125,069
426	823,136	697,877	364,751	171,319	121,75
427	806,216	684,058	354,871	165,924	117,631
428	795,528	676,736	348,774	160,875	114,037
429	782,22	661,948	341,215	157,163	110,945
430	770,487	651,27	335,033	151,947	106,884
431	761,013	640,781	327,641	149,643	105,305
432	748,183	631,324	320,108	142,366	101,033
433	731,982	619,623	316,452	142,218	101,918
434	717,106	606,813	311,904	137,166	99,1632
435	709,075	598,854	306,078	135,288	97,2915
436	691,762	590,332	302,882	131,776	96,7318
437	688,007	578,804	296,898	132,358	95,0938
438	684,463	575,336	295,096	133,045	95,6661
439	672,867	560,105	289,991	130,121	95,5644
440	656,102	552,247	290,081	127,974	92,4214
441	646,767	546,786	282,964	123,304	90,8586
442	641,617	533,718	276,106	123,648	90,2852
443	628,78	523,514	271,362	121,74	88,6108
444	621,078	520,033	269,389	120,618	87,9479
445	606,918	510,146	262,351	117,963	85,9024
446	598,068	500,711	260,519	114,898	86,0985
447	588,411	493,425	256,127	113,995	85,2395
448	576,82	487,022	251,715	115,405	83,7484
449	575,66	483,292	258,666	122,739	85,8418
450	569,569	486,719	260,238	130,192	90,9844
451	560,775	477,102	258,625	128,683	91,7349
452	543,342	464,462	247,793	122,473	87,6937
453	524,013	448,954	242,18	119,053	84,4631
454	515,015	433,051	229,09	113,95	81,3668
455	502,234	425,874	226,943	109,522	79,2948
456	494,736	419,843	227,679	112,029	78,805
457	491,216	419,414	228,262	114,157	80,0474
458	486,683	413,241	228,306	116,212	82,195
459	479,109	412,093	227,205	115,795	80,2028
460	473,951	399,305	222,372	113,188	81,8087
461	467,406	400,044	219,138	114,931	81,8879
462	466,316	402,701	223,369	120,385	86,8289
463	466,986	399,994	231,979	125,722	89,7685
464	460,904	397,671	228,625	130,277	90,501
465	449,139	385,841	220,44	124,229	87,9075
466	441,546	382,222	219,939	122,7	85,5046
467	448,529	390,779	231,734	138,84	94,7659
468	460,993	401,71	241,028	150,918	102,087

469	448,674	397,581	243,897	146,918	105,304
470	426,826	375,585	227,052	134,222	96,8047
471	413,117	357,17	211,721	122,712	88,5775
472	402,093	347,127	203,471	118,159	81,6343
473	392,17	341,988	202,45	121,244	84,4476
474	387,482	336,598	199,761	115,885	82,4378
475	365,617	319,037	183,294	102,815	76,2338
476	354,815	303,764	173,817	97,0064	68,3688
477	344,067	292,991	167,851	92,2596	64,5498
478	336,607	286,839	165,691	89,9513	65,2666
479	333,015	283,212	163,161	90,7707	64,1243
480	331,53	283,049	166,191	94,7307	65,7297
481	329,223	283,65	168,46	101,086	68,7085
482	331,129	283,58	170,143	102,132	71,8775
483	319,765	275,612	165,571	99,5784	70,5963
484	308,825	267,607	159,993	93,5289	67,6985
485	301,05	256,934	154,668	89,2299	63,2798
486	293,329	251,176	145,898	83,4073	60,7202
487	285,668	241,014	141,278	83,317	57,2329
488	277,507	235,019	139,765	79,2699	55,3929
489	271,966	232,268	135,116	78,6991	55,3177
490	266,954	229,294	135,476	78,1128	54,628
491	266,636	228,419	135,669	80,8692	57,8744
492	266,28	231,027	139,271	84,6365	60,3665
493	264,732	228,354	138,876	84,9881	59,2315
494	257,394	223,065	132,414	80,0123	56,1803
495	249,489	212,878	129,1	75,6692	54,3921
496	244,617	207,428	123,242	73,2791	51,8629
497	238,359	203,841	119,534	71,2483	50,2804
498	235,335	197,295	116,913	69,1098	49,254
499	229,808	195,282	116,282	67,387	48,7597
500	225,747	194,616	114,118	66,9328	46,9293
501	223,002	190,155	111,65	65,5111	46,4565
502	220,11	187,108	111,341	65,9155	47,2012
503	218,095	184,373	109,206	65,9737	45,5845
504	214,712	183,681	109,078	64,0289	46,7682
505	213,351	179,203	107,801	64,3305	45,5414
506	206,771	178,678	106,37	62,9495	45,397
507	205,047	177,534	104,804	64,2305	44,5291
508	203,729	171,379	103,206	61,8331	43,3208
509	200,798	172,754	104,305	62,4834	43,6343
510	199,139	169,636	102,426	60,8519	43,6045
511	194,129	168,035	100,714	60,6747	43,4734
512	193,292	167,714	101,411	59,3258	42,9327

513	190,161	164,888	99,2622	60,5177	42,389
514	190,946	164,328	100,337	59,0595	42,2298
515	190,062	162,921	98,2101	59,0117	41,8692
516	185,375	158,932	96,8819	59,6694	41,8696
517	183,868	159,823	98,714	59,4232	41,5809
518	183,809	159,517	96,472	58,5833	42,2088
519	180,589	157,247	95,8923	59,7025	42,1452
520	180,698	156,31	98,6189	59,3457	43,424
521	181,175	157,531	98,0416	61,4955	42,216
522	178,314	153,569	97,6809	61,0776	42,3497
523	175,045	151,649	93,1017	59,2541	41,0658
524	171,984	148,53	92,201	56,4573	38,8125
525	169,343	144,172	88,3119	53,3033	37,4225

Table 2. Excitation spectra with wavelength at 546 nm of difference annealed temperature of 0.5 mol% Ce and 1 mol% Mn – doped $CaAl_2O_4$ un-treated and annealed at 600, 700, 800, and 900^oC in 95% N_2: 5% H_2 with the heating rate of 5^oC/min and the holding time of 1 h

Theta	**900 NO^{3-}**	**800 NO^{3-}**	**700 NO^{3-}**	**600 NO^{3-}**	**Untreated**
250	311,471	296,518	205,568	103,606	96,5626
251	294,638	289,138	197,168	102,73	92,651
252	282,987	272,961	187,386	99,9665	89,8039
253	271,387	259,428	176,344	95,23	87,2964
254	255,572	250,462	168,659	89,3199	84,8018
255	244,166	233,729	158,721	85,9035	79,4837
256	235,218	223,607	152,827	83,5796	77,7521
257	220,64	213,799	147,135	81,0588	72,6088
258	210,559	200,21	137,898	75,9485	70,325
259	199,994	193,903	128,977	72,1531	68,0922
260	191,342	180,883	124,327	68,5257	63,1777
261	185,904	172,356	117,814	64,5962	59,799
262	177,085	163,051	114,066	61,0938	56,954
263	169,608	157,791	108,831	60,5643	54,9286
264	164,339	150,927	103,015	56,8234	51,9173
265	158,968	145,012	100,227	54,0861	50,8077
266	156,072	138,875	96,1103	51,938	48,4709
267	149,952	135,284	92,3767	51,7833	47,1262
268	146,145	131,461	88,4436	48,5087	44,4574
269	144,041	125,457	86,1349	45,9833	43,5238
270	142,208	123,76	83,3384	46,2682	43,7282
271	159,993	145,508	97,5096	61,8037	56,4307
272	270,861	261,236	187,257	133,285	109,728

273	402,752	393,624	306,449	196,703	166,572
274	340,849	328,61	293,62	157,077	141,293
275	192,247	169,781	155,94	71,5703	70,2449
276	135,859	111,922	77,5943	41,0143	37,9815
277	130,339	105,159	68,9074	36,7868	33,2358
278	130,663	103,958	65,7743	36,0224	32,0254
279	129,474	102,04	64,3257	35,0159	32,0555
280	127,343	100,618	64,9193	32,8541	30,2705
281	127,65	101,912	61,9325	31,9567	28,9211
282	127,765	97,8386	60,8243	31,8604	28,1095
283	127,35	98,6677	59,2906	30,6936	27,516
284	127,98	97,5357	60,2302	30,0668	26,782
285	127,811	97,4118	58,9417	28,7065	26,3614
286	130,237	96,6776	59,0393	28,7782	25,7088
287	130,72	96,322	58,2239	27,7191	24,641
288	132,701	98,2291	57,3914	26,3729	24,0786
289	133,329	96,7643	56,0624	26,4927	23,7077
290	132,734	97,3575	56,1781	25,9606	24,1267
291	137,857	98,3755	55,8871	25,8014	22,8865
292	137,682	97,0759	56,4915	24,8679	23,108
293	139,319	98,2569	55,8296	25,1223	22,4318
294	140,813	99,9147	57,2689	25,1458	22,2278
295	140,969	101,313	58,2346	25,6172	21,9134
296	142,737	101,489	57,8923	24,5648	21,6192
297	141,997	101,693	56,917	24,0845	21,519
298	145,16	103,913	57,8769	23,2864	20,3481
299	145,177	105,71	57,759	23,0229	20,7398
300	144,406	106,5	58,8571	22,5017	19,5374
301	148,026	106,94	59,1671	22,5857	19,9761
302	148,988	109,793	58,9725	22,4998	19,8634
303	149,669	110,301	60,7251	22,2866	19,789
304	150,223	111,169	61,9929	21,861	19,172
305	151,939	114,201	62,4725	21,8654	18,8955
306	150,844	115,538	62,5997	21,9493	18,4092
307	152,748	117,871	63,6537	21,6923	18,4075
308	153,083	120,03	65,469	21,5037	18,426
309	155,231	121,642	66,4519	21,6794	18,3069
310	155,475	123,83	66,7619	21,5063	18,2435
311	156,944	125,014	68,2287	21,5408	18,1989
312	156,998	127,764	68,7549	21,2891	17,8179
313	156,982	128,902	69,3195	21,7737	17,5488
314	158,791	131,646	70,4001	21,3673	17,4806
315	159,779	132,319	72,4794	21,8141	17,6879
316	160,861	134,272	73,5666	21,6069	17,3459

317	162,448	137,002	74,604	21,2382	16,9443
318	161,953	137,951	75,429	21,6015	17,3528
319	163,823	139,125	77,6158	21,5571	17,4919
320	164,352	141,621	78,7882	21,158	17,5865
321	164,579	142,314	79,72	21,4358	17,4561
322	166,255	144,971	80,2001	21,6933	16,9267
323	166,429	146,507	82,6795	21,0777	16,8776
324	166,541	148,031	83,1072	21,1461	16,5925
325	167,993	147,804	83,3233	21,1338	16,7159
326	169,124	150,617	85,1428	20,7489	16,5841
327	170,342	152,045	85,7083	21,1047	16,1948
328	170,201	153,165	87,753	21,3596	16,225
329	171,547	154,376	88,2493	20,728	16,3852
330	171,224	155,256	89,4247	20,8878	15,9423
331	170,921	156,518	90,3752	21,0437	16,1462
332	171,857	158,329	91,329	20,777	15,7905
333	172,529	156,979	91,6559	20,8455	15,9377
334	172,627	159,542	93,4006	20,6422	15,3024
335	172,955	159,866	93,6245	20,654	15,4291
336	171,352	160,726	94,7004	20,3359	15,2527
337	172,494	162,279	96,3572	20,3003	15,4031
338	171,868	163,133	95,793	20,3527	14,9974
339	171,444	164,139	97,0239	20,3995	14,8355
340	172,014	165,087	97,6448	20,1066	14,7426
341	171,182	165,09	98,1836	20,3273	14,7053
342	171,348	165,754	98,8281	20,2826	14,476
343	170,508	164,686	99,1079	19,6303	14,575
344	170,021	166,636	99,9212	19,6742	14,542
345	171,357	166,055	100,048	20,1723	14,1364
346	168,739	167,252	101,075	19,9847	14,2423
347	169,335	166,584	101,906	20,0441	13,7716
348	168,076	168,872	102,183	19,6898	14,1696
349	167,13	167,654	102,981	19,6573	13,824
350	167,077	168,067	103,066	19,6081	13,9601
351	166,109	168,449	104,052	19,3116	13,839
352	164,747	167,34	104,144	19,4639	13,8935
353	164,161	167,825	104,988	19,8379	13,678
354	162,959	167,467	104,527	19,7203	13,3026
355	162,443	167,946	105,014	19,3969	13,3946
356	161,385	166,583	104,809	19,5449	13,6362
357	160,157	167,191	105,243	19,1621	13,5514
358	158,713	165,446	105,275	19,4417	13,3981
359	156,678	166,331	107,125	19,2617	13,4122
360	155,225	164,014	106,352	19,3179	13,2527

361	153,144	161,734	106,284	18,9412	13,4291
362	151,132	160,85	104,879	19,1513	13,6636
363	148,758	159,146	105,167	19,1574	13,5703
364	145,6	157,281	103,326	18,8029	13,6911
365	143,981	155,939	104,033	18,589	13,6028
366	141,398	153,401	104,078	18,6774	13,2861
367	137,948	150,9	102,692	18,3274	13,1056
368	134,498	147,639	101,25	18,2778	13,1946
369	131,34	144,983	100,448	18,3293	13,129
370	127,587	140,841	98,3448	17,7141	12,9402
371	124,342	137,469	97,3853	17,5844	12,8338
372	119,789	133,345	95,8354	17,4368	12,7131
373	116,992	130,369	93,9296	17,2956	12,7243
374	111,59	125,913	91,5123	17,1392	12,5384
375	108,306	122,044	89,2403	17,1057	12,5365
376	103,162	117,346	86,6224	16,226	12,0671
377	99,1383	113,676	84,764	16,1768	12,0423
378	94,9592	108,265	81,674	15,9683	12,1252
379	91,0344	103,921	79,1285	15,6343	11,7636
380	87,0411	101,099	77,56	15,4369	11,7718
381	83,0011	96,0757	74,9148	15,0358	11,6437
382	78,9868	92,5904	72,658	14,471	11,7169
383	76,2139	87,7821	69,8113	14,6268	11,1525
384	72,2967	84,3955	68,1139	14,4016	10,9027
385	69,3717	81,2217	65,3052	14,2092	10,9553
386	65,862	77,5901	62,9312	14,1442	11,0708
387	63,0834	74,4859	61,7255	13,7492	10,6448
388	60,2158	70,405	58,8756	13,7047	10,7652
389	57,4019	68,3326	56,7231	13,3556	10,6702
390	54,2725	64,937	54,3562	13,1327	10,3987
391	52,4186	62,4736	52,6192	12,8886	10,3262
392	49,8076	58,6204	50,2013	12,5169	10,1735
393	47,2496	56,2084	48,6692	12,4261	9,8914
394	44,5907	53,2304	45,9032	11,8088	9,8871
395	43,018	50,5727	44,2759	11,8025	9,6209
396	40,5091	48,393	42,7644	11,6118	9,57467
397	38,2962	45,4628	40,45	11,1444	9,25426
398	36,6813	43,3168	38,441	10,9711	8,8517
399	35,1409	41,1131	37,037	10,7644	9,02174
400	33,0999	39,2303	35,5998	10,9125	9,05204
401	31,7071	37,7938	34,1542	10,7962	9,16717
402	30,0619	35,9374	33,2292	10,8395	9,04644
403	29,292	34,2625	31,5831	10,7081	9,3645
404	28,3116	32,7084	30,6773	10,6891	9,28584

405	26,9519	31,0158	29,2063	10,5385	9,18231
406	25,6441	29,7241	27,8732	10,5236	9,18683
407	24,6224	27,9316	26,7158	10,4192	9,08377
408	23,4161	26,9388	25,8725	10,1708	8,97688
409	22,8097	25,9147	24,7209	10,3265	8,83775
410	21,5992	24,7325	23,6376	10,1749	8,85969
411	20,9787	23,6761	22,8518	9,7948	8,77984
412	19,8832	22,5133	21,9578	9,78409	8,82069
413	19,0137	21,7798	21,1979	9,8319	8,65683
414	18,619	20,9977	20,3916	9,5327	8,53661
415	18,1796	20,668	19,891	9,6574	8,62803
416	17,6066	19,9723	19,3573	9,66296	8,62028
417	17,2829	19,4061	18,6967	9,55008	8,63151
418	16,6406	18,4281	18,5121	9,32465	8,54012
419	16,2331	17,9617	17,614	9,26463	8,33829
420	15,6501	17,543	17,1565	9,12412	7,94062
421	15,2612	17,2783	16,697	8,84048	8,1123
422	15,0097	16,9473	16,7056	9,13484	8,27726
423	14,9782	16,8461	16,3706	9,08262	8,20521
424	14,6662	16,5141	16,3414	9,17138	8,18045
425	14,5656	16,3472	16,094	9,04823	8,28929
426	14,1272	16,0829	15,6738	9,20437	8,24832
427	13,7422	15,6472	15,3207	9,03919	8,26157
428	13,8246	15,5229	15,1597	8,94292	8,31967
429	13,5902	15,1462	14,7138	8,90248	8,2094
430	13,475	14,7937	14,4403	8,96357	8,08029
431	13,2001	15,0095	14,2773	9,08072	8,07652
432	12,9397	14,5377	13,9847	9,02665	7,92662
433	12,9688	14,3627	14,0662	8,84649	8,12955
434	12,7796	14,0105	13,7503	9,07235	7,96095
435	12,4758	13,9003	13,5834	8,73209	8,0097
436	12,4246	13,6914	13,173	8,78973	7,95117
437	11,9965	13,4002	13,0968	8,83902	7,89059
438	11,8423	13,1899	12,8461	8,60619	7,65676
439	11,5931	12,9069	12,3946	8,38135	7,51932
440	11,463	12,7559	12,0524	8,32872	7,50963
441	11,3298	12,6212	12,0729	8,56209	7,6597
442	11,3767	12,4465	12,2627	8,30266	7,60229
443	11,26	12,4696	12,1189	8,32982	7,63584
444	11,1576	12,1645	11,9352	8,4956	7,6315
445	11,1797	12,1823	11,9771	8,41225	7,74677
446	10,9875	12,2556	11,5146	8,40145	7,67305
447	10,8576	12,0975	11,4418	8,34746	7,66709
448	10,6589	11,7919	11,5324	8,42949	7,73303

449	10,4638	11,4821	11,0157	8,05671	7,22835
450	9,77983	10,4594	10,2524	7,39968	6,94727
451	9,53534	10,2892	9,63713	7,09047	6,66651
452	9,54611	10,3132	9,94922	7,38861	6,7616
453	9,85794	10,6698	10,2751	7,87865	7,12899
454	10,1811	11,0422	10,5187	8,17952	7,37764
455	10,4605	11,3262	11,1248	8,51825	7,65248
456	10,5786	11,2529	10,9346	8,37363	7,80868
457	10,4598	11,3305	10,7747	8,34065	7,53623
458	10,2532	10,8887	10,5415	8,10154	7,45201
459	10,2486	11,0233	10,8106	8,19019	7,50236
460	10,5475	11,1027	10,6448	8,44712	7,71658
461	10,4489	11,0047	10,6443	8,46771	7,70315
462	10,1724	10,8455	10,4089	8,19637	7,4657
463	9,71873	10,3473	9,71696	7,70388	7,07498
464	9,59791	10,2401	9,74882	7,63489	7,08215
465	9,85125	10,5617	10,0568	8,00161	7,26164
466	10,053	10,6056	10,261	8,05675	7,59131
467	9,50531	10,0367	9,81923	7,71455	6,9786
468	8,56618	9,37986	8,6729	6,734	6,16572
469	8,38534	8,9134	8,467	6,57766	6,01256
470	9,05531	9,31545	9,11133	7,0605	6,53703
471	9,60112	10,2177	9,82165	7,94823	7,33868
472	10,5066	11,1484	10,7602	8,60375	8,01339
473	10,7436	11,3571	10,8788	8,69132	8,35873
474	11,3632	12,4066	11,888	9,38601	8,9908
475	13,018	13,8965	13,9058	10,6228	10,6336

Table 3. Emission spectra with wavelength at 273 nm of 0.5 mol% Ce and 1 mol% Mn – doped $CaAl_2O_4$ un-treated and annealed at 800^{o}C in air, N_2, and 95% N_2: 5% H_2 with the heating rate of 5^{o}C/min and the holding time of 1 h

Theta	N_2H_2	Nitrogen	Air	Untreated
300	2013,37	916,692	790,96	829,596
301	2031,77	926,213	791,088	842,084
302	2022,79	916,241	785,934	839,877
303	1960,48	890,019	764,974	815,649
304	1915,96	860,636	740,686	782,464
305	1885,47	844,755	726,3	762,783
306	1838,62	825,896	711,951	747,723
307	1808,16	806,643	694,593	725,685
308	1782,17	798,908	683,325	714,019
309	1739,47	778,949	663,414	693,874

310	1683,38	757,657	650,97	675,793
311	1652,01	738,537	633,915	663,05
312	1596,45	713,949	615,892	638,61
313	1529,18	690,408	592,604	615,511
314	1465,01	667,031	570,463	584,878
315	1407,87	641,171	554,316	560,722
316	1343,42	616,157	533,507	539,254
317	1290,16	592,569	512,367	513,922
318	1229,87	564,811	488,725	486,347
319	1165,09	537,748	466,338	464,714
320	1108,34	517,592	446,327	440,905
321	1069,33	495,511	428,472	418,07
322	1013,91	471,103	406,491	392,474
323	943,118	438,142	380,81	366,215
324	860,574	400,48	343,45	329,231
325	787,534	363,709	312,968	300,217
326	733,041	336,954	292,517	279,178
327	694,357	320,524	275,93	267,047
328	662,071	308,077	265,222	250,852
329	628,03	293,083	250,5	235,728
330	602,927	279,999	239,222	227,418
331	588,385	270,147	230,799	220,416
332	575,351	262,552	227,04	213,166
333	574,386	259,137	220,657	207,857
334	567,274	258,447	219,752	208,275
335	562,256	256,239	215,417	201,464
336	564,34	251,854	213,873	200,393
337	566,911	254,419	214,29	199,798
338	576,3	251,646	210,604	199,689
339	582,873	255,672	212,459	200,292
340	589,375	254,144	213,355	199,277
341	604,403	256,924	213,456	199,75
342	613,867	255,476	214,829	199,808
343	621,042	257,2	216,072	201,759
344	626,763	259,489	216,077	202,06
345	648,072	258,26	218,267	204,497
346	663,248	260,423	218,488	202,773
347	673,787	263,776	218,34	205,174
348	692,386	266,475	221,033	209,846
349	707,207	268,653	223,948	209,679
350	726,087	270,401	225,596	211,802
351	744,908	273,011	228,066	214,489
352	761,225	275,551	230,516	217,671
353	779,932	280,781	232,743	218,841

354	798,023	279,627	233,261	219,227
355	816,278	286,017	237,887	223,333
356	842,829	287,297	240,267	225,782
357	860,506	292,551	245,553	227,35
358	888,325	298,731	248,546	229,888
359	915,65	303,335	251,649	237,412
360	937,5	305,696	255,35	238,323
361	602,427	153,956	123,447	109,61
362	623,095	156,281	123,914	109,314
363	633,136	157,778	125,065	109,616
364	644,915	157,951	126,229	109,38
365	664,314	158,979	127,137	113,134
366	679,047	160,006	127,291	114,464
367	687,788	162,165	128,47	113,757
368	699,482	161,807	130,241	114,62
369	719,914	162,32	129,706	117,066
370	729,581	163,336	129,902	118,318
371	740,681	165,321	131,071	116,501
372	754,339	166,243	130,345	119,479
373	765,514	165,167	131,259	120,736
374	774,909	164,817	132,454	120,939
375	786,085	168,221	131,954	121,004
376	795,292	167,48	133,498	120,341
377	805,619	166,886	134,864	123,683
378	813,832	167,83	133,611	124,475
379	825,497	168,813	135,039	124,899
380	829,7	170,024	136,682	125,683
381	833,174	169,58	137,316	127,512
382	841,057	169,218	136,655	128,092
383	848,365	168,958	136,583	127,038
384	844,493	169,263	136,516	126,938
385	854,228	168,69	135,349	128,899
386	859,191	168,961	135,207	130,989
387	860,935	168,093	136,215	128,299
388	861,258	168,69	137,337	131,31
389	867,266	169,56	136,921	129,385
390	873,158	171,089	137,712	130,859
391	872,423	173,404	138,534	133,02
392	881,634	171,673	141,328	134,536
393	879,454	173,187	140,7	136,961
394	884,209	174,624	141,896	136,192
395	882,139	174,57	144,182	139,264
396	892,798	175,794	144,224	141,793
397	888,32	178,267	146,89	143,463

398	886,233	177,207	145,75	146,687
399	885,714	175,801	143,618	143,789
400	878,574	174,378	141,421	141,297
401	871,26	171,336	141,309	140,895
402	872,823	169,137	141,487	139,443
403	859,162	167,527	141,04	137,844
404	858,495	168,802	139,432	139,467
405	853,628	167,458	140,199	138,275
406	848,359	170,067	139,118	140,273
407	851,637	169,783	141,349	141,751
408	847,695	171,21	142,061	144,109
409	843,453	173,816	143,154	147,276
410	842,056	173,436	144,451	148,44
411	838,907	178,177	145,416	149,496
412	835,571	178,362	147,634	153,009
413	830,25	180,76	150,763	151,72
414	822,965	181,676	150,519	150,895
415	821,741	179,585	151,257	148,651
416	810,128	177,32	149,99	149,45
417	804,296	177,136	149,228	146,884
418	796,816	176,626	148,056	147,782
419	786,715	174,807	147,169	146,153
420	781,961	176,309	145,53	146,013
421	769,372	171,387	140,499	143,623
422	754,096	165,669	136,211	136,652
423	734,332	158,261	131,074	133,066
424	726,049	152,383	126,07	128,185
425	712,133	150,056	122,357	125,069
426	697,877	143,004	118,718	121,75
427	684,058	139,495	115,502	117,631
428	676,736	133,449	110,793	114,037
429	661,948	130,696	108,903	110,945
430	651,27	125,279	104,46	106,884
431	640,781	123,28	102,544	105,305
432	631,324	120,406	100,568	101,033
433	619,623	116,355	99,3073	101,918
434	606,813	114,233	96,6745	99,1632
435	598,854	113,462	95,1657	97,2915
436	590,332	109,579	93,8765	96,7318
437	578,804	108,979	92,2769	95,0938
438	575,336	110,552	91,8402	95,6661
439	560,105	109,112	92,1485	95,5644
440	552,247	105,568	89,1473	92,4214
441	546,786	103,046	87,9936	90,8586

442	533,718	101,653	86,4423	90,2852
443	523,514	101,969	84,242	88,6108
444	520,033	98,7474	83,2573	87,9479
445	510,146	98,5771	84,9226	85,9024
446	500,711	99,6096	82,3069	86,0985
447	493,425	97,1138	82,2704	85,2395
448	487,022	97,5208	82,3849	83,7484
449	483,292	103,474	86,9077	85,8418
450	486,719	107,869	91,0182	90,9844
451	477,102	107,056	88,7422	91,7349
452	464,462	103,918	86,4695	87,6937
453	448,954	98,8025	81,9855	84,4631
454	433,051	93,7111	80,7312	81,3668
455	425,874	93,3816	78,3682	79,2948
456	419,843	93,91	79,0229	78,805
457	419,414	95,5443	81,795	80,0474
458	413,241	97,01	80,9461	82,195
459	412,093	97,311	80,6814	80,2028
460	399,305	95,0225	81,0705	81,8087
461	400,044	95,4625	81,8648	81,8879
462	402,701	99,4529	84,194	86,8289
463	399,994	103,405	86,1309	89,7685
464	397,671	104,427	88,4075	90,501
465	385,841	100,765	85,8509	87,9075
466	382,222	101,773	86,6312	85,5046
467	390,779	107,144	92,4205	94,7659
468	401,71	115,362	98,9448	102,087
469	397,581	117,855	98,8055	105,304
470	375,585	110,973	92,5398	96,8047
471	357,17	102,075	85,765	88,5775
472	347,127	99,5145	83,662	81,6343
473	341,988	99,5949	85,7133	84,4476
474	336,598	97,3842	82,1963	82,4378
475	319,037	90,2388	76,0483	76,2338
476	303,764	82,2128	70,801	68,3688
477	292,991	78,6417	67,2179	64,5498
478	286,839	77,9738	66,0724	65,2666
479	283,212	78,2344	66,1441	64,1243
480	283,049	80,2533	68,2074	65,7297
481	283,65	81,9194	70,6138	68,7085
482	283,58	85,1777	70,2268	71,8775
483	275,612	81,7913	69,6261	70,5963
484	267,607	79,1455	66,6629	67,6985
485	256,934	76,2481	63,9709	63,2798

486	251,176	72,9233	61,1662	60,7202
487	241,014	69,7596	58,845	57,2329
488	235,019	67,255	57,4719	55,3929
489	232,268	66,9591	56,5415	55,3177
490	229,294	66,6224	57,3724	54,628
491	228,419	67,8832	58,4092	57,8744
492	231,027	71,2708	59,8878	60,3665
493	228,354	71,6061	60,6556	59,2315
494	223,065	68,2645	56,6836	56,1803
495	212,878	65,5246	55,4114	54,3921
496	207,428	63,8608	53,7954	51,8629
497	203,841	61,1959	52,4529	50,2804
498	197,295	58,5961	50,2567	49,254
499	195,282	58,9033	49,6191	48,7597
500	194,616	58,349	49,6526	46,9293
501	190,155	57,8814	49,5982	46,4565
502	187,108	57,4276	49,0154	47,2012
503	184,373	57,8855	48,9822	45,5845
504	183,681	56,6008	48,5537	46,7682
505	179,203	56,8299	47,4294	45,5414
506	178,678	55,4066	47,7805	45,397
507	177,534	55,2962	46,9882	44,5291
508	171,379	55,1204	46,0695	43,3208
509	172,754	54,9619	45,9509	43,6343
510	169,636	54,6137	46,6311	43,6045
511	168,035	53,6102	44,9468	43,4734
512	167,714	53,3315	44,4405	42,9327
513	164,888	53,2672	44,7691	42,389
514	164,328	52,8535	44,0188	42,2298
515	162,921	52,464	45,4749	41,8692
516	158,932	51,3151	43,6048	41,8696
517	159,823	51,9404	44,4919	41,5809
518	159,517	52,4902	44,4988	42,2088
519	157,247	52,0279	44,4775	42,1452
520	156,31	52,8286	45,2087	43,424
521	157,531	52,7314	45,7072	42,216
522	153,569	54,7339	44,9998	42,3497
523	151,649	51,8086	43,1441	41,0658
524	148,53	48,986	41,8971	38,8125
525	144,172	47,858	40,8451	37,4225

Table 4. Excitation spectra with wavelength at 546 nm of of 0.5 mol% Ce and 1 mol% Mn – doped $CaAl_2O_4$ un-treated and annealed at 800^oC in air, N_2, and 95% N_2: 5% H_2 with the heating rate of 5^oC/min and the holding time of 1 h

Theta	N_2H_2	Nitrogen	Air	Untreated
250	296,518	8,34363	79,0964	96,5626
251	289,138	8,14226	76,3381	92,651
252	272,961	7,7036	72,0635	89,8039
253	259,428	7,31168	69,3931	87,2964
254	250,462	7,09046	66,3036	84,8018
255	233,729	6,75838	64,844	79,4837
256	223,607	6,58271	59,6274	77,7521
257	213,799	6,00373	57,8501	72,6088
258	200,21	5,89843	56,0049	70,325
259	193,903	5,60803	53,1977	68,0922
260	180,883	5,48455	51,566	63,1777
261	172,356	5,13201	49,0046	59,799
262	163,051	4,9501	47,1275	56,954
263	157,791	4,68336	44,391	54,9286
264	150,927	4,53942	42,0521	51,9173
265	145,012	4,26959	41,2862	50,8077
266	138,875	4,14242	39,5638	48,4709
267	135,284	4,01539	38,8083	47,1262
268	131,461	3,84502	36,8551	44,4574
269	125,457	3,77593	36,7312	43,5238
270	123,76	3,66704	35,3088	43,7282
271	145,508	4,96394	48,3964	56,4307
272	261,236	8,9209	96,2423	109,728
273	393,624	11,9513	132,962	166,572
274	328,61	9,50246	102,164	141,293
275	169,781	4,89513	48,8374	70,2449
276	111,922	3,14497	29,9432	37,9815
277	105,159	2,86602	28,066	33,2358
278	103,958	2,81466	27,2014	32,0254
279	102,04	2,77064	26,6687	32,0555
280	100,618	2,6105	26,0228	30,2705
281	101,912	2,65791	25,3846	28,9211
282	97,8386	2,50577	24,2447	28,1095
283	98,6677	2,47829	23,4801	27,516
284	97,5357	2,49706	23,5971	26,782
285	97,4118	2,35957	22,3715	26,3614
286	96,6776	2,2618	21,9256	25,7088

287	96,322	2,26173	21,19	24,641
288	98,2291	2,17856	20,8187	24,0786
289	96,7643	2,21815	20,6302	23,7077
290	97,3575	2,20929	20,12	24,1267
291	98,3755	2,06955	19,525	22,8865
292	97,0759	2,06396	19,0619	23,108
293	98,2569	2,11845	19,2595	22,4318
294	99,9147	2,12269	19,49	22,2278
295	101,313	2,0877	19,1199	21,9134
296	101,489	2,04517	18,5529	21,6192
297	101,693	1,93843	18,0253	21,519
298	103,913	1,89749	17,6187	20,3481
299	105,71	1,97019	17,3446	20,7398
300	106,5	1,85932	17,0066	19,5374
301	106,94	1,83317	16,871	19,9761
302	109,793	1,83973	16,7279	19,8634
303	110,301	1,76881	16,6416	19,789
304	111,169	1,77763	16,6046	19,172
305	114,201	1,77925	16,6799	18,8955
306	115,538	1,77524	16,2623	18,4092
307	117,871	1,71068	16,1701	18,4075
308	120,03	1,78617	15,7291	18,426
309	121,642	1,70916	15,9265	18,3069
310	123,83	1,7015	15,5968	18,2435
311	125,014	1,69512	15,3424	18,1989
312	127,764	1,64989	15,3963	17,8179
313	128,902	1,65702	15,2475	17,5488
314	131,646	1,63526	15,0418	17,4806
315	132,319	1,67147	14,9497	17,6879
316	134,272	1,6874	15,306	17,3459
317	137,002	1,61944	15,2221	16,9443
318	137,951	1,63614	15,1404	17,3528
319	139,125	1,64577	14,4584	17,4919
320	141,621	1,5697	14,7668	17,5865
321	142,314	1,58163	14,4434	17,4561
322	144,971	1,61446	14,5083	16,9267
323	146,507	1,58213	14,3141	16,8776
324	148,031	1,528	14,0428	16,5925
325	147,804	1,5873	14,2053	16,7159
326	150,617	1,54691	14,0367	16,5841
327	152,045	1,58031	13,6723	16,1948
328	153,165	1,54401	13,6351	16,225
329	154,376	1,55172	13,7469	16,3852
330	155,256	1,52791	13,5094	15,9423

331	156,518	1,49767	13,3265	16,1462
332	158,329	1,46449	12,9808	15,7905
333	156,979	1,49054	13,1924	15,9377
334	159,542	1,43739	12,9771	15,3024
335	159,866	1,44038	13,2432	15,4291
336	160,726	1,39293	12,9346	15,2527
337	162,279	1,38881	12,9789	15,4031
338	163,133	1,39428	12,7148	14,9974
339	164,139	1,35059	12,56	14,8355
340	165,087	1,32575	12,3504	14,7426
341	165,09	1,30593	12,5779	14,7053
342	165,754	1,28142	12,361	14,476
343	164,686	1,29175	12,2156	14,575
344	166,636	1,23688	12,5101	14,542
345	166,055	1,23556	12,1695	14,1364
346	167,252	1,22744	11,9755	14,2423
347	166,584	1,20525	11,9722	13,7716
348	168,872	1,20168	11,9422	14,1696
349	167,654	1,17405	11,8611	13,824
350	168,067	1,21389	11,9352	13,9601
351	168,449	1,18188	11,9213	13,839
352	167,34	1,16454	11,8758	13,8935
353	167,825	1,19405	11,7567	13,678
354	167,467	1,14985	11,7284	13,3026
355	167,946	1,16134	11,723	13,3946
356	166,583	1,17179	11,9296	13,6362
357	167,191	1,15938	11,8014	13,5514
358	165,446	1,16979	11,9089	13,3981
359	166,331	1,16515	11,9721	13,4122
360	164,014	1,14759	11,9193	13,2527
361	161,734	1,17898	11,956	13,4291
362	160,85	1,12051	11,8166	13,6636
363	159,146	1,15119	11,6302	13,5703
364	157,281	1,15949	11,8518	13,6911
365	155,939	1,12469	11,7951	13,6028
366	153,401	1,11859	11,7715	13,2861
367	150,9	1,0876	11,6437	13,1056
368	147,639	1,1128	11,6021	13,1946
369	144,983	1,10884	11,4678	13,129
370	140,841	1,10662	11,6393	12,9402
371	137,469	1,08685	11,3077	12,8338
372	133,345	1,08439	11,411	12,7131
373	130,369	1,01848	11,1912	12,7243
374	125,913	1,03872	11,276	12,5384

375	122,044	1,02924	10,921	12,5365
376	117,346	1,03156	10,9904	12,0671
377	113,676	1,0081	10,793	12,0423
378	108,265	0,97614	10,635	12,1252
379	103,921	0,956325	10,4822	11,7636
380	101,099	0,95153	10,5543	11,7718
381	96,0757	0,939921	10,3885	11,6437
382	92,5904	0,946	10,1207	11,7169
383	87,7821	0,905135	10,2728	11,1525
384	84,3955	0,918749	9,95328	10,9027
385	81,2217	0,900749	9,89415	10,9553
386	77,5901	0,903694	9,94405	11,0708
387	74,4859	0,884317	9,85079	10,6448
388	70,405	0,900179	9,85322	10,7652
389	68,3326	0,902097	9,66668	10,6702
390	64,937	0,860913	9,47227	10,3987
391	62,4736	0,857294	9,31097	10,3262
392	58,6204	0,825369	9,24324	10,1735
393	56,2084	0,829731	9,00522	9,8914
394	53,2304	0,81052	9,00869	9,8871
395	50,5727	0,791242	8,97506	9,6209
396	48,393	0,777766	8,72097	9,57467
397	45,4628	0,754227	8,68525	9,25426
398	43,3168	0,733986	8,34328	8,8517
399	41,1131	0,748735	8,54266	9,02174
400	39,2303	0,747275	8,40323	9,05204
401	37,7938	0,757116	8,43474	9,16717
402	35,9374	0,76289	8,4503	9,04644
403	34,2625	0,7834	8,46599	9,3645
404	32,7084	0,748414	8,44432	9,28584
405	31,0158	0,754311	8,56452	9,18231
406	29,7241	0,752614	8,55901	9,18683
407	27,9316	0,737676	8,3479	9,08377
408	26,9388	0,735739	8,24307	8,97688
409	25,9147	0,723072	8,23994	8,83775
410	24,7325	0,713899	8,23142	8,85969
411	23,6761	0,711943	8,11169	8,77984
412	22,5133	0,693891	7,96367	8,82069
413	21,7798	0,685786	7,99838	8,65683
414	20,9977	0,700876	8,00679	8,53661
415	20,668	0,700172	7,8649	8,62803
416	19,9723	0,705796	7,82361	8,62028
417	19,4061	0,704851	7,86324	8,63151
418	18,4281	0,713649	7,94114	8,54012

419	17,9617	0,673819	7,77908	8,33829
420	17,543	0,653989	7,5492	7,94062
421	17,2783	0,666399	7,45337	8,1123
422	16,9473	0,672041	7,54779	8,27726
423	16,8461	0,711428	7,64847	8,20521
424	16,5141	0,677474	7,74731	8,18045
425	16,3472	0,685307	7,77484	8,28929
426	16,0829	0,670677	7,68752	8,24832
427	15,6472	0,693477	7,64715	8,26157
428	15,5229	0,669206	7,66029	8,31967
429	15,1462	0,676709	7,57903	8,2094
430	14,7937	0,675757	7,56629	8,08029
431	15,0095	0,659567	7,63602	8,07652
432	14,5377	0,672139	7,53	7,92662
433	14,3627	0,655607	7,64033	8,12955
434	14,0105	0,666399	7,46262	7,96095
435	13,9003	0,647658	7,46818	8,0097
436	13,6914	0,65548	7,27359	7,95117
437	13,4002	0,66444	7,27977	7,89059
438	13,1899	0,634047	7,23488	7,65676
439	12,9069	0,616038	7,16662	7,51932
440	12,7559	0,614411	7,13558	7,50963
441	12,6212	0,625941	7,23952	7,6597
442	12,4465	0,631071	7,13251	7,60229
443	12,4696	0,617632	7,18459	7,63584
444	12,1645	0,641748	7,34905	7,6315
445	12,1823	0,634732	6,94265	7,74677
446	12,2556	0,628886	7,1793	7,67305
447	12,0975	0,633371	7,15057	7,66709
448	11,7919	0,629201	7,19535	7,73303
449	11,4821	0,593425	6,89662	7,22835
450	10,4594	0,542871	6,35758	6,94727
451	10,2892	0,52693	6,30035	6,66651
452	10,3132	0,542027	6,33824	6,7616
453	10,6698	0,572404	6,73835	7,12899
454	11,0422	0,611859	6,92821	7,37764
455	11,3262	0,645965	7,23773	7,65248
456	11,2529	0,622918	7,14271	7,80868
457	11,3305	0,626065	7,27173	7,53623
458	10,8887	0,611647	7,05586	7,45201
459	11,0233	0,611304	7,23544	7,50236
460	11,1027	0,642528	7,3904	7,71658
461	11,0047	0,626908	7,33948	7,70315
462	10,8455	0,607047	7,18059	7,4657

463	10,3473	0,574318	6,9001	7,07498
464	10,2401	0,545144	6,95311	7,08215
465	10,5617	0,578929	7,16621	7,26164
466	10,6056	0,581929	7,19643	7,59131
467	10,0367	0,559063	6,85943	6,9786
468	9,37986	0,485453	6,42321	6,16572
469	8,9134	0,464482	6,17226	6,01256
470	9,31545	0,495987	6,53371	6,53703
471	10,2177	0,569341	7,19955	7,33868
472	11,1484	0,616418	7,68382	8,01339
473	11,3571	0,638928	7,90718	8,35873
474	12,4066	0,667103	8,41126	8,9908
475	13,8965	0,760246	9,33188	10,6336

Table 5. Emission spectra with wavelength at 273 nm of un-dped $CaAl_2O_4$ and Ce and Mn – doped $CaAl_2O_4$ annealed at 800^{o}C in 95% N_2: 5% H_2 with the heating rate of 5^{o}C/min and the holding time of 1 h

Theta	**1mol%Ce and 1mol%Mn – doped $CaAl_2O_4$**	**0.5 mol%Ce and 1 mol% Mn – doped $CaAl_2O_4$**	**1mol%Mn – doped $CaAl_2O_4$**	**$CaAl_2O_4$**
300	1235,55	2013,37	2112,61	2104,09
301	1256	2031,77	2130,79	2106,94
302	1249,63	2022,79	2120,41	2091,35
303	1211,73	1960,48	2076,31	2046,63
304	1187,63	1915,96	2024	1984,81
305	1162,99	1885,47	1987,5	1932,05
306	1134,66	1838,62	1939,85	1903,53
307	1111,87	1808,16	1892,95	1870,92
308	1096,35	1782,17	1862,34	1832,43
309	1065,9	1739,47	1810,39	1781,92
310	1044,99	1683,38	1755,86	1735,73
311	1024,49	1652,01	1703,8	1680,04
312	994,812	1596,45	1644,59	1627,19
313	951,714	1529,18	1580,56	1558,28
314	920,501	1465,01	1510,19	1504,88
315	884,622	1407,87	1448,18	1463,01
316	849,168	1343,42	1387,35	1389,65
317	815,63	1290,16	1319,03	1327,73
318	784,869	1229,87	1254,38	1254,48
319	740,615	1165,09	1189,69	1194,31
320	708,192	1108,34	1136,8	1151,3
321	689,444	1069,33	1089,32	1094,47

322	656,75	1013,91	1018,85	1024,76
323	614,17	943,118	936,532	955,797
324	563,262	860,574	842,151	867,629
325	518,84	787,534	754,478	777,274
326	485,871	733,041	696,476	710,389
327	465,637	694,357	651,666	670,174
328	447,438	662,071	614,439	637,941
329	432,31	628,03	578,187	599,772
330	420,126	602,927	550,029	566,893
331	412,443	588,385	526,958	546,519
332	405,055	575,351	512,425	526,909
333	402,429	574,386	500,238	519,464
334	400,71	567,274	488,404	505,523
335	399,035	562,256	479,795	496,276
336	401,257	564,34	474,675	491,367
337	410,472	566,911	469,046	494,031
338	410,427	576,3	468,062	482,478
339	417,475	582,873	465,368	482,303
340	426,632	589,375	464,163	485,28
341	428,874	604,403	465,347	486,798
342	435,678	613,867	462,11	484,571
343	449,747	621,042	464,095	481,381
344	455,902	626,763	463,123	481,451
345	468,47	648,072	463,015	486,562
346	475,384	663,248	466,672	486,482
347	490,304	673,787	470,669	488,33
348	503,103	692,386	473,521	491,454
349	512,624	707,207	473,539	495,078
350	526,091	726,087	475,753	500,771
351	538,72	744,908	482,93	503,546
352	554,24	761,225	485,105	504,523
353	571,395	779,932	486,443	511,319
354	587,797	798,023	494,582	516,947
355	602,302	816,278	501,896	521,369
356	619,252	842,829	507,411	531,773
357	631,544	860,506	513,333	531,734
358	645,901	888,325	518,193	543,386
359	664,54	915,65	527,968	552,14
360	682,837	937,5	537,636	558,745
361	476,041	602,427	169,228	212,041
362	484,315	623,095	169,302	210,812
363	494,792	633,136	171,059	212,109
364	506,173	644,915	169,125	216,719
365	514,603	664,314	169,598	215,96

366	522,403	679,047	170,509	217,894
367	537,939	687,788	170,007	220,565
368	547,419	699,482	170,296	219,573
369	560,542	719,914	170,545	225,792
370	563,725	729,581	171,591	222,874
371	570,442	740,681	170,59	224,84
372	581,166	754,339	170,395	225,573
373	594,428	765,514	172,423	226,229
374	598,249	774,909	172,469	227,148
375	604,93	786,085	172,269	227,67
376	614,122	795,292	173,171	227,616
377	620,943	805,619	173,474	228,227
378	629,825	813,832	172,662	229,887
379	634,852	825,497	174,183	231,965
380	643,072	829,7	174,779	235,307
381	650,343	833,174	174,354	237,185
382	653,12	841,057	173,937	234,609
383	659,288	848,365	173,314	233,597
384	664,688	844,493	172,978	234,272
385	669,785	854,228	174,179	231,758
386	672,214	859,191	173,627	236,034
387	672,603	860,935	173,912	233,762
388	686,268	861,258	173,317	234,438
389	683,886	867,266	174,126	240,117
390	686,611	873,158	175,947	239,979
391	692,488	872,423	176,602	239,171
392	694,428	881,634	175,975	245,024
393	700,913	879,454	177,951	245,78
394	708,942	884,209	179,083	246,594
395	708,196	882,139	179,014	252,789
396	710,102	892,798	182,207	259,349
397	710,619	888,32	182,232	259,535
398	714,777	886,233	183,349	260,852
399	709,853	885,714	182,199	258,531
400	710,686	878,574	181,512	252,604
401	701,172	871,26	179,524	249,395
402	697,517	872,823	176,735	247,992
403	690,245	859,162	175,39	246,499
404	688,49	858,495	176,503	244,6
405	691,103	853,628	175,846	245,887
406	687,025	848,359	178,211	248,285
407	689,036	851,637	178,402	252,594
408	683,899	847,695	180,059	252,122
409	691,499	843,453	181,855	255,716

410	691,807	842,056	185,274	260,569
411	683,728	838,907	187,292	263,474
412	692,182	835,571	187,304	269,216
413	684,37	830,25	191,148	267,927
414	685,383	822,965	188,219	268,638
415	679,579	821,741	189,574	267,281
416	672,756	810,128	188,609	267,778
417	664,372	804,296	187,362	263,041
418	662,771	796,816	186,203	264,568
419	664,737	786,715	188,795	266,69
420	650,583	781,961	185,888	264,522
421	639,764	769,372	178,328	257,665
422	629,899	754,096	173,35	248,609
423	617,602	734,332	166,552	244,678
424	605,881	726,049	162,475	236,096
425	595,633	712,133	157,021	232,381
426	585,965	697,877	152,939	223,766
427	571,826	684,058	147,865	218,733
428	562,135	676,736	143,775	216,41
429	556,25	661,948	141,263	212,344
430	542,422	651,27	135,959	210,589
431	532,795	640,781	134,772	205,211
432	527,939	631,324	132,357	199,359
433	521,037	619,623	128,598	197,867
434	512,256	606,813	126,534	196,585
435	503,604	598,854	124,783	193,775
436	496,741	590,332	123,019	190,939
437	493	578,804	122,412	193,758
438	490,905	575,336	120,653	190,056
439	480,468	560,105	120,5	192,308
440	474,963	552,247	118,963	189,148
441	464,223	546,786	115,35	185,848
442	455,764	533,718	115,974	182,785
443	450,134	523,514	113,736	183,228
444	444,625	520,033	111,815	182,007
445	437,527	510,146	110,301	181,202
446	426,757	500,711	111,028	179,337
447	421,858	493,425	111,009	176,267
448	418,016	487,022	110,609	180,499
449	416,611	483,292	116,169	186,916
450	426,041	486,719	119,336	196,846
451	413,318	477,102	119,032	194,958
452	399,739	464,462	115,338	186,97
453	391,07	448,954	111,143	184,672

454	377,797	433,051	108,777	173,954
455	367,948	425,874	104,292	173,708
456	365,715	419,843	105,769	174,661
457	366,713	419,414	107,574	177,479
458	361,392	413,241	107,686	181,275
459	358,715	412,093	108,735	181,7
460	352,048	399,305	108,789	179,365
461	352,787	400,044	108,632	179,461
462	355,222	402,701	112,473	187,646
463	362,399	399,994	115,164	198,97
464	359,39	397,671	114,785	200,521
465	349,276	385,841	112,26	192,415
466	339,36	382,222	115,81	189,638
467	357,309	390,779	121,164	206,911
468	371,289	401,71	127,491	222,989
469	363,33	397,581	128,135	223,413
470	337,863	375,585	120,755	207,717
471	325,362	357,17	112,378	192,654
472	309,241	347,127	110,27	183,888
473	312,923	341,988	110,725	186,518
474	303,831	336,598	109,74	181,578
475	285,31	319,037	100,405	170,32
476	270,646	303,764	94,2747	160,313
477	266,544	292,991	91,1165	155,707
478	260,811	286,839	88,714	154,047
479	259,847	283,212	89,7406	155,706
480	261,3	283,049	91,5323	158,904
481	259,451	283,65	94,7094	164,92
482	258,06	283,58	94,7905	167,179
483	254,185	275,612	94,5553	161,155
484	245,072	267,607	90,4503	159,308
485	235,322	256,934	86,4317	152,527
486	233,122	251,176	82,7845	147,275
487	223,859	241,014	80,4156	143,133
488	219,624	235,019	79,1804	138,382
489	210,444	232,268	78,5521	136,022
490	210,776	229,294	78,6475	136,412
491	211,409	228,419	80,2523	141,093
492	215,186	231,027	81,8275	146,485
493	212,336	228,354	82,6485	146,159
494	206,887	223,065	80,0073	142,181
495	199,203	212,878	76,4784	135,965
496	191,369	207,428	74,8631	130,831
497	188,678	203,841	73,2557	128,779

498	183,669	197,295	72,3929	126,834
499	181,427	195,282	72,4383	124,718
500	179,68	194,616	71,4392	121,877
501	179,416	190,155	71,1722	123,23
502	173,434	187,108	70,4994	123,599
503	174,16	184,373	69,9137	123,898
504	171,865	183,681	71,7524	123,711
505	166,413	179,203	70,9835	120,032
506	166,715	178,678	71,1935	118,701
507	165,963	177,534	69,7535	117,867
508	165,035	171,379	70,2437	117,829
509	159,954	172,754	71,7893	117,53
510	160,465	169,636	70,2226	115,212
511	156,103	168,035	69,8133	114,421
512	157,41	167,714	70,8668	115,811
513	155,417	164,888	71,29	114,014
514	154,503	164,328	71,5322	115,133
515	150,814	162,921	71,864	114,72
516	150,858	158,932	73,1247	112,604
517	149,725	159,823	74,0029	111,02
518	147,221	159,517	73,2403	112,802
519	148,134	157,247	75,0078	110,87
520	149,62	156,31	76,5155	111,638
521	146,02	157,531	78,5915	111,057
522	145,794	153,569	77,781	108,888
523	143,866	151,649	77,9617	109,028
524	140,819	148,53	75,3679	104,827
525	137,925	144,172	73,6637	102,593

Table 6. Excitation spectra with wavelength at 546 nm of un-dped $CaAl_2O_4$ and Ce and Mn – doped $CaAl_2O_4$ annealed at 800^{o}C in 95% N_2: 5% H_2 with the heating rate of 5^{o}C/min and the holding time of 1 h

Theta	**1 mol% Ce and 1 mol%Mn – doped $CaAl_2O_4$**	**0.5 mol% Ce and 1 mol %Mn – doped $CaAl_2O_4$**	**1 mol% Mn – doped $CaAl_2O_4$**	**$CaAl_2O_4$**
250	256,626	296,518	284,787	169,941
251	247,552	289,138	270,274	164,534
252	233,784	272,961	257,415	160,956
253	225,051	259,428	247,453	157,179
254	215,855	250,462	231,99	154,247
255	209,704	233,729	221,103	147,855
256	197,233	223,607	207,191	140,956

257	185,014	213,799	196,154	137,353
258	179,987	200,21	184,701	131,691
259	170,37	193,903	173,317	128,406
260	159,314	180,883	163,524	122,68
261	154,35	172,356	156,431	118,167
262	147,86	163,051	145,514	113,177
263	140,107	157,791	135,975	110,071
264	136,455	150,927	127,038	105,284
265	133,384	145,012	121,177	101,037
266	128,32	138,875	115,448	99,3713
267	122,111	135,284	108,018	93,3735
268	121,703	131,461	102,546	93,3365
269	120,213	125,457	97,2218	90,8067
270	116,394	123,76	91,4436	89,8612
271	128,352	145,508	102,053	118,656
272	186,661	261,236	203,079	218,276
273	260,286	393,624	340,218	314,727
274	241,822	328,61	291,799	251,645
275	153,485	169,781	135,454	130,078
276	111,348	111,922	69,0358	76,3887
277	107,417	105,159	60,4833	70,0733
278	105,437	103,958	56,1969	66,4597
279	103,952	102,04	53,0637	65,7987
280	103,668	100,618	51,0891	63,1383
281	104,965	101,912	48,2755	61,2531
282	103,581	97,8386	45,6148	59,9888
283	102,284	98,6677	44,08	56,0294
284	102,031	97,5357	41,3189	55,2166
285	104,2	97,4118	40,6322	53,4783
286	103,419	96,6776	38,4145	53,204
287	103,659	96,322	36,8524	49,0576
288	105,56	98,2291	34,8875	48,537
289	106,115	96,7643	34,2199	47,1613
290	107,499	97,3575	32,5691	45,2707
291	107,291	98,3755	31,7946	43,958
292	108,69	97,0759	30,299	42,6135
293	109,906	98,2569	30,1533	42,5806
294	111,65	99,9147	29,3627	41,0547
295	112,171	101,313	28,9058	41,0172
296	112,418	101,489	27,964	39,8931
297	113,231	101,693	26,7477	37,8983
298	115,274	103,913	25,6758	37,0274
299	115,827	105,71	25,6449	37,1154
300	116,759	106,5	25,1183	35,5291

301	116,039	106,94	24,7202	35,0593
302	117,18	109,793	24,6672	33,8983
303	118,61	110,301	23,6074	33,6943
304	119,921	111,169	23,6375	33,5082
305	120,181	114,201	23,4669	32,1382
306	120,666	115,538	22,9929	32,2845
307	121,514	117,871	22,8628	31,9651
308	121,654	120,03	22,0441	31,8796
309	123,917	121,642	22,473	31,2098
310	125,248	123,83	22,3458	30,6588
311	126,308	125,014	21,9589	30,2537
312	127,002	127,764	22,1232	30,0169
313	127,7	128,902	21,4706	29,592
314	129,776	131,646	21,5167	29,1803
315	130,565	132,319	21,4805	29,1502
316	132,949	134,272	21,1317	28,962
317	134,481	137,002	20,9152	28,8631
318	136,219	137,951	21,0737	27,9126
319	138,556	139,125	20,572	28,0491
320	138,23	141,621	20,2476	28,0224
321	139,855	142,314	20,1547	27,6672
322	144,03	144,971	20,0529	27,2442
323	143,464	146,507	19,5672	27,2595
324	145,927	148,031	19,597	26,6122
325	148,015	147,804	19,5266	26,3268
326	148,808	150,617	19,7505	26,5213
327	151,436	152,045	19,1601	26,5588
328	151,933	153,165	19,0838	26,2039
329	153,727	154,376	19,0146	25,9626
330	154,621	155,256	18,991	26,0092
331	156,681	156,518	18,8162	25,3521
332	157,07	158,329	18,4786	25,2481
333	158,752	156,979	18,4751	25,1183
334	161,264	159,542	18,3256	24,4426
335	161,565	159,866	18,3232	24,7548
336	161,357	160,726	18,1701	24,3881
337	162,299	162,279	18,0237	24,3534
338	164,793	163,133	17,6615	23,7568
339	166,03	164,139	17,7696	24,4333
340	166,872	165,087	17,4598	24,2539
341	167,044	165,09	17,6914	23,3781
342	168,023	165,754	17,5196	24,1295
343	169,865	164,686	17,5381	23,3502
344	170,452	166,636	17,3287	23,4294

345	171,275	166,055	17,2429	23,3828
346	171,723	167,252	17,2542	23,2933
347	173,373	166,584	16,9359	23,035
348	173,459	168,872	17,0593	23,1115
349	172,671	167,654	16,9121	23,0125
350	175,737	168,067	17,1991	22,4675
351	175,138	168,449	17,2341	22,6006
352	176,176	167,34	16,8986	22,031
353	178,442	167,825	17,0311	21,9593
354	178,286	167,467	16,9942	22,3966
355	178,696	167,946	17,0388	22,3757
356	179,314	166,583	17,018	21,9967
357	179,186	167,191	16,9048	21,7804
358	181,012	165,446	16,9865	21,8349
359	180,026	166,331	17,0143	21,7428
360	179,799	164,014	17,4763	21,5205
361	179,322	161,734	17,1553	21,8013
362	179,826	160,85	17,3128	22,0542
363	177,47	159,146	17,3631	21,4438
364	177,489	157,281	17,3922	21,7647
365	175,359	155,939	17,4518	21,8089
366	174,792	153,401	17,0249	21,1482
367	173,982	150,9	17,3828	21,2893
368	171,216	147,639	16,9248	20,9536
369	167,907	144,983	17,0413	20,7275
370	164,822	140,841	16,8708	20,8455
371	162,645	137,469	16,8232	20,2207
372	158,319	133,345	16,7092	20,1392
373	156,485	130,369	16,5896	20,3174
374	152,784	125,913	16,4028	19,9123
375	148,798	122,044	16,4949	19,703
376	143,581	117,346	16,2066	18,9414
377	139,01	113,676	15,7837	18,9419
378	135,474	108,265	15,6918	18,7402
379	131,194	103,921	15,5561	18,6751
380	127,17	101,099	15,2907	17,9893
381	122,487	96,0757	15,0783	18,0705
382	118,663	92,5904	15,1753	17,4731
383	113,9	87,7821	15,1165	17,4384
384	109,761	84,3955	14,8203	17,2752
385	106,059	81,2217	14,6292	17,0818
386	101,979	77,5901	14,4198	16,998
387	98,1871	74,4859	14,3178	16,7683
388	94,6855	70,405	14,3055	16,1903

389	90,4579	68,3326	14,1362	16,1953
390	87,2551	64,937	13,6613	15,8528
391	83,284	62,4736	13,6407	15,6335
392	79,7003	58,6204	13,4775	15,4979
393	76,3429	56,2084	13,3916	15,2268
394	72,8642	53,2304	13,2523	15,0632
395	69,5712	50,5727	13,0648	14,8095
396	66,8979	48,393	12,8388	14,3417
397	63,5451	45,4628	12,5353	13,8269
398	60,0673	43,3168	12,3852	13,5563
399	57,9267	41,1131	12,1591	13,5723
400	55,0071	39,2303	12,2126	13,68
401	52,2971	37,7938	12,2401	13,8059
402	49,9059	35,9374	12,2553	13,5731
403	47,53	34,2625	12,2789	13,7476
404	45,5945	32,7084	12,2962	13,7903
405	43,5805	31,0158	12,2393	13,6966
406	41,383	29,7241	12,0273	13,6093
407	39,5854	27,9316	12,0152	13,2724
408	37,6654	26,9388	11,8736	13,0387
409	36,1213	25,9147	11,6551	12,8875
410	34,1564	24,7325	11,8302	12,7324
411	32,7634	23,6761	11,4489	12,561
412	30,9778	22,5133	11,5168	12,5187
413	29,6953	21,7798	11,446	12,323
414	28,2956	20,9977	11,4629	12,394
415	27,4641	20,668	11,6883	12,4665
416	26,6467	19,9723	11,5693	12,212
417	25,9938	19,4061	11,5169	12,2637
418	24,63	18,4281	11,4878	12,2061
419	23,8244	17,9617	11,3056	12,0052
420	23,1876	17,543	11,1237	11,4975
421	22,429	17,2783	11,2828	11,2984
422	21,6871	16,9473	11,3539	11,6532
423	21,6298	16,8461	11,4874	11,987
424	21,277	16,5141	11,6882	12,0061
425	20,718	16,3472	11,6874	11,8253
426	19,9622	16,0829	11,7271	11,9343
427	19,5436	15,6472	11,6513	11,5221
428	18,8993	15,5229	11,5685	11,6833
429	18,4526	15,1462	11,6503	11,3646
430	18,4718	14,7937	11,5281	11,3064
431	17,6595	15,0095	11,5364	11,5048
432	17,3547	14,5377	11,5261	11,4541

433	17,2855	14,3627	11,2642	11,2018
434	16,801	14,0105	11,5753	11,2444
435	16,4755	13,9003	11,3469	11,2462
436	15,9707	13,6914	11,2227	11,0651
437	15,5274	13,4002	11,0437	11,1024
438	15,2969	13,1899	11,0014	10,8605
439	14,8078	12,9069	10,8673	10,6458
440	14,7244	12,7559	10,8822	10,6353
441	14,6663	12,6212	10,8458	10,6723
442	14,5287	12,4465	10,7889	10,7621
443	14,1444	12,4696	10,6493	10,8479
444	13,8923	12,1645	10,7151	10,6736
445	13,8012	12,1823	10,7744	10,7063
446	13,8138	12,2556	10,7426	10,6859
447	13,6735	12,0975	10,706	10,6039
448	13,2514	11,7919	10,6821	10,6239
449	12,8	11,4821	10,2572	10,3008
450	11,8827	10,4594	9,5498	9,47662
451	11,3551	10,2892	9,45619	9,0915
452	11,4138	10,3132	9,43523	9,4308
453	12,141	10,6698	9,90893	9,88226
454	12,216	11,0422	10,1718	10,1165
455	12,5365	11,3262	10,3862	10,6624
456	12,4357	11,2529	10,4055	10,5763
457	12,2494	11,3305	10,3105	10,6079
458	12,138	10,8887	10,1745	10,2484
459	11,9178	11,0233	10,2459	10,3258
460	12,1329	11,1027	10,4943	10,4867
461	12,0277	11,0047	10,3813	10,4763
462	11,5238	10,8455	10,2654	10,0838
463	11,0344	10,3473	10,0556	9,71394
464	10,9761	10,2401	9,80916	9,48898
465	11,2379	10,5617	10,0071	9,757
466	11,4436	10,6056	10,3138	10,133
467	10,6266	10,0367	9,79102	9,2381
468	9,64761	9,37986	9,09302	8,56242
469	9,37043	8,9134	8,90343	7,98031
470	10,1209	9,31545	9,48405	8,56879
471	11,0622	10,2177	10,0052	9,73111
472	11,8041	11,1484	10,4973	10,3061
473	11,8921	11,3571	10,7538	10,501
474	12,542	12,4066	10,9245	10,988
475	13,8784	13,8965	12,6083	12,2411

Table 7. Emission spectra with wavelength at 273 nm of un-dped $CaAl_2O_4$ and Ce and Mn – doped $CaAl_2O_4$ annealed at800^oC in 95% N_2: 5% H_2 with the heating rate of 5^oC/min and the holding time of 1 h

Theta	0.5 mol% Ce and 5 mol% Mn – doped $CaAl_2O_4$	0.5 mol% Ce and 3 mol%Mn – doped $CaAl_2O_4$	0.5 mol% Ce and 1 mol% Mn – doped $CaAl_2O_4$	0.5 mol% Ce– doped $CaAl_2O_4$	$CaAl_2O_4$
300	1576,43	1942,85	1961,23	1814,3	2104,09
301	1578,01	1957,08	1981,16	1833,01	2106,94
302	1578,12	1949,2	1972,91	1822,87	2091,35
303	1537,02	1898,47	1921,3	1780,84	2046,63
304	1486,62	1845,44	1870,17	1739,46	1984,81
305	1462,56	1817,11	1835,37	1707,83	1932,05
306	1430,21	1777,95	1799,8	1677	1903,53
307	1402,42	1740,08	1757,87	1644,75	1870,92
308	1379,93	1707,52	1724,03	1603,22	1832,43
309	1345,12	1660,35	1687,1	1568,61	1781,92
310	1315,14	1617,41	1646,46	1521,28	1735,73
311	1283,98	1581,75	1609,07	1478,98	1680,04
312	1250,88	1529,21	1553,45	1427,94	1627,19
313	1207,07	1468,62	1496,11	1364,89	1558,28
314	1164,87	1414,17	1430,79	1316,12	1504,88
315	1127,45	1363,7	1381,85	1264,6	1463,01
316	1087,89	1309,4	1319,36	1213,39	1389,65
317	1040,56	1250,22	1258,15	1152,19	1327,73
318	1000,11	1193,52	1204,57	1099,36	1254,48
319	961,759	1136,07	1141,99	1039,35	1194,31
320	918,977	1074,31	1088,24	995,065	1151,3
321	890,135	1030,91	1048,99	954,912	1094,47
322	848,193	975,697	990,061	901,825	1024,76
323	798,953	904,143	922,401	827,365	955,797
324	741,571	820,824	838,533	750,677	867,629
325	683,803	743,191	765,061	682,677	777,274
326	646,582	690,879	711,52	632,867	710,389
327	619,987	657,186	676,189	598,504	670,174
328	600,346	627,753	652,38	574,239	637,941
329	577,564	596,842	615,006	535,844	599,772
330	561,395	569,217	595,433	517,63	566,893
331	549,804	554,022	574,416	500,095	546,519
332	543,641	541,034	559,813	489,507	526,909
333	542,255	532,669	553,64	482,904	519,464
334	541,284	530,441	547,97	481,742	505,523
335	541,901	524,7	544,551	474,885	496,276
336	546,328	525,194	545,44	475,339	491,367
337	549,392	523,502	548,993	474,282	494,031

338	556,551	526,612	553,335	479,243	482,478
339	559,878	534,185	556,93	484,016	482,303
340	569,76	539,177	563,627	488,796	485,28
341	581,606	543,778	575,515	495,395	486,798
342	589,798	553,027	581,188	496,998	484,571
343	601,291	560,749	590,236	504,204	481,381
344	608,065	566,012	599,405	511,235	481,451
345	622	574,468	610,888	521,837	486,562
346	633,303	583,649	621,714	527,755	486,482
347	640,634	592,401	636,342	537,131	488,33
348	658,41	606,466	651,643	548,329	491,454
349	667,997	619,235	665,553	563,885	495,078
350	685,677	626,187	677,669	574,886	500,771
351	696,172	639,946	694,894	581,549	503,546
352	712,265	654,827	709,088	594,311	504,523
353	718,338	669,275	724,54	605,579	511,319
354	732,559	684,423	741,059	621,073	516,947
355	740,615	697,156	759,841	633,806	521,369
356	758,373	712,565	779,214	649,454	531,773
357	767,197	729,049	794,759	659,711	531,734
358	780,655	743,809	814,106	675,71	543,386
359	787,994	759,799	834,527	689,286	552,14
360	800,913	778,089	853,6	707,635	558,745
361	531,386	441,085	525,429	393,854	212,041
362	535,462	454,451	533,639	400,315	210,812
363	538,135	462,769	550,278	410,102	212,109
364	542,453	471,235	556,629	418,276	216,719
365	547,217	476,074	568,654	426,781	215,96
366	546,77	485,753	578,697	435,14	217,894
367	551,968	491,264	593,984	443,14	220,565
368	549,412	504,242	600,61	448,589	219,573
369	548,607	510,025	613,545	456,704	225,792
370	548,419	516,638	626,508	465,621	222,874
371	553,527	522,934	632,94	469,051	224,84
372	550,922	531,436	642,95	480,056	225,573
373	551,394	534,547	652,056	478,572	226,229
374	547,832	540,595	654,426	488,074	227,148
375	547,598	546,553	667,392	495,809	227,67
376	546,618	550,077	673,763	498,682	227,616
377	546,507	556,033	677,907	502,697	228,227
378	543,96	557,101	684,428	508,348	229,887
379	541,808	563,45	688,852	508,583	231,965
380	538,955	566,465	696,214	514,297	235,307
381	536,755	572,289	702,31	517,995	237,185

382	534,171	571,785	708,056	519,424	234,609
383	529,43	572,294	710,405	524,763	233,597
384	527,598	575,451	715,817	525,879	234,272
385	522,457	573,861	716,706	527,457	231,758
386	518,353	576,172	721,129	531,242	236,034
387	514,653	582,443	721,826	535,665	233,762
388	511,516	583,281	724,136	534,657	234,438
389	507,649	582,539	729,515	539,899	240,117
390	504,386	585,538	732,838	540,663	239,979
391	503,273	586,144	735,897	541,586	239,171
392	494,544	588,224	737,602	544,955	245,024
393	494,985	589,104	738,297	543,875	245,78
394	490,261	589,467	740,616	548,827	246,594
395	484,14	589,536	738,058	551,571	252,789
396	481,624	593,706	740,967	550,686	259,349
397	474,477	593,24	741,805	553,833	259,535
398	470,618	587,87	740,745	551,605	260,852
399	465,034	583,487	733,878	548,758	258,531
400	460,482	580,639	729,199	545,294	252,604
401	453,412	579,194	729,43	547,196	249,395
402	447,538	574,743	722,324	544,096	247,992
403	439,073	567,93	720,691	538,652	246,499
404	433,058	568,069	716,45	537,592	244,6
405	429,251	564,302	714,445	538,857	245,887
406	424,5	560,825	709,958	536,136	248,285
407	420,358	559,704	709,427	533,197	252,594
408	417,506	557,562	703,292	529,11	252,122
409	414,8	557,792	701,749	531,723	255,716
410	412,097	555,695	702,177	531,839	260,569
411	408,66	556,719	697,176	529,304	263,474
412	404,053	555,176	694,672	532,307	269,216
413	400,95	553,792	694,708	530,046	267,927
414	397,043	548,911	689,151	526,933	268,638
415	390,41	544,169	683,67	522,53	267,281
416	384,851	538,761	677,491	520,512	267,778
417	381,989	533,135	673,469	513,677	263,041
418	374,392	527,818	666,658	511,04	264,568
419	369,65	525,238	660,355	509,144	266,69
420	365,273	518,078	656,147	503,239	264,522
421	354,416	509,538	642,623	495,402	257,665
422	342,592	496,215	631,699	487,352	248,609
423	334,083	486,621	618,222	476,161	244,678
424	326,47	476,542	608,801	468,767	236,096
425	316,236	464,501	595,132	461,239	232,381

426	307,464	453,793	582,066	452,446	223,766
427	299,696	446,28	571,932	444,335	218,733
428	292,125	434,902	562,998	438,161	216,41
429	284,707	426,683	553,008	430,09	212,344
430	276,747	418,862	542,903	424,988	210,589
431	270,821	413,613	531,242	415,703	205,211
432	264,823	402,94	522,23	409,031	199,359
433	260,322	397,976	512,658	402,698	197,867
434	255,319	389,503	506,068	396,653	196,585
435	251,102	383,678	494,552	393,573	193,775
436	244,628	377,961	485,494	386,053	190,939
437	240,337	370,806	481,962	381,013	193,758
438	238,01	367,538	473,37	377,512	190,056
439	231,839	360,363	466,527	371,743	192,308
440	227,4	358,846	457,878	367,176	189,148
441	224,232	346,37	450,169	361,835	185,848
442	217,816	340,809	442,027	355,791	182,785
443	215,625	339,321	434,166	349,38	183,228
444	211,271	331,848	429,856	345,191	182,007
445	208,306	326,374	424,417	340,406	181,202
446	204,154	322,68	416,707	335,761	179,337
447	203,137	318,54	409,354	330,315	176,267
448	198,627	312,077	405,969	326,466	180,499
449	202,088	311,744	403,555	324,875	186,916
450	202,771	315,94	401,657	325,884	196,846
451	199,238	311,778	394,715	320,7	194,958
452	191,742	300,096	384,721	310,689	186,97
453	184,892	292,17	370,457	303,597	184,672
454	180,284	281,653	363,751	295,566	173,954
455	176,084	277,354	354,753	289,726	173,708
456	173,754	274,467	351,302	287,151	174,661
457	172,778	272,068	349,77	284,615	177,479
458	173,495	271,621	347,359	282,674	181,275
459	171,553	266,856	341,186	280,426	181,7
460	169,044	265,046	338,807	275,991	179,365
461	166,336	261,862	331,357	272,407	179,461
462	169,423	264,773	334,622	270,245	187,646
463	170,228	263,059	334,853	272,174	198,97
464	171,096	262,804	329,198	268,368	200,521
465	166,684	256,23	322,143	265,256	192,415
466	164,41	255,556	317,228	262,611	189,638
467	171,204	262,962	321,883	263,97	206,911
468	176,267	267,539	330,19	270,339	222,989
469	172,789	265,11	325,5	263,747	223,413

470	164,622	254,631	312,943	254,166	207,717
471	156,431	242,234	299,718	245,137	192,654
472	153,587	235,475	292,256	240,97	183,888
473	153,308	234,524	289,892	240,159	186,518
474	149,007	230,345	282,884	234,691	181,578
475	140,115	215,731	272,883	224,121	170,32
476	132,928	206,078	259,392	215,656	160,313
477	128,224	200,573	251,584	208,497	155,707
478	124,679	195,958	246,204	203,615	154,047
479	125,123	194,645	240,205	202,02	155,706
480	126,926	195,214	240,305	201,605	158,904
481	129,443	193,671	239,599	202,764	164,92
482	127,621	194,525	238,512	199,528	167,179
483	125,008	192,696	236,253	194,509	161,155
484	119,851	186,384	226,765	187,16	159,308
485	115,911	179,608	220,166	184,774	152,527
486	111,482	172,671	212,547	178,01	147,275
487	108,817	166,284	202,989	174,022	143,133
488	105,371	163,986	201,568	170,576	138,382
489	105,121	160,668	197,638	166,592	136,022
490	104,48	157,644	193,338	164,628	136,412
491	105,151	159,16	194,751	165,02	141,093
492	106,643	160,863	196,532	163,567	146,485
493	106,406	160,214	194,021	161,918	146,159
494	102,811	157,721	189,255	159,634	142,181
495	100,768	152,354	184,005	154,808	135,965
496	97,2429	148,184	179,994	152,306	130,831
497	94,9654	142,809	175,035	149,124	128,779
498	94,5021	142,898	172,874	144,907	126,834
499	93,3496	140,405	170,633	143,72	124,718
500	92,7819	138,149	167,592	140,699	121,877
501	90,7793	137,265	165,768	140,088	123,23
502	90,002	135,403	163,058	138,096	123,599
503	90,882	133,733	163,187	137,841	123,898
504	89,2489	133,579	159,009	134,264	123,711
505	88,8923	132,427	157,61	132,507	120,032
506	88,0526	130,147	156,283	131,223	118,701
507	89,0677	130,655	154,529	129,728	117,867
508	88,3647	127,89	153,88	127,808	117,829
509	86,8517	126,937	151,271	127,082	117,53
510	87,7427	127,476	149,104	123,445	115,212
511	88,6893	126,8	148,54	122,34	114,421
512	87,8166	124,992	148,325	119,339	115,811
513	88,2602	126,194	147,044	119,198	114,014

514	88,0587	124,625	142,289	116,807	115,133
515	88,9026	123,462	143,175	115,691	114,72
516	88,5234	124,495	142,528	114,273	112,604
517	88,9842	124,357	140,474	113,129	111,02
518	89,7687	123,475	140,63	111,3	112,802
519	90,3797	123,098	139,436	109,593	110,87
520	92,8304	123,626	139,832	109,035	111,638
521	93,5552	125,007	138,929	109,746	111,057
522	94,2687	124,818	138,991	107,144	108,888
523	94,3121	121,008	136,072	106,193	109,028
524	94,3689	120,472	132,449	101,9	104,827
525	93,2263	115,749	130,226	98,4078	102,593

Table 8. Excitation spectra with wavelength at 546 nm of un-dped $CaAl_2O_4$ and Ce and Mn – doped $CaAl_2O_4$ annealed at800^oC in 95% N_2: 5% H_2 with the heating rate of 5^oC/min and the holding time of 1 h

Theta	**0.5 mol% Ce and 5 mol%Mn – doped $CaAl_2O_4$**	**0.5 mol% Ce and 3 mol% Mn –doped $CaAl_2O_4$**	**0.5 mol% Ce and 1 mol% Mn –doped $CaAl_2O_4$**	**0.5 mol% Ce –doped $CaAl_2O_4$**	**$CaAl_2O_4$**
250	191,571	311,774	284,864	110,995	169,941
251	185,311	297,82	271,934	106,495	164,534
252	176,315	281,24	261,816	104,281	160,956
253	169,167	270,831	249,968	99,5975	157,179
254	161,74	255,828	238,254	98,007	154,247
255	152,588	244,011	226,188	94,0939	147,855
256	149,113	231,92	215,362	90,2144	140,956
257	140,631	221,092	206,255	89,2564	137,353
258	134,266	207,798	193,806	86,4976	131,691
259	130,682	198,47	183,219	81,8693	128,406
260	123,3	184,367	174,753	80,7558	122,68
261	119,197	175,566	166,359	78,0253	118,167
262	114,156	166,696	156,112	77,215	113,177
263	108,149	158,368	150,819	76,3938	110,071
264	105,935	148,937	143,614	74,2334	105,284
265	104,182	141,386	135,684	72,8645	101,037
266	102,528	137,26	129,259	72,4823	99,3713
267	99,8321	128,619	126,754	70,8519	93,3735
268	100,872	124,341	121,881	70,3925	93,3365
269	100,111	120,566	117,834	70,2319	90,8067
270	102,807	118,561	115,568	70,8322	89,8612
271	122,501	148,547	143,569	92,0698	118,656
272	198,866	272,297	257,647	191,632	218,276

273	291,974	395,454	353,42	301,237	314,727
274	264,702	312,669	303,001	247,096	251,645
275	157,789	158,25	160,878	122,442	130,078
276	118,614	101,95	102,448	71,5172	76,3887
277	117,104	91,4871	95,7447	66,9022	70,0733
278	120,466	91,2675	93,1773	65,394	66,4597
279	124,159	87,503	90,8709	65,3886	65,7987
280	129,783	87,0068	90,4729	64,8592	63,1383
281	132,437	84,6668	88,8709	64,0919	61,2531
282	137,967	83,3732	88,6534	64,0096	59,9888
283	141,572	81,8127	87,3361	62,96	56,0294
284	147,135	81,9079	85,5732	63,9577	55,2166
285	152,209	80,8132	85,2689	63,6706	53,4783
286	157,826	80,3845	83,9248	63,2512	53,204
287	165,193	80,3007	83,8777	62,7892	49,0576
288	171,574	80,0023	84,0448	63,0328	48,537
289	176,936	79,7442	84,2846	63,0891	47,1613
290	181,488	79,9042	83,3682	62,0862	45,2707
291	189,01	79,9997	83,6252	62,7858	43,958
292	193,76	79,9159	84,5867	62,9053	42,6135
293	198,192	79,0946	84,8787	63,1826	42,5806
294	203,643	80,4021	85,1316	63,4062	41,0547
295	208,471	81,079	86,1376	64,2096	41,0172
296	213,055	81,4341	86,8988	63,6492	39,8931
297	213,491	81,9366	87,6885	64,0695	37,8983
298	217,334	81,2494	87,2273	64,5412	37,0274
299	216,802	82,7602	89,229	64,148	37,1154
300	216,784	83,7925	89,3891	64,992	35,5291
301	217,286	84,2425	91,187	66,329	35,0593
302	213,576	85,3757	92,3362	66,4845	33,8983
303	213,802	85,5393	93,2925	67,9626	33,6943
304	212,482	88,4775	94,4981	68,1416	33,5082
305	209,08	89,1691	96,837	69,7175	32,1382
306	207,158	89,9653	97,8953	70,3167	32,2845
307	203,145	90,9696	99,0163	71,0493	31,9651
308	203,273	93,4627	100,63	72,3157	31,8796
309	199,579	93,9457	102,192	72,395	31,2098
310	198,01	94,8819	103,246	73,1679	30,6588
311	196,016	95,4642	105,263	74,2482	30,2537
312	195,868	97,1979	107,21	74,8301	30,0169
313	193,085	98,3868	109,562	76,3377	29,592
314	193,015	99,9177	109,432	75,9061	29,1803
315	192,458	100,3	111,719	77,1327	29,1502
316	189,766	101,369	113,019	77,9578	28,962

317	188,92	102,543	114,93	79,3045	28,8631
318	188,387	103,74	116,418	79,5955	27,9126
319	187,253	105,086	117,973	80,3675	28,0491
320	186,047	106,763	120,359	81,2016	28,0224
321	185,073	105,999	120,706	81,6673	27,6672
322	183,967	106,621	122,41	82,1899	27,2442
323	183,223	107,766	124,264	82,8088	27,2595
324	182,806	109,305	124,648	83,7057	26,6122
325	182,227	110,303	125,25	84,2138	26,3268
326	180,19	110,73	127,527	85,0539	26,5213
327	178,291	111,496	128,868	85,2915	26,5588
328	175,422	112,831	129,447	84,9495	26,2039
329	172,843	112,335	131,105	86,2489	25,9626
330	167,813	113,309	132,148	85,7962	26,0092
331	162,417	113,53	133,254	85,6114	25,3521
332	156,49	113,842	133,858	85,9293	25,2481
333	150,872	114,661	135,609	86,983	25,1183
334	143,87	114,933	135,88	87,4396	24,4426
335	137,344	114,016	137,351	87,347	24,7548
336	130,841	114,653	137,021	87,2664	24,3881
337	124,117	115,625	138,952	86,9406	24,3534
338	117,572	115,193	140,131	87,2151	23,7568
339	110,522	115,763	140,011	87,3237	24,4333
340	105,35	116,386	141,211	87,5047	24,2539
341	100,738	115,259	141,249	87,8023	23,3781
342	95,802	115,446	141,913	86,5165	24,1295
343	91,1915	115,421	142,902	86,2757	23,3502
344	87,911	115,095	143,36	87,1761	23,4294
345	84,6083	115,329	144,49	86,5029	23,3828
346	81,6456	115,67	143,937	85,5247	23,2933
347	79,139	115,242	144,884	85,6038	23,035
348	77,5417	114,596	145,4	85,3491	23,1115
349	75,3325	114,825	145,896	84,2449	23,0125
350	74,0452	115,236	146,215	84,0173	22,4675
351	72,0523	114,486	146,741	83,3201	22,6006
352	70,6444	114,155	146,419	82,6643	22,031
353	69,1204	114,877	146,019	82,1487	21,9593
354	67,753	113,398	147,207	81,675	22,3966
355	66,7627	113,565	147,276	81,4303	22,3757
356	66,0745	114,579	147,077	80,371	21,9967
357	65,142	112,29	146,76	80,1772	21,7804
358	63,8085	113,808	147,093	79,1725	21,8349
359	62,4651	113,112	147,533	77,7628	21,7428
360	62,0639	111,718	146,651	77,0868	21,5205

361	61,126	110,813	145,706	75,7326	21,8013
362	60,3365	110,648	144,651	74,778	22,0542
363	59,662	109,712	142,944	74,519	21,4438
364	58,2568	108,734	142,164	72,3975	21,7647
365	57,4343	107,434	141,365	71,1345	21,8089
366	57,0638	106,465	139,364	70,6777	21,1482
367	54,8722	104,286	137,4	68,3353	21,2893
368	54,0511	102,709	134,378	66,3368	20,9536
369	52,5107	101,427	132,661	65,0488	20,7275
370	51,7584	99,0155	130,303	63,0502	20,8455
371	50,2752	97,9063	127,423	61,4065	20,2207
372	49,0637	95,4278	123,671	59,4742	20,1392
373	47,5181	92,3844	121,148	57,4608	20,3174
374	45,9621	90,0881	118,207	56,2735	19,9123
375	44,3721	87,1239	114,993	54,2184	19,703
376	42,8603	84,8103	111,107	52,3451	18,9414
377	41,6554	82,2268	107,64	50,3327	18,9419
378	39,8968	80,025	103,833	48,3863	18,7402
379	38,3806	76,6411	99,5033	46,8259	18,6751
380	37,0678	73,9752	96,1107	44,6378	17,9893
381	35,6518	71,3565	92,6158	43,1667	18,0705
382	34,4853	68,8508	89,2268	41,6383	17,4731
383	33,1798	66,595	85,703	39,8659	17,4384
384	32,1586	63,3882	81,5469	38,6715	17,2752
385	30,8792	61,59	79,2264	37,3899	17,0818
386	29,5018	58,7458	75,7465	35,6394	16,998
387	28,9298	56,8172	72,4321	34,07	16,7683
388	27,4657	54,7069	69,824	32,9252	16,1903
389	26,8803	52,603	67,3276	31,8006	16,1953
390	25,7397	50,6487	64,4771	30,5873	15,8528
391	25,1976	48,5246	61,509	29,4028	15,6335
392	23,9646	46,3329	58,4758	28,1036	15,4979
393	23,2322	44,29	55,963	27,2744	15,2268
394	22,2318	42,4021	53,3962	26,1886	15,0632
395	21,6327	40,692	50,9091	25,248	14,8095
396	20,6913	38,8175	48,69	24,1345	14,3417
397	19,8	37,0648	46,0898	23,5272	13,8269
398	19,2828	35,1158	43,9608	22,6222	13,5563
399	18,6592	33,9651	42,0289	21,7602	13,5723
400	18,2139	32,4568	39,9203	21,1532	13,68
401	17,9154	31,172	38,2019	20,6557	13,8059
402	17,4157	30,5818	36,8721	20,2075	13,5731
403	17,1742	29,2026	35,071	19,4522	13,7476
404	16,6181	27,8919	33,7256	18,7669	13,7903

405	16,3389	26,9678	32,2045	18,4218	13,6966
406	16,0563	25,7667	30,8016	17,906	13,6093
407	15,9628	24,6571	29,2248	17,4891	13,2724
408	15,9172	23,8141	27,7954	16,8854	13,0387
409	15,9652	22,938	26,9074	16,6739	12,8875
410	15,9932	22,1422	25,7974	16,1366	12,7324
411	16,4865	21,3361	24,582	15,7188	12,561
412	16,7918	20,6097	23,5755	15,2986	12,5187
413	17,0464	20,4441	22,7974	15,2143	12,323
414	17,0592	19,7614	21,8434	14,5275	12,394
415	16,9049	19,4471	21,3612	14,3503	12,4665
416	16,5981	19,0843	20,6795	14,2898	12,212
417	15,871	18,7656	20,4345	13,8817	12,2637
418	15,064	18,4786	19,5673	13,6952	12,2061
419	14,7071	18,2222	19,0386	13,4291	12,0052
420	14,0969	18,1005	18,6027	13,1998	11,4975
421	13,8535	18,1028	18,2413	12,8523	11,2984
422	13,5941	18,0446	18,1378	12,7895	11,6532
423	13,6792	18,0955	18,0881	12,5753	11,987
424	13,7976	18,1162	17,5434	12,6356	12,0061
425	13,4635	17,8997	17,3962	12,4116	11,8253
426	13,4177	17,863	17,0371	12,2036	11,9343
427	13,2378	17,5475	16,8467	12,0986	11,5221
428	13,289	17,1459	16,4684	12,0888	11,6833
429	13,1505	17,1887	16,4239	12,0011	11,3646
430	13,108	16,853	15,9967	11,9296	11,3064
431	13,0322	16,6222	15,5833	11,8069	11,5048
432	12,9069	16,5564	15,4713	11,7467	11,4541
433	12,6971	16,4627	15,5154	11,6267	11,2018
434	12,7869	16,1654	15,0439	11,5995	11,2444
435	12,8425	15,8578	14,9165	11,3932	11,2462
436	12,4973	15,6347	14,776	11,3594	11,0651
437	12,2408	15,4739	14,4383	11,2292	11,1024
438	12,2099	15,2307	13,9811	11,0793	10,8605
439	11,9778	14,6942	13,8654	11,0002	10,6458
440	11,787	14,8194	13,5042	10,8465	10,6353
441	12,0448	14,4864	13,3574	10,9305	10,6723
442	11,7674	14,3366	13,4266	10,9707	10,7621
443	11,5782	14,2925	13,0679	10,7594	10,8479
444	11,5375	14,1292	13,011	10,7466	10,6736
445	11,4944	13,9786	12,8403	10,8636	10,7063
446	11,4635	13,9303	12,8201	10,7519	10,6859
447	11,4649	13,6358	12,6292	10,6756	10,6039
448	11,3252	13,3895	12,4345	10,6308	10,6239

449	11,1187	12,7446	11,9821	10,432	10,3008
450	10,451	12,144	11,3496	9,83383	9,47662
451	10,064	11,6761	10,8781	9,77555	9,0915
452	10,2308	11,6446	11,0222	9,88972	9,4308
453	10,4636	12,2243	11,2385	10,2237	9,88226
454	10,9846	12,1179	11,4205	10,4447	10,1165
455	11,114	12,8138	11,7897	10,8335	10,6624
456	10,96	12,4833	11,8658	10,7684	10,5763
457	10,9372	12,5401	11,7347	10,6804	10,6079
458	10,7676	12,2206	11,621	10,6972	10,2484
459	10,9682	12,201	11,4829	10,7119	10,3258
460	10,9885	12,5056	11,6451	10,8783	10,4867
461	11,1275	12,5857	11,6924	10,9283	10,4763
462	10,6736	12,1082	11,4221	10,7462	10,0838
463	10,4725	11,8317	11,1987	10,4679	9,71394
464	10,3352	11,6594	11,1423	10,5735	9,48898
465	10,5166	12,0478	11,2823	10,5588	9,757
466	10,8285	12,019	11,3962	10,8033	10,133
467	10,1453	11,6516	10,8599	10,3964	9,2381
468	9,7403	10,7917	10,0881	9,8	8,56242
469	9,4584	10,5403	9,9326	9,29961	7,98031
470	9,99666	11,0724	10,4926	9,90979	8,56879
471	10,5454	11,9647	11,1185	10,6953	9,73111
472	10,9512	12,6352	11,7927	10,9839	10,3061
473	11,106	12,7016	11,8101	11,3163	10,501
474	11,7895	13,441	12,5069	11,8231	10,988
475	12,856	15,2737	13,9233	12,879	12,2411

AUTHOR BIOGRAPHY

A Marsha Alviani obtained his B.E (Bachelor of Engineering) in Materials and Metallurgical Engineering Department from Institut Teknologi Sepuluh Nopember (ITS) in Indonesia, 2015, under supervision of Dr. Widyastuti, with a thesis on "Magnetic properties and morphological analysis of Barium Hexaferrite doping Ni-Zn prepared by sol gel auto combustion method with the variation of pH and sintering temperature". She did his B.E with only 3.5 years. Then, she was worked as research assistant under supervision of Dr. Widyastuti. She was published some books, such as Derap Kampus Perjuangan, Saga, 2015; Integrasi Teknologi dan Entrepreneurship (as an editor), ITS Press 2016; Tracer Study ITS 2016, ITS Press 2016; Survey Kepuasan Pengguna 2016 (as an editor), ITS Press 2016; and Tracer Study ITS 2017, ITS Press 2017. Currently, she is completing her M.Eng (Master of Engineering) degree in Materials Engineering from ITS and her M.Sc (Master of Science) in Material Science and Engineering Department at National Taiwan University of Science and Technology (NTUST), Taiwan by joining the double-degree program. She has been working under supervision of Professor Shao-Ju Shih (NTUST), Dr. Widyastuti (ITS), and Dr.Eng. Hosta Ardhyananta (ITS) with thesis addressed to preparation and characterization of glassy Ce^{3+} and Mn^{2+} -doped $CaAl_2O_4$ powder using spray pyrolysis. This thesis work has led the author to get his M.Eng in ITS as well as M.Sc in NTUST.

Corresponding author.

Tel. : +62 8775 2072 710

a.marshaalviani@gmail.com

(*This page intentionally left blank*)